

SNOWMASS NEUTRINO FRONTIER: NF10 TOPICAL GROUP REPORT NEUTRINO DETECTORS

SUBMITTED TO THE PROCEEDINGS OF THE US COMMUNITY STUDY
ON THE FUTURE OF PARTICLE PHYSICS (SNOWMASS 2021)

JOSH KLEIN^{*1}, ANA MACHADO^{*2}, DAVID SCHMITZ^{*3}, RAIMUND STRAUSS^{*4},
MILIND DIWAN^{†5}, CHRISTOPHER JACKSON^{†6}, JOSE MANEIRA^{†7}, KOSTANTINOS MAVROKORIDIS^{†8},
NICOLA MCCONKEY^{†9}, TANAZ MOHAI^{†10}, GIANLUCA PETRILLO^{†11}, AND JOSEPH ZENAMO^{†10}

¹UNIVERSITY OF PENNSYLVANIA, PHILADELPHIA, PA, USA

²UNIVERSITY OF CAMPINAS, BRAZIL

³UNIVERSITY OF CHICAGO, CHICAGO, IL, USA

⁴TECHNICAL UNIVERSITY MUNICH, MUNICH, GERMANY

⁵BROOKHAVEN NATIONAL LABORATORY, UPTON, NY, USA

⁶PACIFIC NORTHWEST NATIONAL LABORATORY, RICHLAND, WA, USA

⁷LABORATÓRIO DE INSTRUMENTAÇÃO E FÍSICA EXPERIMENTAL DE PARTÍCULAS - LIP, 1649-003 LISBOA,
PORTUGAL AND FACULDADE DE CIÊNCIAS - FCUL, UNIVERSIDADE DE LISBOA, PORTUGA

⁸UNIVERSITY OF LIVERPOOL, LIVERPOOL, UK

⁹UNIVERSITY COLLEGE LONDON, LONDON, UK

¹⁰FERMI NATIONAL ACCELERATOR LABORATORY, BATAVIA IL, USA

¹¹STANFORD LINEAR ACCELERATOR CENTER, STANFORD, CA, USA

Contents

1	Introduction	6
2	Noble Element Detectors	7
2.1	Advanced Technologies for Liquid Argon TPCs	7
2.1.1	New Charge Readout Technologies	7
2.1.2	Dopants to Increase Charge Yields	10
2.1.3	Optical TPCs and the ARIADNE Program	11
2.1.4	Scintillation Detection in LArTPCs	13
2.1.5	The ARAPUCA Light Collector	14
2.1.6	Dopants to Increase Photon Yields	16
2.1.7	Simulation and Calibration in LArTPC Neutrino Detectors	16
2.1.8	Gaseous Argon TPCs	19
2.1.9	Low-Radioactivity Argon	19
2.2	Novel Large Liquid Argon Detector Concepts	20
2.2.1	Solar Neutrinos in LAr (SoLAr)	20
2.2.2	A SURF Low Background Module (SLoMo)	21
2.2.3	Neutrinoless Double Beta Decay with Xe+LArTPC	23
2.2.4	Detecting Cherenkov and Scintillation Photons in LAr (ArCherS)	24
2.3	Liquid and Gaseous Xenon Detectors	24
3	Photon-Based Neutrino Detectors	26
3.1	Enabling Technologies for Hybrid Cherenkov/Scintillation Detectors	26
3.1.1	Water-based Liquid Scintillator	28
3.1.2	Slow fluors	28
3.1.3	Fast Photomultiplier Tubes and LAPPDs	29
3.1.4	Spectral Sorting and Dichroicons	29
3.1.5	Using Angular Information	32
3.1.6	Comparing Cherenkov/scintillation Separation Approaches	33
3.1.7	Further Technological Needs	33
3.2	Isotopic Loading Techniques for Low-energy Physics Programs	35
3.2.1	Metal Loading in WbLS	35
3.2.2	Te Loading in Liquid Scintillator for $0\nu\beta\beta$	36
3.2.3	^6Li Loading in Plastic Scintillator	36
3.2.4	Quantum Dots	37
3.3	Improvements in Simulation and Analysis	39
3.3.1	GPU-Accelerated Photon Ray Tracing (<i>Chroma</i>)	39
3.3.2	GEANT4-based toolkits <i>RAT-PAC</i>	40
3.3.3	Machine Learning Approaches	43
3.4	Prototypes and Large-Scale R&D Platforms	43
3.4.1	ANNIE	43
3.4.2	NuDOT	44
3.4.3	Eos	46
3.5	Large-Scale Detector Ideas	47
3.5.1	THEIA	47

3.5.2	LiquidO	49
3.5.3	SLIPs	51
4	Low-Threshold Neutrino Detectors	53
4.1	Common challenges of low-energy neutrino detectors	54
4.2	The eV frontier of neutrino detectors	55
4.2.1	Cryogenic particle detectors for CEvNS	55
4.2.2	CCD-based detectors for CEvNS	57
4.2.3	Detectors for neutrino mass	57
4.2.4	Future detectors for relic neutrinos	58
4.2.5	New detector concepts	58
4.3	Optimized conventional detectors to exploit CEvNS	59
4.3.1	HPGe detectors	59
4.3.2	Photon-based low-threshold detectors	60
4.3.3	Bubble chambers	61
4.3.4	Gaseous detectors	61
4.3.5	Liquid noble gas detectors	62
4.4	Dark Matter detectors for next-generation neutrino measurements	63
4.4.1	Multi-ton liquid noble detectors	64
4.4.2	Large-scale cryogenic detectors	65
4.4.3	Directional detectors	65
5	High- and Ultra-High-Energy Neutrino Detectors	67
5.1	Advanced High- and Ultra-High-Energy Neutrino Telescopes	67
5.1.1	Detector Requirements	67
5.1.2	Optical Cherenkov Approaches	69
5.1.3	Radio Detection in Ice	69
5.1.4	Air-shower detection techniques for UHE ν_τ s	71
5.1.5	Air-shower radio detection	71
5.1.6	Air-shower imaging	72
5.2	Detectors for the Forward Physics Facility at the LHC	72
5.2.1	Detector Requirements	72
5.3	Technical Considerations	73
5.3.1	Experimental Technologies	73
6	Additional Detector Ideas	76
6.1	Hydrogen and Deuterium Detectors	76
	References	79

Executive Summary

Neutrino physics spans an enormous range of energies and scales: from detection of low-energy cosmic neutrinos; to keV-scale recoils in coherent neutrino scattering; to MeV-scale solar, reactor, and neutrinoless double beta decay events; to GeV and TeV-scale detection of neutrinos from accelerators and the atmosphere; to cosmic sources in the PeV–ZeV range. While any particular experiment tends to focus on just one or two detection approaches, the great breadth of neutrino physics means that there is an equally broad spectrum of neutrino detection technologies and methodologies.

At any one time, there are a dozen or more medium- to large-scale neutrino detectors operating worldwide, several more in the design or construction phases, and many future detectors planned. Beyond this are a diverse set of smaller scale prototypes distributed across universities and labs.

The focus in this report is on new technologies and approaches that will enable future neutrino detectors, and thus experiments that are already built and running, are under construction, or for which technical designs exist are not discussed in great detail.

Recommendations for Next-Generation Neutrino Detectors While there are many exciting detectors and enabling technologies described in this report, there are a few ideas that have had a particularly large community interest, and we formulate these into a set of recommendations below:

- **Broaden the Noble Liquid and Gas Physics Program:** Many ideas are being pursued for improving LArTPCs, including new charge readout technologies, the use of underground argon for low-background physics, the addition of various dopants (xenon, photo-ionizing) to increase photon or charge yields, or light traps like the ARAPUCAs for improved light detection. Many of these ideas may enable a broader physics program than can be done with existing detector designs.
- **Pursue hybrid Scintillation/Cherenkov Detectors:** Many different technologies are being developed for these, including water-based liquid scintillator, slow fluors, fast timing with LAPPDs and other devices, and spectral photon sorting with dichroicons. At very large scales like the proposed Theia detector, these could have very broad physics programs.
- **Optimize low-threshold neutrino detectors:** To expand the ever-growing CE ν NS program and to fully exploit the physics reach of CE ν NS in the next decade requires not just lowering energy thresholds but improving background rejection techniques, understanding detector responses at the eV-scale, and moving toward larger detector masses. The enabling technologies have many synergies with direct neutrino mass measurements and recoil-imaging directional dark matter detectors.
- **Develop Technologies for Neutrino Detection at the TeV Scale and Beyond:** Observations of high-energy neutrinos at large neutrino telescopes have provided a wealth of physics and multi-messenger astrophysics, and new opportunities for studying neutrino interactions at the LHC, including possibly tagging the production vertex, are particularly exciting. Enabling technologies for neutrino telescopes include radar echo detection, Askaryan effect detection, and ever-larger scale optical detection, while at the LHC they include picosecond timing synchronizations, intelligent triggering, and high-resolution tracking.

- **Co-develop neutrino and dark-matter detectors:** Both the development of noble liquid and gas detectors and low-threshold detectors of various technologies are likely to lead to new technologies that are useful for both the Neutrino Frontier and the Cosmic Frontier.

Detector and Technology Summary Through the Snowmass LOI process, plus several community discussions, it has become clear that many ideas for new neutrino technologies and detectors fall into a few broad classes:

- **Noble gas and liquids:** New detector ideas here typically focus on improved reconstruction (e.g., by using pixellated TPCs or high-pressure gas), and broad physics programs accomplished by effectively moving to lower energy thresholds.
- **“Photon-based” detectors:** Enabling technologies here are various approaches to development of hybrid Cherenkov/scintillation detectors, new approaches to segmentation, and new isotopic loading techniques for particle ID, neutrino detection, and neutrinoless double beta decay.
- **Low-threshold neutrino detectors:** These include a broad array of technologies many of which are aimed at detection of low-energy nuclear recoils created by coherent neutrino-nucleus scattering ($\text{CE}\nu\text{NS}$).
- **High-energy neutrino detection:** New approaches here include large-scale detectors for neutrinos from cosmic sources including radar echo technology, and space-based geo-observations, and new techniques for detecting and vertexing neutrinos from the LHC.
- **Novel Detector Ideas:** Some of the detectors fall into no particular technical category but are nevertheless novel in themselves, putting together in some cases existing technologies to create new neutrino physics capabilities.

Liquid Noble and Gas Detectors Since the last Snowmass, there has been enormous progress and diversity in detectors that use either noble liquids or gases as their target material. Such detectors have been used for dark matter searches by experiments like DarkSide [1], DEAP [2], and LZ [3], for neutrinoless double beta decay with experiments like EXO-200 [4], and as part of both the Short-Baseline Neutrino program at FNAL [5] with MicroBooNE, SBND, and ICARUS, and the DUNE experiment at SURF [6]. There are many new ideas for doing more with these detectors, from scaling upwards (e.g., nEXO [7]), to improving reconstruction capabilities by using pixelated charge readout in LArTPCs (e.g., LArPix, QPix) or moving to high-pressure (e.g. ND-GAr, NEXT) or atmospheric-pressure (e.g. CYGNUS) TPCs, to lowering thresholds by using underground sources of LAr. There is also interest in new approaches to detecting scintillation light in these detectors, including pixelated SiPM arrays, photo-ionizing dopants, or by increasing light coverage with ARAPUCA light-traps deployed on TPC cathodes using power-over-fiber. A common theme in the LArTPC community is the pursuit of a broader physics program than currently planned, including low-energy solar neutrinos or neutrinoless double beta decay, much of which would be leveraged by underground or low-background argon.

Thus some of the highest technical priorities in this area are:

- Larger-scale production of underground argon sources, or ways to remove ^{39}Ar and ^{42}Ar

- Development of pixelated charge readout for TPCs
- Development of pixelated light readout for TPCs
- Investigations of new ways for photon detection in liquid noble detectors, including photo-ionizing dopants
- Advanced triggering schemes at low-energies, including machine learning techniques

Photon-based Detectors Neutrino detectors that use photons as their primary carrier of neutrino interaction information have an incredibly successful history in neutrino physics. They include Cherenkov detectors like IMB, Kamiokande, SNO, and Super-Kamiokande, and scintillation detectors like KamLAND, Double CHOOZ, Daya Bay, RENO, BOREXINO, NOVA, PROSPECT, and SNO+. Of particular interest in the past decade or so are *hybrid* Cherenkov/scintillation detectors, which can detect and discriminate between Cherenkov and scintillation photons (“chertons” and “scintons”) in the same detector, thus allowing a very broad neutrino physics program. Enabling technologies that would allow this have been and continue to be developed over the past decade, including new materials like water-based liquid scintillator and slow fluors, new and faster devices like LAPPDs, and spectral photon sorting with devices like dichroicons. These new technologies, employed either separately or in concert, make large-scale hybrid detectors a real possibility. The most developed of these ideas is the proposed Theia experiment, which could sit in the LBNF beam at SURF.

In addition to hybrid Cherenkov/scintillation detectors, new ideas for segmented detectors have also been developed. The most developed of these is LiquidO, which would use scintillator with short scattering lengths and an array of fiber optics to create a “self-segmented” detector that could allow precision track reconstruction at both high and low energies. The SLIPS idea, which removes physical segmentation by floating a scintillator volume, could allow very low-background experiments by eliminating radioactive sources in the volume.

Looking even further ahead, some of the highest technical priorities seen in this area, which could be explored between this Snowmass and the next, are:

- Lower-cost, large-area, high-quantum efficiency ($\sim 40\%$) photon sensors
- Lower-cost, fast-timing (≤ 100 ps) photon detectors
- Dichroic filters that can be deposited on non-flat surfaces and with sharper cut-on/cut-off curves, even at high incidence angles
- Narrow-band fluors for liquid scintillators
- High-yield scintillators with attenuation lengths > 40 m
- High-yield “slow” (≥ 10 ns risetime) fluors
- Low-background fiber optics
- New approaches to radiologic background reductions, beyond levels seen in Borexino

Low-threshold Neutrino Detectors The development of low-threshold neutrino detectors with eV-scale resolution has become a priority in neutrino physics during the last decade since it has opened up new portals for the study of neutrino properties and the search for new physics. The COHERENT program has pioneered a detector technology which enabled the first observation of $\text{CE}\nu\text{NS}$ and is driving since then a blooming new research field under US leadership. This technological breakthrough triggered R&D activities worldwide of low-threshold neutrino detectors based on a wide range of technologies. A broad and complementary $\text{CE}\nu\text{NS}$ program based on small-scale experimental projects will enable precision measurements and pave the way for applications. The community will profit from multiple technological synergies with direct neutrino mass measurements and a variety of proposed approaches. To achieve the technological goals the following challenges have to be addressed:

- Improve detector thresholds towards the eV scale.
- Develop advanced techniques for suppressing backgrounds, including the community-wide observed low-energy excess.
- Establish multiplexing techniques to scale-up active detector mass.
- Understand the detector response at the eV scale.
- Increase level of automatization for applications in science, industry, and for society.

Exploiting the strong technological connections with direct dark matter (DM) searches is essential and of mutual interest for both communities. The $\text{CE}\nu\text{NS}$ community will profit from the ongoing R&D efforts on low-threshold directional recoil detectors for DM searches. Multi-ton DM detectors will play a crucial role for the measurements of solar and supernova neutrinos in the next decade.

High-Energy and Ultra-High-Energy Neutrino Detectors Detection of neutrinos at the TeV scale and beyond has been pioneered by big neutrino telescopes like ICECUBE and KM3NET. The amount of physics and astrophysics and multi-messenger possibilities from these detectors is remarkably broad, and they have been exceptionally successful. Future plans for these detectors focus on moving toward even higher energies, into the EeV and ZeV regimes, which require scales going well beyond km^3 or new technologies, exploiting the Askarayan effect or radar echoes off ionization trails. In many cases, the enabling “technology” for these telescopes is a piece of geography: polar or Greenland ice sheets, mountain ranges that can be used as targets, etc. At the same time, there is a new opportunity at the LHC with the “Forward Physics Facility” (FPF) to detect neutrinos produced in collisions, perhaps with the possibility of tagging the neutrino production vertex in a collider detector. High priorities over the next several years for these detectors are:

- Develop further the capability of radio detection of neutrinos interacting in ice or the atmosphere.
- Demonstrate at larger scales the detection of neutrinos via radar echoes off ionization cascades.
- Create low-cost ways of scaling to ever-larger telescopes sizes.
- Create intelligent triggers for background rejection at the FPF.
- Create larger-scale high-resolution tracking options for FPF neutrino events.

1 Introduction

Neutrino physics spans an enormous range of energies and scales: from detection of low-energy cosmic neutrinos; to keV-scale recoils in coherent neutrino scattering; to MeV-scale solar, reactor, and neutrinoless double beta decay events; to GeV and TeV-scale detection of neutrinos from accelerators and the atmosphere; to cosmic sources in the PeV–ZeV range. While any particular neutrino experiment tends to focus on just one or two detection technologies—say, ionization and photon detection—the great breadth of neutrino physics means that there is an equally broad spectrum of detection technologies and methodologies. At any one time, there are a dozen medium- to large-scale neutrino detectors operating worldwide, several more in the planning or construction phases, and many future detectors planned. Beyond this are a diverse set of smaller scale prototypes distributed across universities and labs.

The focus of NF10, “Neutrino Detectors,” is on enabling technologies in the context of neutrino detection. We have in this report focused on new approaches that will enable *future neutrino detectors* and thus, experiments that already exist, or are under construction or for which advanced technical designs already exist are not discussed in great detail. Table 1 lists the contributed Snowmass White Papers relevant to the NF10 topical group. In addition, during the summer of 2020 the neutrino physics community submitted nearly a hundred relevant LOIs that can be found linked from the snowmass21.org website.

1	Future Advances in Photon-Based Neutrino Detectors	arXiv:2203.07479
2	Coherent elastic neutrino-nucleus scattering: Terrestrial and astrophysical applications	arXiv:2203.07361
3	Recoil imaging for dark matter, neutrinos, and physics beyond the Standard Model	arXiv:2203.05914
4	Low-Energy Physics in Neutrino LArTPCs	arXiv:2203.00740
5	SoLAr: Solar Neutrinos in Liquid Argon	arXiv:2203.07501
6	Low Background kTon-Scale Liquid Argon Time Projection Chambers	arXiv:2203.08821
7	Measuring the Neutrino Event Time in Liquid Argon by a Post-Reconstruction One-parameter Fit	arXiv:2004.00580
8	Adding Stroboscopic Muon Information For Reduction of Systematic Uncertainties in DUNE	link
9	DUNE Software and High Performance Computing	arXiv:2203.06104
10	High-pressure TPCs in pressurized caverns: opportunities in dark matter and neutrino physics	arXiv:2203.06262
11	Passive low energy nuclear recoil detection with color centers – PALEOCCENE	arXiv:2203.05525
12	Bubble Chamber Detectors with Light Nuclear Targets	arXiv:2203.11319
13	The COHERENT Experimental Program	arXiv:2204.04575

Table 1: Table of submitted White Papers relevant to the NF10 topical group on Neutrino Detectors.

2 Noble Element Detectors

Noble element detectors play a significant role in neutrino physics today. Several new experimental programs have been built and operated during the past few years, each one advancing the technology further, and efforts are underway now to build detectors at massive scale and take advantage of this technology’s capabilities for precision neutrino physics. Of particular interest are liquid argon time projection chambers (LArTPCs), discussed next.

2.1 Advanced Technologies for Liquid Argon TPCs

Liquid argon time project chamber (LArTPC) detectors offer the possibility of individual particle tracking and fine-grained calorimetry over very large volumes, making them an ideal technology for precision neutrino physics and searches for rare phenomena. LArTPCs have been used in frontier experiments in both accelerator neutrino physics and dark matter searches (e.g. ICARUS, ArgoNeuT, LArIAT, MicroBooNE, ProtoDUNE, SBND, LArIAT, WArP, ArDM, DarkSide). Over the years, many different types of charge and light readout have been developed or proposed: single phase TPC (only liquid argon), dual phase TPC (liquid and gaseous argon which profits from charge amplification in gaseous phase), wire or PCB-based charge readout, light detection with photon multipliers and silicon sensors, etc.

The international particle physics community is currently working to build a next generation neutrino observatory and long-baseline oscillation experiment, DUNE (the Deep Underground Neutrino Experiment), based on this technology. The DUNE design includes four massive detector modules, each containing 10-kilotons of active argon mass, located in a deep underground cavern at the Sanford Underground Research Facility (SURF) in South Dakota. The 2014 P5 report strongly endorsed this program, and in addition recommended several efforts to pave the way to DUNE by executing a set of smaller-scale liquid argon experiments to develop the technology and build up the international community and expertise for the DUNE program. This recommendation has been realized in the SBN program at Fermilab, the ProtoDUNE program at CERN, and other experimental R&D efforts. The eight years since the 2014 P5 Report have seen tremendous progress in the design, construction, operation, and physics outputs of the liquid argon time projection chamber neutrino detector.

To realize the full potential of the LArTPC technology, R&D efforts continue. Large LArTPCs are well-matched to physics at accelerator beam neutrino energies (GeV-scale). A particular motivator for many current R&D efforts is to push the reach of the detectors to lower and lower energies (MeV-scale) to optimize the performance for supernova neutrinos, solar neutrinos, and even the possibility of searches for neutrinoless double beta decay in a large-scale detector. DUNE is comprised of four 10-kiloton LArTPC modules (active mass). Construction has started on the first modules, but the fourth “module of opportunity” presents a platform to further enhance the physics capabilities of the experiment in exciting ways through successful R&D efforts, now underway. This section highlights some of those efforts.

2.1.1 New Charge Readout Technologies

Charge readout is fundamental to the TPC and improved performance (signal-to-noise, granularity, etc.) can lead directly to improved particle reconstruction, energy resolution, and general physics performance. Many ideas are being actively pursued within the neutrino research community.

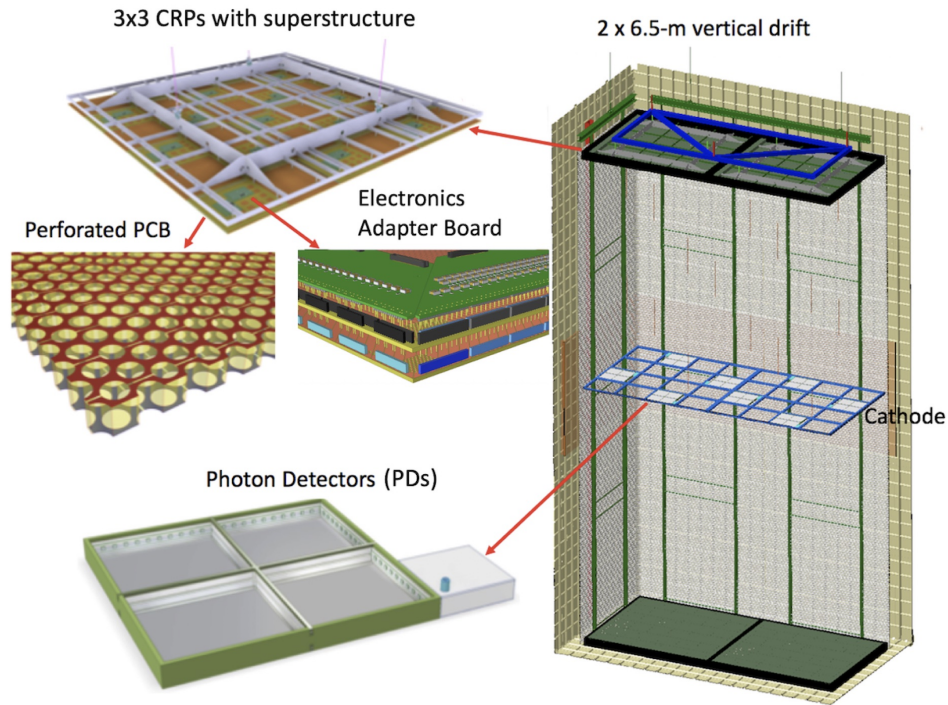


Figure 1: DUNE vertical drift design with PCB-based charge readout.

Charge Readout Planes (CRPs) and the Vertical Drift: The first DUNE far detector module will use a single-phase TPC technology, horizontal drift field, and wire-based charge readout, as has been already successfully demonstrated in ICARUS, MicroBooNE, ProtoDUNE-SP [1], and other detectors. For the second DUNE far detector module, however, a new design, known as Vertical Drift, has been recently under development (see Snowmass LOI [8]). Figure 1 shows the concept. A horizontal cathode plane is placed at mid-height in the active volume of the cryostat, dividing it into two vertically stacked equal volumes, each 6.5m in height. The anode planes are constructed of perforated printed circuit boards (PCBs) with etched electrodes forming a three-view charge readout. The top anode plane is placed close to the cryostat top, just below the surface of the LAr, and the other is located as close to the bottom of the cryostat as possible. Ionization electrons will drift vertically towards the anode plane at the end of the drift volume in which they are released. The vertical drift design offers a slightly larger instrumented volume compared to the first module design as well as a substantially simpler, more cost-effective construction and installation due to its geometry and structure.

LArPix: Pixelated charge readout is a highly attractive alternative to traditional wire-based readouts as pixels can provide unambiguous 3D imaging in LArTPCs. To prove viable in a large LArTPC, such as the DUNE far detectors, pixelated readout systems must meet stringent requirements on noise, power, reliability in a cryogenic environment, and scalability to systems with order 10^9 channels. The first-generation LArPix system provided a proof-of-concept for pixelated LArTPC readout by 2018 [9], and since then the R&D effort has focused on scalability and use of commercial production of components. The LArPix system is now being tested at a scale relevant for the DUNE near detector in the ArgonCube prototype detectors. Figure 2 shows a LArPix anode panel and two examples of typical raw data from cosmic ray interactions in ArgonCube. Further R&D and prototyping will be needed to prepare a pixel-based readout system for use at DUNE far detector scale.

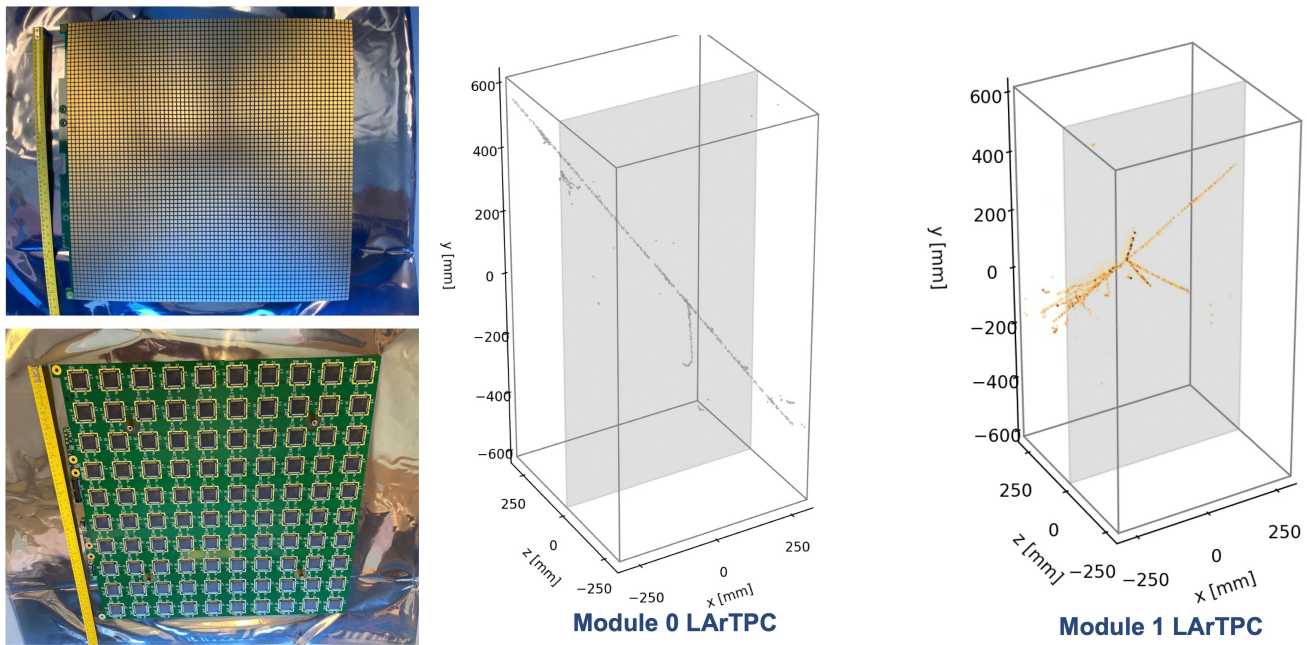


Figure 2: Left: A single LArPix-v2 pixel anode panel. Right: Typical raw data from the LArPix charge readout system as deployed in the ArgonCube prototype detectors.

Q-Pix: Another approach to pixelated LArTPC readout is the Q-Pix design. The Q-Pix approach aims at low readout thresholds, vast reduction in data rates, and maximizing the protection against single point failures. The design explicitly targets an underground environment, such as a DUNE far detector, where most of the time there is nothing of interest happening, but you need to be able to instantly capture any signals coming above threshold. Technical details are available in [10], and impacts on the physics performance of pixel-based detectors vs. wire readout have been studied in [11] and [12].

Consortia of institutions have formed around advancing the LArPix and Q-Pix designs for pixel charge readout, and in a joint Snowmass submission these groups advocate for a coherent R&D collaboration to achieve the scalable designs needed for future large-scale LArTPC detectors [13].

Multi-modal Pixels: One challenge presented by pixel-based charge readouts is that the anode is then opaque, preventing the standard approach (in wire-based TPCs) of detecting scintillation light from behind the anode plane. One rather elegant solution would be a pixel plane that is simultaneously sensitive to both VUV photons and charge, and R&D is ongoing [14]. Figure 3 shows a basic concept starting from the Q-Pix pixel design. A central pixel is sensitive to ionization charge, but there is an additional material coating on the pixel plane that converts VUV light also to charge, and then the same (or similar) electronics reads out the signal from the photoconverted charged. Further R&D is needed to produce a viable design, but such a dual mode pixel system would be an important advance for TPCs.

Electron Multiplication: Another potential enhancement to charge readout in large LArTPCs that is under development involves multiplication of the drifting electrons before the amplification stage of the readout electronics [14]. The goal of such multiplication is to improve the energy sensitivity of a large LArTPC to very low-energy physics signals down to the keV scale. Multiplication has been used previously in gaseous TPCs, and an R&D effort has been initiated to pursue controlled and stable

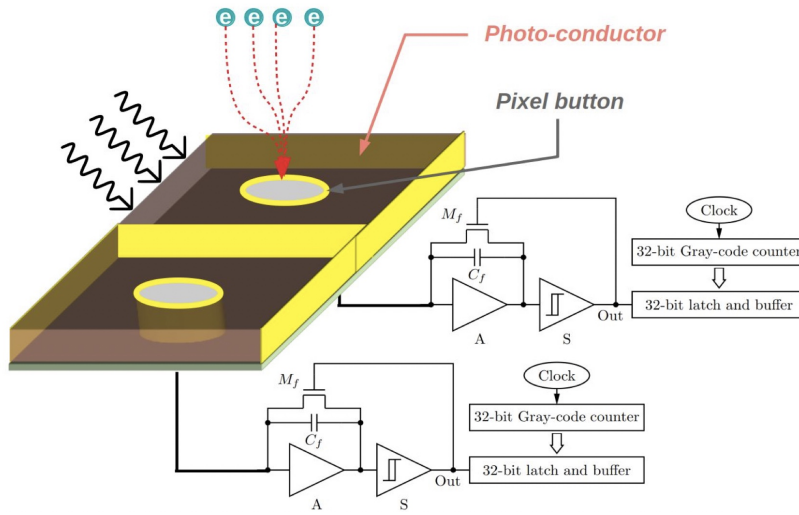


Figure 3: Q-Pix pixel readout combined with a photoconducting material coating could lead to a pixel system that is simultaneously sensitive to ionization charge and VUV photons.

electron proportional multiplication of drift electrons directly in liquid argon. The approach consists of using sub-micrometric anodic electrodes, a scaled down version of the geometries successfully adopted in gaseous TPCs, in order to generate a local electric field large enough (> 100 kV/cm) to trigger the proportional multiplication of charge carriers. Different anode geometries are being explored in a controlled test-stand to quantify gain at different strengths of the electric field, and a simulation toolkit capable of studying the potential for amplification in a variety of anode geometries has also been developed, with promising results. Transitioning from proof-of-principle demonstrations with simplified anode geometries to scalable readout sensors, and appropriate readout electronics, will require continued R&D going forward.

Dual Readout (ion detection): The dual-readout TPC concept refers to a high pressure gaseous TPC capable of collecting charge from both the ionization electrons at the anode and the positive ions at the cathode. Due to the lack of diffusion effects on the heavier ions, the use of positive ions collected at the cathode would push the intrinsic physical resolution of such a chamber in the 10-100 micron region. The challenge associated with this scheme is the development of a sensor that can reliably detect slow positive ions with the required granularity. Possible technology solutions are discussed in [15]. Detection at micron-scale pitches in large detectors has the potential to push dark matter detection under the neutrino floor and could enable an exploration of ν_τ interactions, which is essential to testing the unitarity of the neutrino mixing matrix.

2.1.2 Dopants to Increase Charge Yields

When energy is deposited into liquid argon (LAr), it is split between ionization and scintillation signals. In pure LAr at a fixed electric field, the ratio of ionization to scintillation depends on the amount of energy deposited. For low energy, stopping particles, or very heavy particles, understanding the fraction of energy that creates scintillation light is critical for reconstructing the particle's energy. The NEST Collaboration [16] has shown that LArTPCs can improve the energy reconstruction of MeV-scale electrons by augmenting the charge measurements with a light collection efficiency near 50%. Collecting 50% of the scintillation light in a large LArTPC is challenging due to the large detector size, isotropic emission, and the requirement to wavelength shift the light. A different concept has been proposed in Refs [17] and [18], which is to dope the LAr with a photosensitive dopant [19, 20],

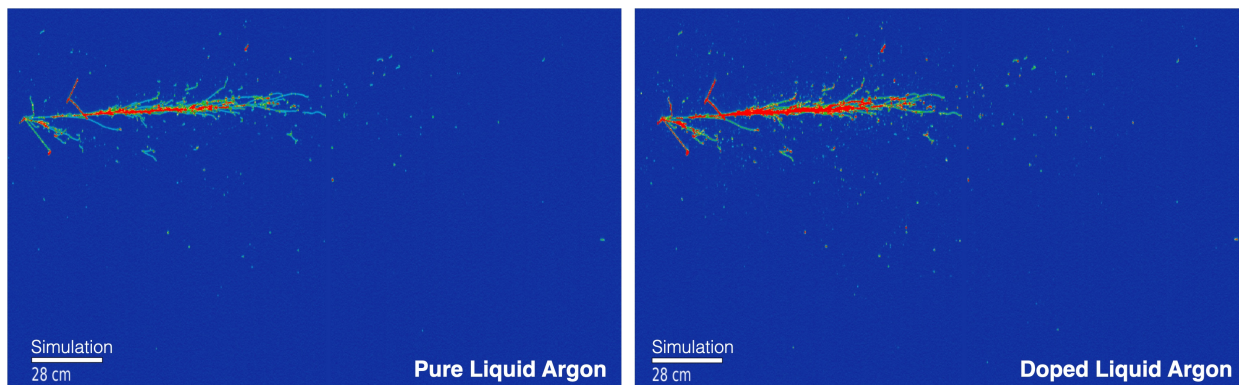


Figure 4: A simulation of a GeV-scale electron antineutrino simulated in (left) pure LAr and (right) with a photosensitive dopant. This simulation utilizes the LArSoft [21] simulation framework, and the photosensitive simulation converts the number of scintillation photons into ionization charge at the point of creation. This conversion leads to larger signals, a more linear detector response, and enables the visualization of a larger amount of soft deposits from neutron and low energy photon scatters.

which directly converts the isotropic scintillation signal to a directional ionization signal with high efficiency, with estimates up to 60% [19]. Recently, the capabilities of LArTPCs with extended MeV-scale energy resolution have been explored, and it has been found that LArTPCs could, with a few R&D advances, reach normal-ordering sensitivity to neutrinoless double-beta decay with xenon doping and the introduction of these photosensitive dopants [17].

The introduction of photosensitive dopants would lead to an enhanced ionization signal, especially where scintillation signals are large. This is expected to improve the energy reconstruction of low-energy signals [16, 17]. It would also lead to a more linear detector response for highly quenched processes. Together these would lead to an improved reconstruction of alpha particles and low-energy protons. When looking toward GeV-scale neutrino interactions, these improvements could lead to improved neutrino energy reconstruction by improving vertex energy reconstruction, neutron and low energy photon reconstruction efficiency, and shower energy reconstruction, as well as reducing thresholds. These gains in LArTPC GeV-scale performance coupled with the MeV-scale enhancements highlight the need for a robust R&D program to enable this technique for use in large LArTPCs. The four primary areas of focus of such R&D would be (1) understanding the optimal doping strategy at the MeV and GeV scales, (2) understanding the impact of dopants on long term detector stability, (3) understanding the triggering and timing of a LArTPC with limited scintillation information, and (4) studying if any light survives the photoconversion process [22].

2.1.3 Optical TPCs and the ARIADNE Program

The ARIADNE program is dedicated to the development of optical readout of dual-phase LArTPCs, as a cost-effective and powerful alternative approach to the existing charge readout methodology. As first demonstrated in the 1-ton dual-phase ARIADNE detector, the secondary scintillation (S2) light produced in THGEM holes can be captured by fast TimePIX3 cameras to reconstruct in 3D the primary ionisation track.

The operation principle of a dual phase optical TPC read out with a TimePIX3 system is shown in Figure 5. When a charged particle enters the LAr volume it causes prompt scintillation light (S1) and ionisation. The free ionisation electrons are drifted in a uniform electric field to the surface of the

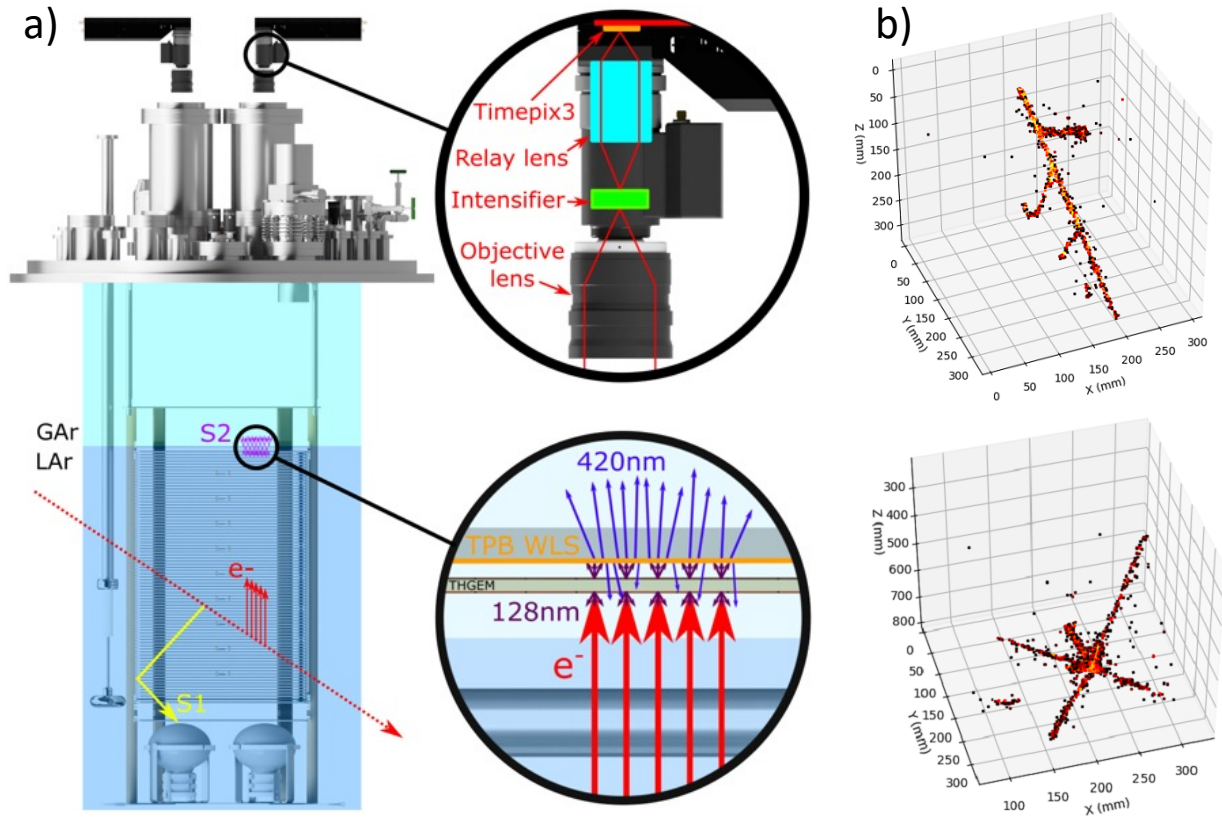


Figure 5: a) Detection principle of dual phase optical TPC readout with TimePIX3 camera, first demonstrated in the 1-ton ARIADNE detector. b) LAr interactions from cosmics. Figures taken from [23] and [24].

liquid. A higher field induced between an extraction grid and the bottom electrode of the THGEM extracts the electrons to the gas phase. Once in gas, the electrons are accelerated within the $500\ \mu\text{m}$ holes of the THGEM at a field set between 22-31 kV/cm. As well as charge amplification, secondary scintillation (S2) VUV light is produced. The light is shifted with a TPB coated sheet to 430 nm and then detected by cameras mounted on optical viewports above the THGEM plane.

Originally optical readout was tested with EMCCD cameras within the 1-ton ARIADNE detector at the T9 charged particle beamline at CERN [23] and later was upgraded with fast TimePIX3. Within the TimePIX3 camera assembly, a lens coupled to a Photonis Cricket image intensifier ($\approx 33\%$ quantum efficiency at 430 nm) boosts the S2 light signal. The amplified photons hit light sensitive silicon, bump bonded to a TimePIX3 chip ($55\ \mu\text{m}$, 256×256 pixel array). The camera measures simultaneously 10-bit Time over Threshold (ToT) and Time of Arrival (ToA); ToT allows accurate calorimetry and ToA gives accurate timing (1.6 ns resolution). The TimePIX3 chip then sends a packet containing 4 pieces of information: x and y pixel position, ToA (z) and ToT allowing for full 3D reconstruction using a single device. The camera provides a “Data driven readout” where pixels are read out asynchronously allowing for very efficient sparse readout; the maximum readout rate is 80 Mhits/s. The high readout rate, natively 3D raw data and low storage due to zero suppression make TimePIX3 ideal for optical TPC readout.

The TPX3camera system was first tested in low pressure CF₄ gas within the ARIADNE 40 l TPC prototype [24]; following this demonstration, a TimePIX3 camera was mounted on ARIADNE and

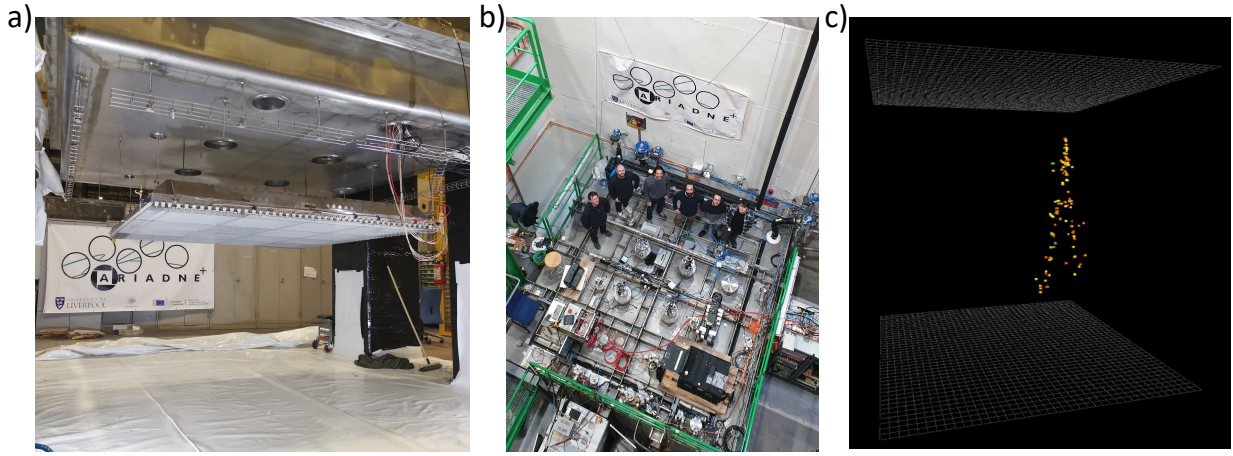


Figure 6: a) The LRP under the cryostat lid. b) The ARIADNE+ team on top of the cryostat. c) A LAr interaction.

particle tracks from cosmic showers were successfully imaged in 3D for first time (see Figure 5) [25]. The cameras are shown to be sensitive even to pure electroluminescence light generated at the lower end of the THGEM field; this mitigates difficulties often faced when trying to operate THGEMs at a higher field where there can be issues with stability. Use of cameras has additional benefits such as ease of upgrade as they are externally mounted, they are decoupled from TPC and acoustic noise and as, large areas can be covered with one camera bringing cost and operational benefits.

In order to demonstrate this technology further and at a scale relevant to the 10 kton DUNE detector modules, a larger-scale test (ARIADNE+) was proposed [26] and recently performed at the CERN Neutrino Platform. Four cameras, each imaging a 1 m x 1 m field of view were employed of which one utilised a novel VUV image intensifier negating the need for wavelength shifter. The test also showcased a light readout plane (LRP) comprising of 16, 50 x 50 cm glass THGEMs supported within an Invar welded structure. The novel manufacturing process for the glass THGEMs allows for mass production at the large-scale [27]. Successful, stable operation was achieved, and cosmic muon data were collected from both the visible and VUV intensifiers showcasing optical readout technology in combination with a novel glass THGEM array. An image of the detector setup is shown in Figure 6 and publication is pending.

2.1.4 Scintillation Detection in LArTPCs

The LAr is known to be an abundant scintillator: it emits about 40 photons per keV of energy deposited by minimum ionizing particles. The scintillation proceeds through the formation of the excited dimer Ar_2^* and in particular the photons are emitted by the de-excitation of the lowest lying singlet and triplet states $^1\Sigma_u$ and $^3\Sigma_u$. The transition from the $^1\Sigma_u$ state to the dissociative ground state ($\text{Ar} + \text{Ar}$) is very fast ($\tau_{fast} \sim 5$ ns) while the transition from the $^3\Sigma_u$ is much slower, being prohibited by the selection rules, and has a characteristic decay time of $\tau_{slow} \sim 1300$ ns [28]. The time evolution of LAr scintillation light can be described as the sum of two decaying exponential functions:

$$L(t) = \frac{A}{\tau_{fast}} e^{-\frac{t}{\tau_{fast}}} + \frac{B}{\tau_{slow}} e^{-\frac{t}{\tau_{slow}}} \quad (1)$$

where $A+B = 1$. The relative abundance of the fast to slow components depends heavily on the type of particle that caused the excitation and is 0.3 for electrons, 1 for alphas and 3 for neutrons. This property of LAr is responsible of its exceptional pulse shape discrimination capability that is extensively used by DM experiments to discard γ/e^- and α background over neutron-like WIMPs (Weakly Interacting Massive Particles) signals.

The fast component is often used for triggering purposes and for determining the time of occurrence of the event (t_0 time) that is fundamental in LArTPC for position and calorimetric reconstruction. Scintillation light is also used to perform calorimetric measurements eventually in combination with charge detection.

Unfortunately LAr scintillation spectrum lies in the Vacuum Ultra Violet (VUV) region of the electromagnetic spectrum: it is a 10 nm band centered around 127 nm. This complicates its detection because common cryogenic photo-sensors have glass or fused silica windows, which are not transparent to these wavelength.

The most common paradigm for LAr scintillation light detection is based on the down conversion of VUV photons into visible ones by means of a wavelength shifter. Widely used shifters are TetraPhenyl Butadiene (TPB) and para-Terphenyl which absorb 127nm photons and re-emit around 430nm and 350nm, respectively. Down converted photons are then eventually collected with photo-collectors (ARAPUCA, light guides, optical fibers) and detected with cryogenic photo-sensors (PMT, SiPM, APD, CCD...)

The most commonly used cryogenic photo-sensors in LArTPCs in the last years are the photomultiplier (PMT), however, a new generation of photo-sensors based on silicon technology (APD, CCDs, and SiPMs, in particular) has been developed and is actually promising to surpass the PMTs in the next few years. This technology is growing fast, driven by applications in communications and medicine and by the competition among many producers. These devices are mainly constituted by a Si wafer, few electrical connections, an optical window and an almost inessential packing. The overall amount of material is on the order of grams and sensors can be manufactured with more or less any desired level of radio-purity. They do not need HV and have detection efficiencies comparable or better than those of the most performing PMTs. These are ideal devices to be coupled with cryogenic noble liquids because their performances strongly increase at low temperature (dark counts at the level of few Hz). SiPMs in particular have a gain per single photo-electron comparable to that of PMTs, and allow single photon counting in principle without amplification.

2.1.5 The ARAPUCA Light Collector

Detecting light in LAr and specially in a strong electric field like the one needed to operate a Time Projection Chamber (TPC), can be difficult with a standard PMT. A new approach consist in the development of ARAPUCAs [29], which are light traps built out of short pass dichroic filters and wavelength shifters. The dichroic filter is a multilayer film, that has the property of being highly transparent for wavelength below a certain cutoff and highly reflective above it. The device is a flattened box with highly reflective internal surfaces. The open side hosts the dichroic filter that is the acceptance window. The filter is deposited with two shifters – one on each side.

LAr scintillation light is shifted by the external shifter (paraTerphenyl - PTP) from the ultraviolet (127nm) to 350nm (emission wavelength of PTP) and passes through the filter. On the internal side

the second shifter (TetraPhenyl Butadiene - TPB, emission wavelength around 430nm) absorb 350nm photons and down-converts them to a wavelength above the filter cutoff. In this way the internal side of the filter becomes reflective to re-emitted photons and the photon is trapped inside the reflective cavity of the ARAPUCA. After some reflections the light will be eventually detected by the array of SiPMs installed on the internal surface of the ARAPUCA. The working principle of the ARAPUCA is illustrated in Fig. 7(a))

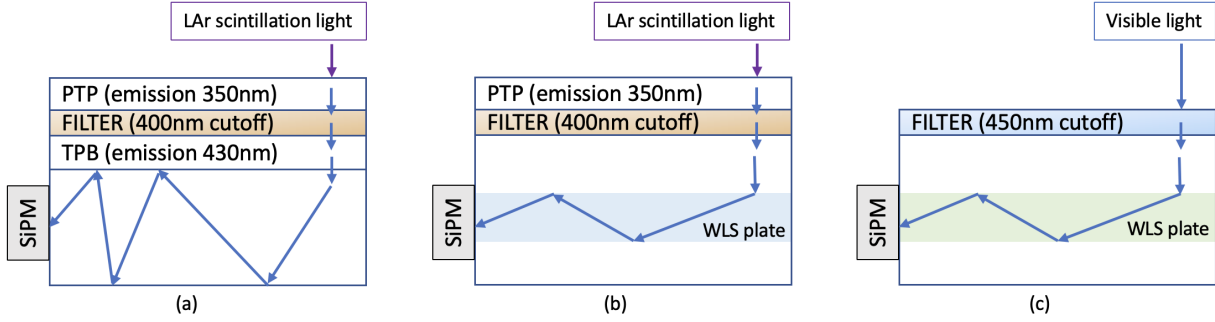


Figure 7: a) Working principle of the ARAPUCA device. b) X-ARAPUCA for LAr scintillation light. c) X-ARAPUCA for visible light.

The coupling of the passive ARAPUCA photon trap with SiPMs has the advantage of increasing their effective area since trapped photons have more than one chance of hitting the SiPM sensitive surface. The ARAPUCA validation program has demonstrated an amplification factor of the effective SiPM area around 4.

The ARAPUCA technology was proposed to be used in the far detector of the DUNE experiment in 2016 and was extensively tested during the first run of protoDUNE (CERN2018-2020) [30]. An evolution of the ARAPUCA device, the X-ARAPUCA [31], has been chosen as the baseline choice for the Photon Detection system of the DUNE far detector in 2019. The X-ARAPUCA also make part of the photon detection system of SBND experiment.

The X-ARAPUCA represents an optimization of the ARAPUCA design. In this case, the second wavelength shifter (deposited on the internal side of the filter) is replaced with a light guide in form of a plate, doped with a secondary shifter, see Fig. 7(b). This design has the advantage of increasing the trapping efficiency with respect to an ARAPUCA, since a fraction of the photons converted inside the light guide suffers total internal reflection and is guided towards the edge of the plate, where the SiPM are installed. In addition, the construction of the device is simpler and the production is faster, since it is necessary to evaporate just one side of the dichroic filter.

Some experiments may want to detect the visible component of light as well. In this case, a type of X-ARAPUCA specific to this need can be developed. This is the case of the SBND experiment which, in addition to VUV photons, can also detect visible photons converted by TPB deposited on reflective foils installed on the cathode of the experiment. The X-ARAPUCA for visible light is showed in Fig. 7(c)).

The X-ARAPUCA has been demonstrated to have a detection efficiency 30% higher than the standard ARAPUCA in several experimental tests [32] and [33].

The X-ARAPUCA represents the baseline choice for the two modules of the DUNE far detector.

The TPC of the two modules have different designs and use different charge read-out technologies: traditional wires for far detector one (also referred as horizontal drift) and printed PCB for far detector two (vertical drift). The differences in the designs of the TPC are also reflected on the geometrical shapes of the X-ARAPUCA modules: those for far detector one are in the form of bars (210 x 10 cm, see Fig. 8(a)), while those for far detector two are squares (60 cm x 60 cm, see Fig. 8(b)).

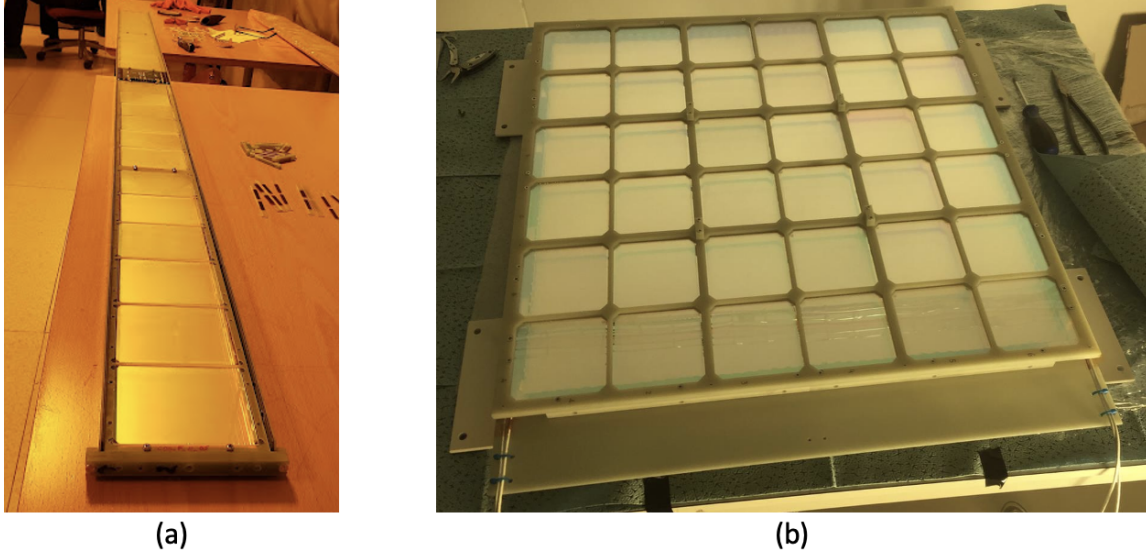


Figure 8: a) X-ARAPUCA photon detection module of DUNE far detector one (horizontal drift). b) X-ARAPUCA photon detection module of DUNE far detector two (vertical drift).

The ARAPUCA and X-ARAPUCA devices were proposed for large LArTPC detectors with the idea of improving the response to low energy events, such as supernova neutrino bursts and solar neutrinos. However, the use of the ARAPUCA technology is not limited to Liquid Argon detectors and can be extended to other areas, such as, for example, Cerenkov and Water Cerenkov detectors. A dedicated R&D program is currently investigating the optimization of the optical components of the X-ARAPUCA for the detection of Cerenkov radiation produced in water by cosmic particles. This program, called C-ARAPUCA, is developing specific dichroic filters, waveshifting plates and SiPMs for this application.

2.1.6 Dopants to Increase Photon Yields

LAr is a particularly bright scintillator, with around 40,000 photons/MeV with no electric field, and with excellent discrimination between β s and heavier particles. Because the scintillation light is very short, at 128 nm, it needs to be wavelength shifted to be detected by PMTs or SiPMS, and the wavelength-shifter of choice is usually TPB. Adding Xe to the LAr, however, shifts the light in advance of getting to the TPB, overall increasing light yield. The DUNE Collaboration has performed a large-scale demonstration of the effect by adding Xe to the ProtoDUNE-SP prototype at CERN's Neutrino Platform [34]. The fact that the shifted light tends to be the LAr triplet state also means that one might be able to do pulse-shape discrimination using spectral discrimination.

2.1.7 Simulation and Calibration in LArTPC Neutrino Detectors

Scintillation light detectors at LArTPC neutrino experiments are often used for timing measurements and triggering on non-beam events (e.g. proton decay). Additionally, they may provide better energy measurements when combined with ionization data from the TPC. In all of these applications, there

must be precise understanding of initial scintillation light yields, effects of Rayleigh scattering, and light detector acceptance and quantum efficiency beyond what current measurements can provide. The simulation of the optical signal is usually divided in a few steps. The simulation of passage of particles through argon (GEANT4, FLUKA, ...) yields the amount of energy deposited along the particle path. Starting from it, a sequence of steps decides which fraction turns into scintillation light and how many scintillation photons, where they end their life ("propagation"), and if they convert into a signal in a photodetector. The simulation of their electronics signal follows.

The deposited energy contributes to both scintillation and ionization, and these two processes compete against each other. Relevant physics parameters includes the electric field and the electron-ion recombination model and parameters. While simple models featuring their anticorrelation are already in use, work is ongoing by the NEST collaboration to extend to liquid argon the results already delivered for liquid xenon detectors. The standard approach includes two scintillation times, 1.6 μ s and 6 ns, although hints of a third scintillation time have appeared.

The propagation of scintillation light can in principle be performed via detailed photon-by-photon simulation. Relevant physics parameters include the scattering and absorption lengths in liquid argon, the refraction index and group velocity of the light, and the optical properties of the surfaces in contact with argon. While possible, this approach to simulation is deemed too computing-intense to be performed individually for each of the million photons (similarly to the ionized electrons drifting to the anode), and parametrizations are commonly in use mapping each position in the detector to the fraction of photons reaching each photodetector and their arrival time. The first practical approach to the problem is to finely dice the detector volume and to represent the mapping in a precomputed discrete table with one cell per small volume. This soon hits computational limitations when large detector volumes need to be covered. Conversely, simple physics-based parametrizations are cheaper, but often inadequate in at least some regions. Good promise is shown by hybrid approaches that attempt to decouple geometry effects, simpler to describe analytically, from light interaction effects, reducing the space where the latter need to be mapped. These techniques fail to describe the visibility of regions with little or no line of sight to the optical detectors, where physics effects dominate. Such limitation is relevant in configurations with optical detectors outside the active TPC volume, while they do not concern light-hermetic LArTPC modules. Another alternative approach is being studied using machine learning techniques[SIREN] that tune an existing map from simulation using actual detector response to long tracks. This technique achieves a compact description of the mapping, and also improves its quality. The commonly used photodetectors are not sensitive to the argon scintillation wavelength (128 nm), so somewhere in the path a wavelength shift needs to happen. The relevant parameters, mainly the conversion efficiency, depend not only on the wavelength shifting material, but also critically on its deployment on the surfaces. This requires dedicated measurements specific to each detector design. An aspect often neglected by the simulation is the 50% of visible light which is emitted back into argon by the wavelength shifter coating a photodetector. In detectors using photomultipliers with curved cathode there can be a direct optical path connecting their sensitive areas, enhancing the chance of one illuminating the other. If the photodetection system is sensitive to different wavelengths, multiple maps will be needed, one describing each of them. Such setups can be chosen to resolve light reflecting on the far surface of the detector (like in SBND) or light scintillating from other materials (like in xenon doping).

The simulation of the photodetector response is very specific to the detector itself. In general, in the signal formation both the amount of charge and its time distribution need to be correctly simulated: seeking a time resolution at nanosecond level requires a careful characterization of the setup which is

typically included as part of the detector calibration.

Simulation of readout electronics features most of the aspects common to the one for the TPC charge. While the number of channels in the optical detector readout is significantly lower than the TPC counterpart, the requirement of nanosecond time resolution imposes a significantly higher sampling rate. As a result, full readout for the optical detector is no more possible than for the TPC charge, and data reduction techniques (selective readout, including lossy compression) need to be applied, and simulated. One special aspect arises in experiments whose the trigger is based on the optical detection system, which is a common feature because of its prompt response, and where the trigger signal is used to determine a selective readout. For example, a large detector may decide to read out channels only in an area close to where activity is being noticed. In such cases, the readout simulation effectively requires a trigger simulation as well, and the two are in fact intertwined.

The capability of the present and upcoming LAr-TPC based neutrino physics detectors in reaching their required precision in particle tracking and calorimetry is based on the performance and precision of the detector models for simulation and reconstruction, and therefore on the capabilities of calibration techniques. Due to the size of neutrino detectors and the long data-taking times, an essential component of a calibration program is the measurement and validation of spatial and time variations, both of low-level detector description parameters – efficiency of ionization charge and scintillation light detector components, uniformity of electric field and drift velocity, electron diffusion, lifetime and recombination – and high-level detector performance metrics – trigger efficiency, track and cluster reconstruction efficiency and uncertainties, energy resolution and scale uncertainty, for different particle species.

Natural sources, such as cosmic ray muons or natural radioactivity, are extensively used, for instance in MicroBooNE [35] and the DUNE prototype ProtoDUNE [36] at CERN. Samples of stopping charged particles, typically muons and protons, are used to measure the recombination model parameters and a work function scaling [37], both needed for the absolute energy scale. The calibration of the electromagnetic energy scale can typically be done with Michel electrons in the tens of MeV range or, at higher energies, with π^0 decay samples [38], whether from cosmic ray or beam events. Through-going muons can be used to map the detector efficiency, including the effect of electric field distortions from space-charge [39] or to measure electron lifetime [40].

However, the use of cosmic ray muons presents limitations when the detectors are placed deep underground. For this reason, calibration methods based on UV laser ionization, external neutron pulsed, or the "classical" deployment of radioactive sources, are being actively pursued [41].

Since several decades, argon gas TPCs have been calibrated with ionizing laser beams [42], and more recently the technique has been further developed for use in liquid TPCs [43–45]. The method is based on employing UV laser beams intense enough to ionize the LAr, directed at various locations in the TPC via steerable cold mirrors. It was first employed in a large detector in MicroBooNE [46], where detailed electric field distortion maps were carried out [47]. Due to the underground location, DUNE is also planning to use UV lasers to calibrate the far detectors [41], and a prototype system will be installed at ProtoDUNE-II at CERN [48], where additional measurements, based on charge and not just position, will be tested.

Other recent ideas for LAr TPC calibration include the use of external neutron generators creating pulses that propagate into the detector. Due to an anti-resonance [49] where the cross-section for

neutron scattering in LAr is quite low and to the small energy loss per scatter, the travel range for neutrons in LAr is large. Therefore, only a few well-shielded commercial neutron DD generators installed on a few locations outside the cryostat are enough to cover a large fraction of a large detector such as DUNE. The capture of neutrons in ^{40}Ar leads to a 6.1 MeV (total) gamma ray cascade [50], allowing the calibration of the energy range relevant for Supernova and solar neutrino physics. Initial encouraging tests were carried out at ProtoDUNE-I, but further development is upcoming in ProtoDUNE-II.

2.1.8 Gaseous Argon TPCs

In the DUNE near detector complex [51], one of the detectors will be a high-pressure gaseous-argon time projection chamber (HPgTPC) surrounded by a calorimeter and a magnet (ND-GAr) [52]. In the direction of the neutrino beam, ND-GAr will be positioned downstream of a modular liquid-argon time projection chamber (ND-LAr). ND-GAr can complement ND-LAr by reconstructing the momentum and sign of charged particles ranging out of ND-LAr [53]. ND-GAr will also collect its own independent sample of neutrino interactions on argon, offering a unique cross-section and BSM physics program. In particular, due to its lower detection threshold than a liquid argon TPC, ND-GAr's HPgTPC will be able to reconstruct low energy pion and proton tracks and constrain uncertainties in the oscillation analysis by pinning down neutrino-argon interaction models [52]. HPgTPC is also less likely to confuse primary and secondary interactions since secondary interactions are rare in the lower density gas detecting medium [52]. This makes it possible to collect a neutrino event sample with less influence from the detector response and secondary interaction models [52]. Additionally, ND-GAr's excellent PID capabilities will allow it to constrain backgrounds to achieve a strong BSM reach [52]. While much of ND-GAr's baseline design takes advantage of the ALICE TPC and the CALICE calorimeter designs, there are some optimizations that need to be done to adapt the designs for the DUNE near detector environment [52]. Dedicated and novel R&D efforts, including gas-mixture studies, light collection studies, charge readout, electronics and data acquisition development, high voltage studies, and detector calibration, are underway to optimize the designs and explore new technological developments [52]. These efforts will offer DUNE the opportunity to expand its capabilities.

2.1.9 Low-Radioactivity Argon

Argon from underground sources, depleted in ^{39}Ar and ^{42}Ar , has been important for the current and next-generation argon dark matter experiments [54, 55]. Recent interest has been in using these underground sources within the neutrino frontier to fill next-generation detectors such as Coherent or a low background DUNE module [7, 8] or to provide shielding for neutrinoless double beta decay experiments such as LEGEND. Experiments targeting sub-MeV signals are sensitive to both ^{39}Ar and ^{42}Ar , while MeV-scale experiments are sensitive primarily to the decay progeny of ^{42}Ar .

^{39}Ar decays primarily via a beta with a $Q_\beta = 565$ keV and a half-life of 269 years. This large rate of counts can overwhelm rare process searches and lead to challenges with multisite tagging due to pile-up. In a liquid argon detector filled with atmospheric argon, there is a 2% chance that a ^{39}Ar will decay within 32 cm of any arbitrary point within the detector. ^{42}Ar decays via a beta decay with a 599 keV endpoint and a half-life of 33 years. This decay also produces the radioactive isotope ^{42}K , which beta decays with $Q_\beta = 3.5$ MeV and a cascade of de-excitation photons with a half-life of 12 hours. This long half-life means that coincidence tagging would be unreliable, and the high Q_β falls across many critical regions of interest for MeV-scale physics searches. In the atmosphere, the ^{39}Ar isotope is primarily produced through cosmogenic spallation, leading to 1 Bq/kg concentrations [55].

^{42}Ar is less easily produced, requiring the fusion of two neutrons into the stable ^{40}Ar [56], and the atmospheric argon level is $92\ \mu\text{Bq/kg}$ [55, 57].

DarkSide-50 has demonstrated a depleted underground argon source for a dark matter search. The argon was extracted from a commercial CO_2 gas stream, and after deployment in the detector, ^{39}Ar levels were reduced by a factor of 1400. ^{42}Ar was found to be below detection levels. Recent calculations accounting for the reduced cosmic flux level underground estimate this level to be greater than 10^{10} below atmospheric levels [58]. Such reductions are crucial for the next-generation argon dark matter experiments. There is also evidence that the underground argon stream was contaminated by an air leak during processing, indicating that these measured ^{39}Ar levels are due to residual atmospheric argon so that the ultimate level could be lower. A processing facility (URANIA) is being constructed to process the required amounts for DarkSide-20k and the proposed ARGO (300 tons) next-generation experiments. The maximum production of such a facility is 300 kg/day, which though large enough for these dark matter experiments, is too small to fill a DUNE-scale (10+ ktons) module.

A new facility will be required to provide underground argon at the scale needed for a DUNE module [54]. This will require addressing a number of challenges. A major challenge is finding suitable sources of underground argon. Ideally, a commercial gas stream including a high concentration of chemically enriched underground argon should be identified. PNNL has identified such streams in discussion with a commercial supplier. The producer estimated that 10+ kilo-tonne-scale production might cost as little as a factor of three more than commercially available atmospheric underground sources. Another challenge to address will be monitoring the quality of the argon during production. Low background proportional counters can measure ^{39}Ar levels to approximately 5% of atmospheric levels. The DART liquid argon detector can assay 1 liter of argon to a factor 1000 below atmospheric ^{39}Ar levels, which will be used to check batches of argon for DarkSide-20k production. Alternate indirect methods include searches for associated air contaminants or ^{36}Ar : ^{40}Ar ratios. A final challenge will be the storage of the large amounts of argon to prevent cosmogenic activation before the experiments begin. Calculations for the dark matter experiments show that significant activation requires several years of storage above ground [59].

2.2 Novel Large Liquid Argon Detector Concepts

Opportunities to deploy combinations of new enabling technologies in future large-scale liquid argon detectors are actively being considered by the neutrino physics community. Low-energy physics in LArTPCs is a topic of great community interest, particularly as it would broaden the already exciting program of DUNE. To do just about any physics in LArTPCs below about 6 MeV would require first, shielding for ambient neutrons in combination with extremely low-background materials for the cryostat (ensuring very low (α, n) reactions). In addition, a critically important enabling technology would be production of large quantities of low-background argon, likely through the extraction of underground argon at scales much larger than have been done to date. Underground argon would significantly reduce the levels of ^{39}Ar and ^{42}Ar . Below we describe several current ideas for optimizing large LArTPCs performance at low-energies and expanding the physics reach over first-generation LArTPC neutrino detector designs.

2.2.1 Solar Neutrinos in LAr (SoLAr)

The SoLAr design (see Snowmass white paper [60]) is aimed at measuring physics at the MeV-scale in a large liquid argon neutrino detector, leveraging technological developments to expand the physics

reach of next-generation devices to include solar neutrinos. This novel concept will significantly improve the precision on solar neutrino mixing parameters and will enable observation of the “hep branch” of the proton-proton fusion chain.

The SoLAr technology will be based on the concept of monolithic light-charge pixel-based readout which addresses the main requirements for such a detector: a low energy threshold with excellent energy resolution (7%) and background rejection through pulse-shape discrimination. The SoLAr concept is also timely as a possible technology choice for the DUNE “Module of Opportunity”, which could serve as a next-generation multipurpose observatory for neutrinos from the MeV to the GeV range.

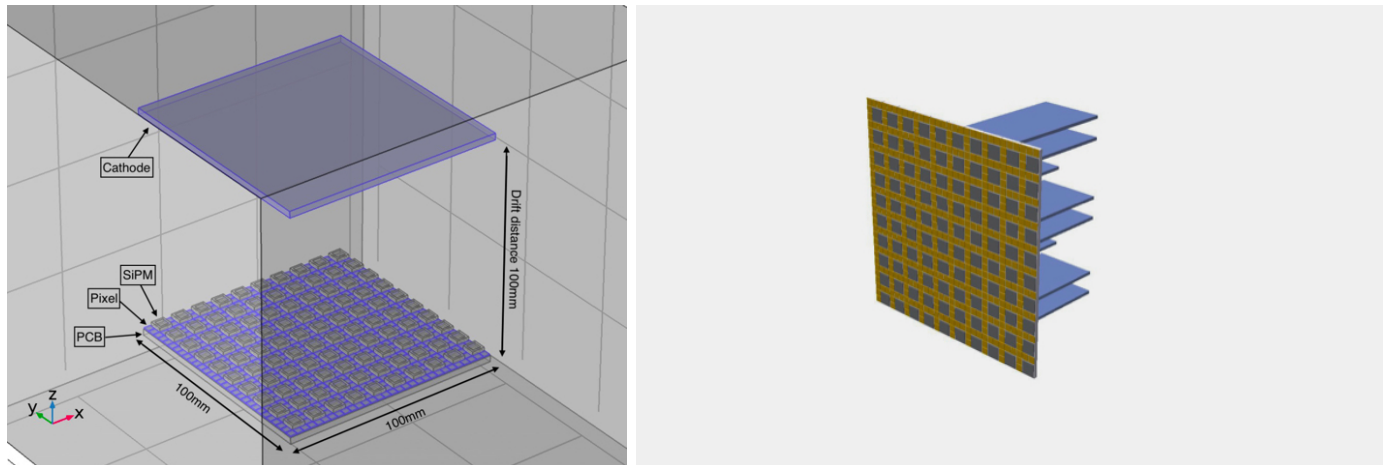


Figure 9: SoLAr detector concept.

The SoLAr readout unit will be a pixel tile in CMOS technology that embeds charge readout pads located at the focal point of the LArTPC field shaping system and collects VUV photons in thousands of microcells operated in Geiger mode. Each monolithic sensor produces analog signals corresponding to the charge of the electrons collected in each pixel and to the photons collected in the pixel frame, respectively. SoLAr leverages the independent technology development of both VUV SiPMs and CMOS pixel readout, combining them to develop a detector technology which is scalable to the multi-kiloton scale.

The goal of SoLAr is to observe solar neutrinos in a 10 ton-scale detector and to demonstrate that the required background suppression and energy resolution can be achieved. To achieve this, SoLAr is adopting a staged approach, building from the current table-top prototype (see figure 9) whose design and assembly is ongoing, to a medium sized demonstrator module.

2.2.2 A SURF Low Background Module (SLoMo)

The possibility of building a low background kTon-scale liquid argon time projection chamber (the SURF Low Background Module – SLoMo), that could be a design for the 3rd or 4th module of the Deep Underground Neutrino Experiment (DUNE), has been explored in [61]. Such a module would allow the physics scope of that experiment to be increased with the addition of several low-energy physics topics, without disrupting the main oscillation physics program. This includes enhanced supernova and solar neutrino sensitivity, and even searches for neutrinoless double beta decay and Weakly Interacting Massive Particle (WIMP) dark matter. The detector design will take as a starting point the standard DUNE vertical drift single phase TPC design [62]. It will be modified with

the addition of an optically isolated inner volume, where fiducialization allows significantly lower background levels, and photosensor coverage can be increased to improve energy resolution. The proposed design is shown in Figure 10.

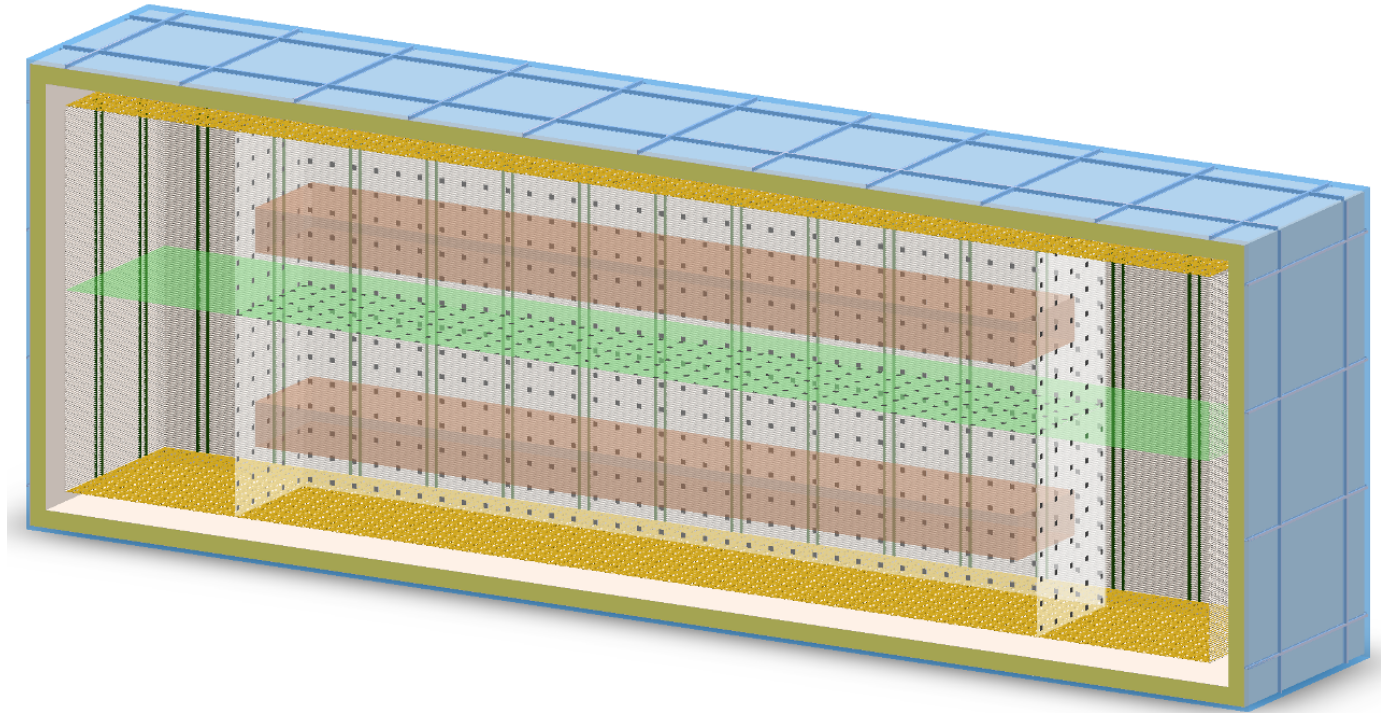


Figure 10: Shown is the baseline design for the proposed low background detector. Blue shows external water “bricks”. The top and bottom yellow planes are the Charge Readout Panels unchanged from the Vertical Detector design. The central cathode is in green. The white box of acrylic (full interior volume) is of dimensions $6 \times 12 \times 20$ ($12 \times 12 \times 60$) m^3 . The black points are SiPM modules shown here at a low coverage of 10% for viewing’s sake. A proposed fiducial volume totaling 2kT is shown in the two beige boxes.

Methods to control radioactive backgrounds have been explored. In particular, the large size of such a module (~ 17 kTons) allows the self-shielding properties of the argon to be exploited and fiducialization of a 1-3 kTon volume allows a radioactively clean central part of the detector to be utilized. Further techniques to control backgrounds that may reach the fiducial volume include:

- External neutrons from the cavern. As first proposed in [63] [64], a 40 cm layer of water shield will reduce external neutrons by a factor 10^3 . Such a water shield could be implemented around the current DUNE cryostat design, within the structural supports.
- Cryostat and detector background. An intensive materials assay campaign will allow selection of construction materials with radioactive backgrounds reduced by a factor 10^3 . Such material purity has been exceeded by a further two orders of magnitude in current dark matter experiments (e.g. [65]). Additional internal shielding can also be added, including neutron absorbers such as boron, lithium or gadolinium loaded cryostat layers.
- Radon in the liquid argon. Active purification of the inner volume and an emanation measurement campaign will reduce radon levels by a factor 10^3 . This factor has been exceeded by current dark matter experiments [66].

- Internal argon-42, argon-39, krypton-85. As demonstrated in DarkSide-50 [67], underground sources of argon can have depleted amounts of critical background isotopes, with ^{39}Ar reduced by a factor 1400. No ^{42}Ar was measured in DarkSide, and reduction factors are expected to be of 10^8 or more. To fill a DUNE-scale detector new sources must be found, and work is underway to identify viable commercial options. Discussion of a future underground argon facility can be found in [54].

The light collection will be enhanced in the inner volume with at least $\sim 10\%$ coverage of SiPM tiles on walls and cathode, additional reflectors on the inner walls and anode collection planes, and additional argon purity requirements. This will allow energy resolution of $\sim 2\%$ at 1 MeV when combined with the TPC charge signal [16] and allow a pulse shape discrimination measurement for background reduction.

A number of important physics topics can be explored with this detector. For supernova neutrino physics lower neutron levels allow the lowering of energy threshold for the search to 600 keV, permitting access to interesting low energy and late or early time information. The reduction in backgrounds allows improvements to the trigger sensitivity, and the detector will be fully sensitive to supernova from the Magellanic cloud. In addition, the increased light collection allows the supernova neutrino $\text{CE}\nu\text{NS}$ interactions within the detector to be measured. For solar neutrino physics lowering the threshold and improving the energy resolution will increase sensitivity to Δm_{21}^2 allowing a precision measurement. This would also improve non-standard interaction constraints or explain the solar anomaly between reactor and solar measurements of Δm_{21}^2 . A precision measurement of the CNO flux is also possible.

Loading the detector with a few-percent of xenon-136 allows a sensitive search for neutrinoless double beta decay beyond the coming ton-scale experiments. As first discussed in [68], the increased light coverage allows pulse shape discrimination to remove electron recoil backgrounds (primarily argon-39) to a WIMP dark matter search through nuclear recoils of at least 100 keV and perhaps just 50 keV. Such a search will be competitive with coming dark matter searches on a reduced timescale. Due to the unrivaled large mass of 3 ktons and a potentially very long DUNE operation of one decade (or even several), this concept can offer a unique seasonal variation detection at sufficient statistical significance for providing a smoking gun signature for the nature of WIMPs. This would be particularly of interest in the case upcoming generation-2 experiments such as LZ, XENONnT and/or DarkSide-20k have evidence for WIMPs near their sensitivity. It would be nearly impossible for the planned generation-3 experiments to make such a smoking gun detection proving the WIMP nature of dark matter.

This concept takes full advantage of the planned DUNE far-detector facilities to create a true multipurpose detector to address important questions in high energy physics, astronomy, and nuclear physics.

2.2.3 Neutrinoless Double Beta Decay with Xe+LArTPC

With several of the exciting enabling technologies described above—underground argon for very low radioactivity, photo-ionizing dopants, and xenon doping in LArTPCs—there is the possibility of performing an extremely sensitive neutrinoless double beta decay search in a DUNE module, as described by Mastbaum, Pshihias, and Zennamo in Ref. [17]. The photo-ionizing dopants improve the energy resolution substantially over exclusive primary ionization and direct photon detection, and by re-using a DUNE module infrastructure costs would be dramatically lower than an entirely new detector.

2.2.4 Detecting Cherenkov and Scintillation Photons in LAr (ArCherS)

Distinguishing Cherenkov and scintillation (C/S) photons is challenging in organic liquid scintillators because the short-wavelength end of the Cherenkov spectrum, where most of the photons reside, is buried by the more intense scintillation spectrum. In contrast, liquid Ar (LAr) scintillates narrowly around 128 nm, leaving the broad Cherenkov spectrum isolated above this wavelength, which is readily detected by common devices such as PMTs. The scintillation photons can be detected with the same devices upon coating their photosensitive surface with a wavelength shifter like TPB. The narrow range of scintillation photons ensures that the uncoated PMTs see purely Cherenkov light. This pure sample of Cherenkov photons can be used to cleanly reconstruct the position, direction, and energy of events from several MeV and above, depending on the PMT photocoverage and efficiency. The photons detected by the TPB-coated PMTs would be primarily from scintillation due to its far greater yield and could be used to independently reconstruct the position and energy of events as low as a few MeV. Using both photon samples together would provide more robust particle ID and reconstruction.

Relative to liquid Ar time projection chambers like those proposed for DUNE, this type of detector would provide the same particle interaction channels while requiring simpler hardware (no charge readout) and event analysis (like a scintillator or Cherenkov detector). Collaborators at Penn and Berkeley are studying the capabilities of a LAr detector to distinguish C/S photons. GPU-accelerated simulations of a large liquid Ar detector with TPB-coated and -uncoated PMTs is performed using the Chroma package and pyrat wrapper.

2.3 Liquid and Gaseous Xenon Detectors

Detectors that use liquid xenon for both scintillation and charge readout—typically as a TPC—have had great success in exploring low-energy physics, particularly for dark matter searches [3, 69, 70] and neutrinoless double beta decay [4].

For dark matter searches, LXe has the advantage of a high cross section and very low backgrounds (no real analog of ^{39}Ar). It is also a better neutron shield than LAr. And liquid detectors lend themselves to large, monolithic designs, which help attenuate external backgrounds like γ rays.

For neutrinoless double beta decay, LXe has similar advantages, although clearly cross section (other than the cross section for neutron scattering) is not relevant. The high density of LXe is, however, important, as it helps to attenuate γ rays even in small volumes. In addition, the apparent anti-correlation of scintillation light and charge [4], helps to provide better energy resolution than simple counting statistics would imply, a fact that is important for searches near the endpoint of the $2\nu\beta\beta$ spectrum, as well as for general background reduction.

Clearly, there are synergies between LXe dark matter detectors and neutrinoless double beta decay detectors, although also significant differences. Dark matter experiments have very low threshold requirements—to see the $\sim 10\text{keV}_{\text{ee}}$ recoils from WIMPs, while neutrinoless double beta decay experiments have low-background (at much higher energies) requirements, which depend in part on requirements on energy resolution that are less critical for dark matter searches.

Nevertheless, it is likely there are many places where LXe detectors can be co-developed, including on low-background materials, veto systems, front-end electronics, etc. This would seem to be a very good opportunity for the Cosmic Frontier and the Neutrino Frontier to work toward common goals.

There are many new ideas for xenon-based detectors for both dark matter and neutrinoless double beta decay. Future ideas for LXe dark matter detectors assume a two-phase detector, where electroluminescence converts drifting charge into photons at a liquid/gas transition layer. Like previous LXe dark matter experiments, the fast scintillation light is used to provide a t_0 that allows position reconstruction of events via timing as well as the pixelization of the electroluminescence photon sensors. Many details of this approach, including its physics program, can be found in Ref. [71]. The two-phase LXe detector described there will also likely be able to measure solar neutrinos, down into the pp energy regime.

For neutrinoless double beta decay, the next-generation LXe detector planned, nEXO [7], is a single-phase detector that detects both light and charge. At the 5-tonne scale, nEXO is part of the Office of Nuclear Physics’ “tonne-scale” double beta decay program.

Looking further ahead, the NEXT experiment plans to use high-pressure xenon gas which, like the ND-GAr detector described above, allows tracking of the two β s emitted in a double beta decay event. The possibility of detecting the barium daughter ion via fluorescence is being actively investigated, as this would be a tremendous reduction in non- $\beta\beta$ backgrounds.

3 Photon-Based Neutrino Detectors

Between the last SNOWMASS and now, there has been an explosion of new ideas and new, enabling technologies that will significantly expand the capabilities of next-generation photon-based neutrino detectors. Detectors that use photons as the primary carrier of interaction information have a long, rich history in neutrino physics, going as far back as the discovery of the neutrino itself. Large-scale, monolithic detectors that use either Cherenkov or scintillation light have played major roles in nearly every discovery of neutrino oscillation phenomena [72–76] or observation of astrophysical neutrinos [73, 77–81]. New detectors at even larger scales are being built right now, including JUNO [82], Hyper-Kamiokande [83], and DUNE [84]. Photon-based detectors have been so successful because they are inexpensive, remarkably versatile, and have dynamic ranges that reach all the way from tens of keV [85] to PeV [81].

The new photon-based technologies that NF10 has surveyed include neutrino physics and astrophysics programs of great breadth: from high-precision accelerator neutrino oscillation measurements, to detection of reactor and solar neutrinos, and even to neutrinoless double beta decay measurements that will probe the normal hierarchy regime. They will also be valuable for neutrino applications, such as non-proliferation via reactor monitoring.

Of particular community interest is the development of *hybrid* Cherenkov/scintillation detectors, which can simultaneously exploit the advantages of Cherenkov light—reconstruction of direction and related high-energy PID—and the advantages of scintillation light—high light-yield, low-threshold detection with low-energy PID. Hybrid Cherenkov/scintillation detectors could have an exceptionally broad dynamic range in a single experiment, allowing them to have both high-energy, accelerator-based sensitivity while also achieving a broad low-energy neutrino physics and astrophysics program. Recently the Borexino Collaboration [86] has published results showing that even in a detector with standard scintillator and no special photon sensing or collecting, Cherenkov and scintillation light can be discriminated well enough on a statistical basis that a sub-MeV solar neutrino direction peak can be seen. Thus the era of hybrid detectors has begun, and many of the enabling technologies described here will make full event-by-event direction reconstruction in such detectors possible.

There were many relevant letters-of-intent and several white papers including one aimed explicitly at these kinds of detectors and their technologies, and far more details can be found in that reference [87].

3.1 Enabling Technologies for Hybrid Cherenkov/Scintillation Detectors

The physics accessible in large Water Cherenkov (WC) detectors such as Super-Kamiokande (SK) is limited in many areas of interest by the inability to detect particles with energy below the Cherenkov threshold. One example is the sensitivity to the Diffuse Supernova Neutrino Background (DSNB) [88] due to backgrounds from low-energy atmospheric neutrino interactions, and reduced signal from the inability to detect positron annihilation, which enhances the prompt signal from the leading reaction $\bar{\nu}_e + p \rightarrow e^+ + n$. Similarly for proton decay, the kaon from $p \rightarrow \bar{\nu} K^+$ is below Cherenkov threshold, and for solar neutrinos the ${}^7\text{Be}$ and CNO neutrinos are practically undetectable as much of the energy from the neutrino electron scattering reaction is invisible.

Organic liquid scintillators (LS) have been used to enhance sensitivity for particles below Cherenkov threshold, and to provide high light yield and thus narrow energy resolution needed to see monoenergetic signals like the 0ν peak in neutrinoless double beta decay. Liquid scintillators also typically allow

excellent discrimination between heavy particles like α s or protons and electrons or γ rays, through the differences in the scintillation time profile. These detectors thus typically aim for a primarily low-energy program, like reactor antineutrinos (KamLAND, Daya Bay, and JUNO), solar neutrinos (Borexino and SNO+), or neutrinoless double beta decay (KamLAND-Zen and SNO+).

Yet the narrow energy resolution and low-energy particle ID of scintillation detectors comes at the cost of the high-energy particle ID possible with Cherenkov light, and the reconstruction of direction from Cherenkov rings which helps identify events from point sources like the Sun. Most high-energy neutrino physics programs—from accelerator beams or atmospheric neutrinos (or nucleon decay)—use ring imaging and counting to eliminate backgrounds.

Hybrid neutrino detectors, which leverage both the unique topology of Cherenkov light and the high light yield of scintillation, have the potential to revolutionize the field of low- and high-energy neutrino detection, offering unprecedented event imaging capabilities and resulting background rejection. Such detectors would be more than the sum of scintillation and Cherenkov physics programs, as the information from one source of light leverages background rejection for physics in the other. One example of this is the rejection of radioactive backgrounds in a low-threshold scintillation measurement of solar neutrinos using direction [89]; another is the rejection of atmospheric neutrino backgrounds to DSNB neutrinos, by counting Cherenkov rings and using the Cherenkov/scintillation ratio to remove mostly hadronic final states [90]. At high energies, it may be possible to use scintillation light to precisely reconstruct the neutrino interaction vertex in a charged-current event, thus helping to eliminate backgrounds from NC π^0 production.

Discrimination between “chertons” and “scintons” can be achieved in several ways, each of which has its own advantages and drawbacks, but which ultimately fall into four broad classes:

- Make chertons easier to see by increasing the Cherenkov/scintillation ratio, typically through suppression of the scintillation light
- Separate chertons from scintons by timing, by using fast photons sensors, or by slowing down the scintillation time profile, or by having a large enough detector that dispersion between “blue” scintillation light and broadband Cherenkov light allows them to be resolved
- Exploiting the differences in the spectra of Cherenkov and scintillation light to distinguish chertons from scintons, either by sorting the photons with devices like dichroicons [91], or using filters on some subset of the photon sensors to exclusively see long-wavelength Cherenkov light.
- Use the angular distribution of Cherenkov light to identify it, through analysis techniques.

Which approach works best depends on many things, including the dominant backgrounds for the physics of interest, cost, development status, robustness, etc. The tensions between them typically contrast the required number of detected Cherenkov photons against scintillation light yield; direction reconstruction against vertex resolution; and backgrounds and robustness of new scintillation cocktails against high costs of new photon sensing or collecting devices. A program of both benchtop R&D, and mid-scale prototypes is underway to help answer these questions. In principle, all of the approaches above could be used in a single detector, as they are for the most part not mutually exclusive.

Below we detail the various enabling technologies for hybrid Cherenkov/scintillation neutrino detec-

tors. Far more detail can be found in the related white paper [87].

3.1.1 Water-based Liquid Scintillator

The development of Water-based Liquid Scintillator (WbLS) [92] has the potential to significantly impact and enhance hybrid particle detection capabilities. WbLS is essentially liquid scintillator encapsulated in surfactant micelles that are thermodynamically stable in water (see Fig. 11). By introducing varying amounts (typically 1%-10%) of liquid scintillator into water, the liquid yield can be adjusted to allow detection of particles below Cherenkov threshold while not sacrificing directional capability, cost, or environmental friendliness. First developed at Brookhaven National Lab (BNL), WbLS is a leading candidate for the main target medium for the proposed THEIA detector, which would enhance the scientific program at the LBNF significantly, as described in the THEIA White Paper [93].

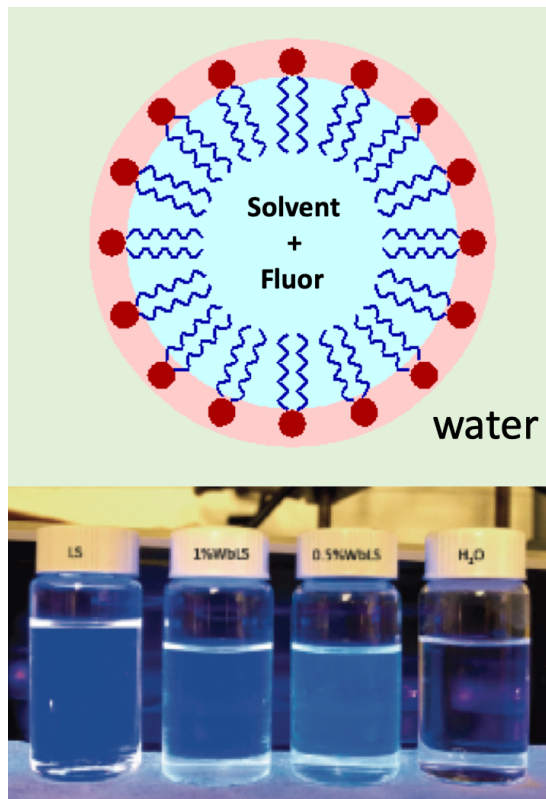


Figure 11: Top: Liquid scintillator encapsulated in a surfactant micelles, which are typically around 10 nm in size. Bottom: From right to left: water, 0.5% WbLS, 1% WbLS, pure liquid scintillator.

3.1.2 Slow fluors

The properties of four slow fluors have been studied in the context of LAB-based liquid scintillator mixtures to provide a means to effectively separate Cherenkov light in time from the scintillation signal with high efficiency. This allows for directional and particle ID information while also maintaining good energy resolution. Such an approach is highly economical (i.e. small compared to other experimental costs) and can be readily applied to existing and planned large-scale liquid scintillator instruments without the need of additional hardware development and installation. Using this technique, Cherenkov/scintillation separation has been demonstrated on a bench-top scale, showing clear directionality, for electron energies extending below 1 MeV.

While the use of slow fluors means that the vertex resolution may be worse than typical large-scale liquid scintillator detectors (but better than typical large-scale Cherenkov detectors), the balance between position resolution, Cherenkov separation purity and energy resolution can be tuned for a particular physics objective by modifying the fluor mixture. This balance is also affected by the presence of fluorescence quenchers, which may be naturally present in the case of loaded scintillator mixtures or could be purposely introduced to change the balance.

3.1.3 Fast Photomultiplier Tubes and LAPPDs

Resolving Cherenkov and scintillation light via timing can be done even with “standard” scintillation cocktails, because the Cherenkov light is created promptly while scintillation light has both a risetime of hundreds of picoseconds and fall types that are in the multi-nanosecond regime, even without intentionally using a “slow” scintillator. In addition, in large detectors, the dispersion of the broadband Cherenkov light means that many Cherenkov photons can arrive at a photon sensor a nanosecond or more before the scintillation light.

In the past decade there have been significant improvements in the time resolution of even standard photomultiplier tubes (PMTs). Hamamatsu, for example, has developed 8” high-quantum efficiency PMTs that have transit time spreads (TTS) with FWHM of around 1.5 ns, or $\sigma \sim 700ps$ [94]. With this kind of resolution, scintillator risetimes of 1 ns or so are slow enough to allow a prompt signal to be seen. Smaller PMTs already have TTSs in the regime of 250 ps or so, and these can be “ganged” together to make larger-area arrays [95].

The most aggressive approach to timing for photon sensors has been the development of Large Area Picosecond Photodetectors (LAPPDs). LAPPDs are 20 cm x 20 cm microchannel plate photomultiplier tubes (MCP-PMTs) [96] now in use by the neutrino community and capable of millimeter-scale spatial resolutions, tens of picosecond sPE time resolutions, and gains exceeding 10^6 [97].

The combination of spatial and temporal information make LAPPDs ideal for Scintillation-Cherenkov separation. The <100 psec resolution of LAPPDs makes it possible to separate between the two components on the basis of timing alone.

3.1.4 Spectral Sorting and Dichroicons

One approach to separating Cherenkov and scintillation light is by discriminating photons by wavelength, as scintillation is typically within a narrow emission band, while Cherenkov is a broad spectrum of light, falling as roughly $1/\lambda^2$.

A simple approach to doing this would be to add filters in front of some subset of the photon sensors in a detector, filtering out the blue scintillation light and allowing longer-wavelength Cherenkov light to pass. This has the advantage of simplicity, and in a detector with low photocathode coverage would be reasonable, if the size of the “red-sensitive” PMTs were large enough to detect enough long-wavelength Cherenkov photons. As the coverage increases however, using filters in front of a subset of the PMTs means that some of the scintillation light is lost, and for physics that requires narrow energy resolution, every photon is important.

Dichroicons, get around this problem by *sorting* photons by wavelength. As shown in Figure 14 below, the dichroicon can follow the off-axis parabolic design of an ideal Winston light concentrator but is built out of a tiled set of dichroic filters. The filters are used to direct long-wavelength light

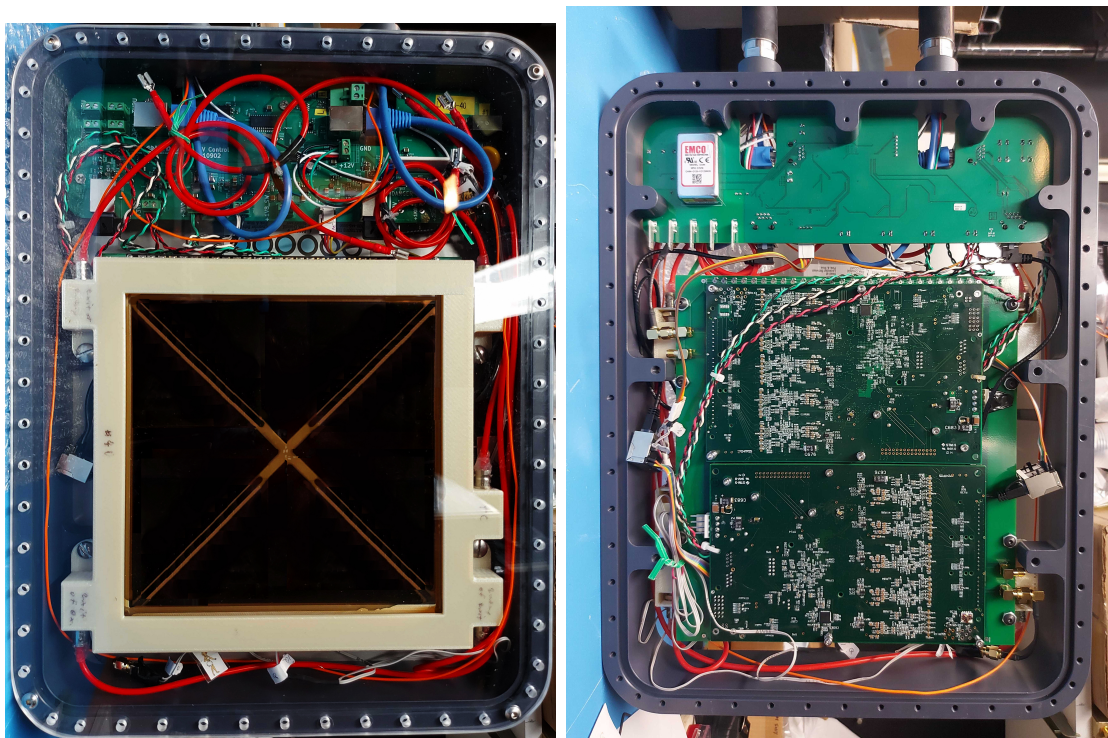


Figure 12: Left: Front view of an ANNIE LAPPD Module. Right: The back of an LAPPD module with the back plate off.

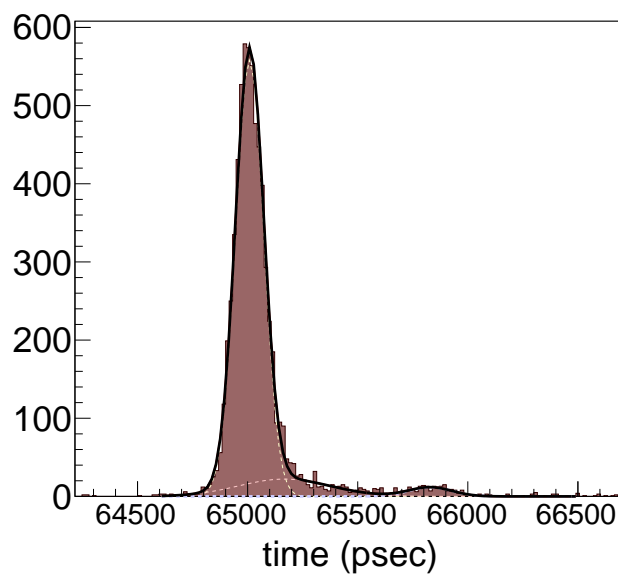


Figure 13: The Transit Time Spread (TTS distribution) for ANNIE LAPPD-25. The time resolution for the prompt pulses is below 70ps, where roughly 30ps of smearing is due to the pulse duration of the diode laser used.

towards a central red-sensitive PMT, while transmitting the shorter wavelength light through the “barrel” of the Winston cone to secondary photodetectors. This is possible because of the remarkable property of the dichroic reflectors, which reflect one passband of light (below or above a ‘cut-on’ wavelength) while transmitting its complement, with very little absorption. As shown schematically

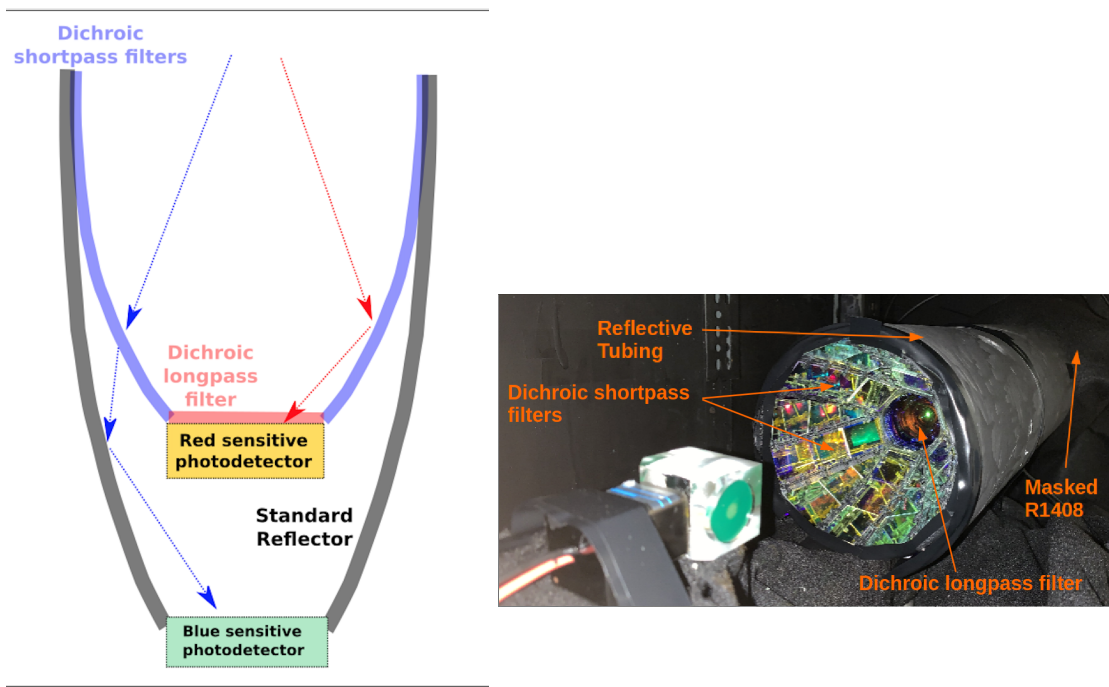


Figure 14: Left: Schematic of a “nested” dichroicon configuration, with shortpass filters on the barrel and a longpass filter at the aperture. Right: Dichroicon in benchtop test setup, viewing ^{90}Sr source embedded in an acrylic block containing LAB-PPO.

in one possible design in Figure 14, the barrel of the dichroicon is built from shortpass dichroic filters (cutoff wavelength near 480 nm) and a longpass dichroic filter is placed at the aperture of the dichroicon. The shortpass filter passes short-wavelength light while reflecting long-wavelength light; the longpass has the complementary response. In the “nested” design shown, the back PMT detects the short wavelength light.

There are many possible configurations of the dichroicon; the ones built to date are not necessarily optimal, and different detectors may have different needs. The nested photon sensor configuration of the design above requires more than one photon sensor and is thus most useful when the available detection area is limited (for example, when the desired coverage is $> 50\%$, or in a segmented detector where each segment is viewed by a single sensor). Simpler designs could simply offset the dichroicon and its aperture PMT, collecting the low-yield Cherenkov photons while allowing the scintillation light to be detected by the rest of the PMT array. Using a pixelated photon sensor, such as an LAPPD or an array of SiPMs, would also work, with the pixels then mapping to different wavelength bands. A complementary design—with Cherenkov light passing through the barrel and scintillation light reflected toward the aperture—might be most useful when ring imaging is a high priority. To achieve more than two passbands, the “nested” design could be extended using multiple dichroicons.

A simulation model of the dichroicon has been developed in *Chroma* (See Section 3.3.1) and calibrated against the measurements of a benchtop prototype, for use in simulating dichroicon performance large-scale detectors. This model was simplified and scaled up to use a 20" diameter large area PMT to collect photons passed by the short-pass dichroic filters, and a cylindrical 5" PMT to collect the long wavelength photons reflected by the dichroic filters shown at the top of Fig. 15. This dichroicon unit was then tiled around a cylindrical volume to simulate a large-scale neutrino detector, seen from the inside at the bottom of Fig. 15. In this model a 50 kt volume of the scintillator LAB with 2g/L of PPO

[10] is surrounded by 90% coverage of simplified dichroicons, which gives effectively 90% coverage of

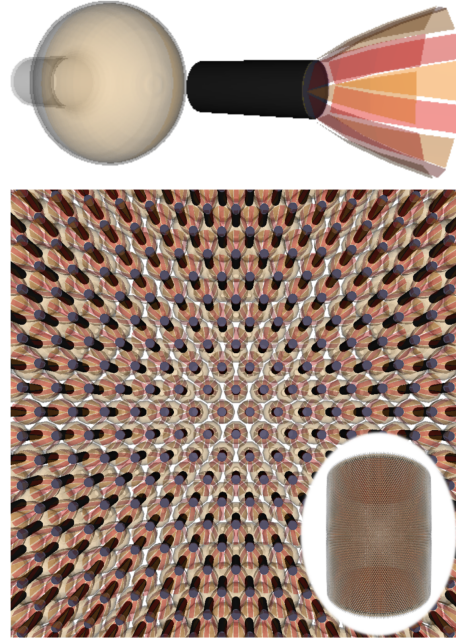


Figure 15: A rendering of the *Chroma* geometry for (top) a dichroicon unit with (left to right) 20" large area PMT, cylindrical 5" long-wavelength PMT, and dichroic filter concentrator, and (bottom) the dichroicon units tiled to create a 50 kt neutrino detector, viewed from inside the detector, with the full cylindrical geometry shown in the inset.

both long and short wavelength photons, as the dichroic filters allow the long and short PMTs share the same solid angle. Using this model, we have begun to evaluate the impact of spectral photon sorting on future neutrino experiments.

A reconstruction algorithm developed in [98] has been modified such that it uses hit time information from all (short and long wavelength) PMTs to perform a position and time fit, and then uses the angular distribution of photons detected on long wavelength PMTs to perform a direction fit.

Alpha particle identification has been explored by simulating alpha and beta particles with the same quenched energy (number of scintillation photons) and inspecting the signal on the long-wavelength PMTs, which are primarily sensitive to Cherenkov photons. A quenched energy comparable to neutrinoless double beta decay in ^{130}Te is chosen to highlight potential background rejection capabilities. The mean number of long-wavelength hits is indeed higher for betas than alphas as shown in Fig. 16 due to Cherenkov production with betas. The detected long wavelength photons from alphas are all scintillation, and indicate that the filters could be optimized for better rejection of scintillation. Fig. 17 shows a clear Cherenkov signal in the hit time residuals of betas at early times, which would allow for discrimination of alphas in a neutrinoless double beta decay region of interest. A similar method provides some discrimination between single and double beta events, as can be seen in the ^{130}Te $0\nu\beta\beta$ plots in Figs. 16 and 17, which could further constrain backgrounds.

3.1.5 Using Angular Information

The ring topology itself can be used to identify Cherenkov photons, essentially by reconstructing events using PDFs in time and angle. The CHESSE array [95] has shown this works for cosmic-ray

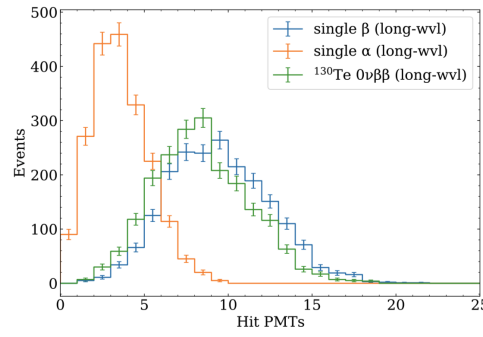


Figure 16: Number of long-wavelength PMTs that detected photons for alpha and beta events with the same quenched energy as ^{130}Te neutrinoless double beta decay, showing alpha/beta discrimination based on Cherenkov photon identification in a 50 kt liquid scintillator detector.

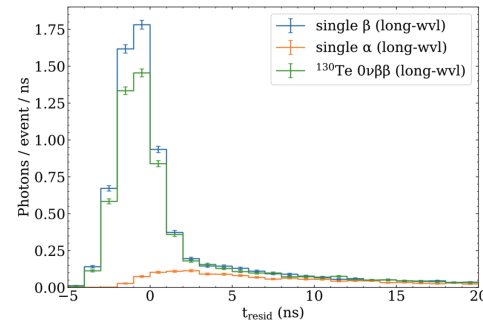


Figure 17: The hit time residuals of long-wavelength PMTs for the events shown in Fig. 16. The Cherenkov is clearly visible at early times for the beta events.

muons, and work with simulations [98] has shown that even at lower energies the separation can be good enough if the scintillation light yield is low (as one would see in a WbLS detector, or a detector with a low level of secondary fluor added).

3.1.6 Comparing Cherenkov/scintillation Separation Approaches

Any comparison between the approaches discussed above is dangerous because they have all been done on the benchtop, with different sources, photon sensors, analyses, and other conditions. And because they will each scale differently in large detectors, depending on the target material and size of the detector itself. Nevertheless, it is interesting to see side-by-side so many different successful ways of doing this discrimination which, at the time of the last SNOWMASS, was mostly just an idea. Figure 18 shows distributions from the various approaches side-by-side.

3.1.7 Further Technological Needs

Despite the success of the development of these technologies, there are still many areas where additional development would have great benefit. We describe these below:

- **Lower-cost, large area, high-quantum efficiency photon sensors:** While improvements in timing and quantum efficiency in traditional photomultiplier tubes has been dramatic over the past several years, clearly the biggest single win for future large-scale detectors would be if these could be made less expensively, or with even higher photocathode efficiencies.

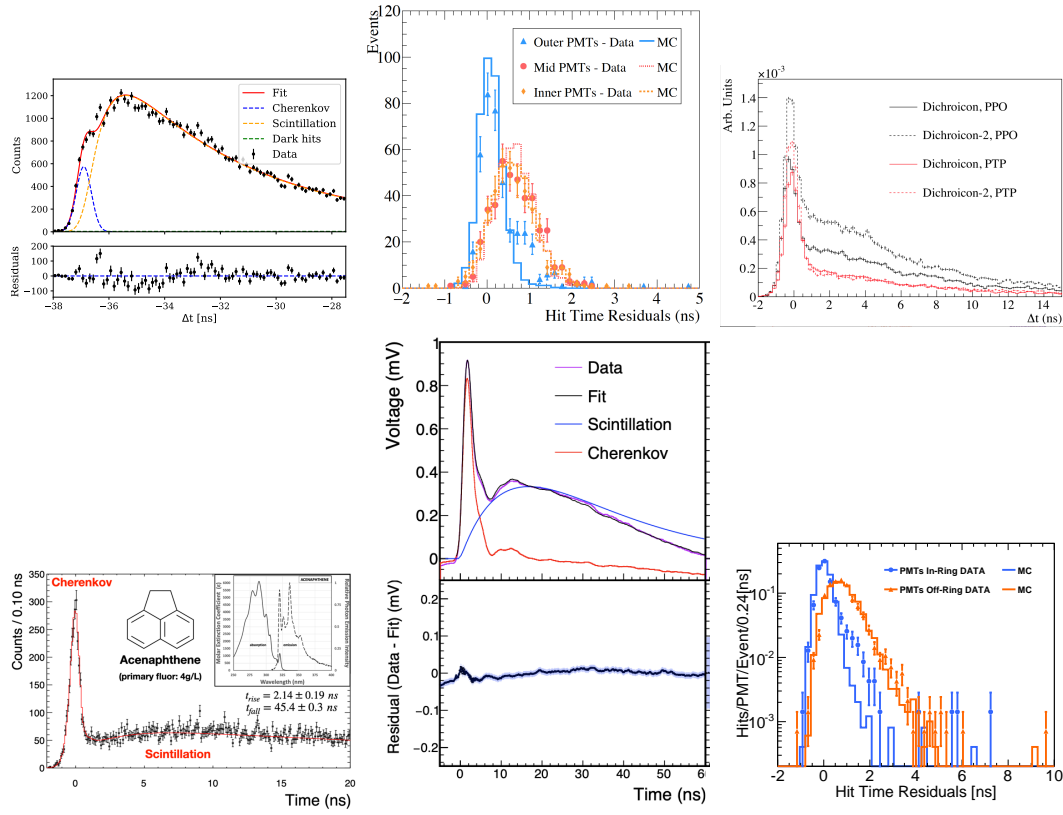


Figure 18: The hit time residuals for several different approaches to separating out Cherenkov and scintillation light.

- Further advances in dichroic filters:** Dichroic filters are still expensive, and their production in large areas and on curve surfaces (like the dichroicon) has not yet been done. In addition, improvements in the angular response of such filters, with sharp cut-on and cut-off transmission and reflection curves as a function of angle would enable much better photon-sorting capabilities.
- Narrow-band fluors:** Any Cherenkov/scintillation separation using wavelength is hampered by the fact that most organic fluors are relatively broad-band compared to the sensitivity of typical photocathodes; they leave little room for “clean” long-wavelength Cherenkov detection. A fluor that had an emission band from just 400-450 nm or something similar would make spectral sorting much more effective.
- High-yield scintillators with attenuation lengths > 40 m:** Limitations on the size of big detectors using scintillation light come primarily from the short attenuation lengths these scintillators have. WbLS is one approach to improving this, but it may come at the cost of lower light yield than some physics requires. A high-light yield scintillator that had 40 m attenuation lengths or longer for the primary emission bands would make very large-scale (e.g., 250 ktonne) detectors possible.
- High light-yield “slow” (~ 10 ns or longer) fluors:** Existing slow fluors already look very good, but if the fluor is too slow, position reconstruction is poor, and particle ID may also be compromised. A fluor that has a long risetime to allow identification of Cherenkov light, but maintains a light yield like some of the brightest scintillators while keeping good β - α discrimination would be an important step forward.

- **New approaches to radiological background reduction:** Although not specific to hybrid detectors, for all Cherenkov and scintillation detectors that aim for a broad program that includes low-energy physics, continued reductions in radiological contamination is always critical. This may be particularly important for new materials like WbLS or slow fluors.

3.2 Isotopic Loading Techniques for Low-energy Physics Programs

One of the great ways of expanding and improving the physics programs of photon-based detectors is through the loading of various isotopes. These isotopes can be the source of the physics itself—as in neutrinoless double beta decay experiments—or leverage additional physics, such as the Gd loading of water to detect neutrons from supernova neutrinos, or ^6Li to improve pulse-shape discrimination. We discuss some of the possibilities below.

3.2.1 Metal Loading in WbLS

Water-based liquid scintillator (WbLS) described above in Section 3.1.1, as an additional advantage in that loading of many isotopes is possible, using a mix of surface-active agents with hydrophilic as well as hydrophobic chelating groups to bridge aqueous (polar) and organic solvents (nonpolar). WbLS allows inorganic metal salt to be first dissolved in water, followed by directly blended into any type of scintillator solvents, regardless of the chemical property of each scintillator. WbLS has 100% metallic extraction efficiency and is particularly operative in extracting the hydrophilic elements (e.g. Boron, Lithium) into organic solvents. The metal-doped principal for oil-based WbLS (>80% scintillator) has been successfully demonstrated by PROSPECT experiment, a $\sim 0.1\%$ ^6Li -doped DIPN-based WbLS, with good light yield (>10,000 ph/MeV) and superior pulse shape discrimination.

A summary of applications and competences of metallic targets doped in WbLS, either being deployed or still under development, is presented in Table 2.

Target	Loading (mass)	Potential Applications
Indium	>8% In	Solar ν
Tellurium	> 6% Te	$0\nu\beta\beta$
Lithium	0.1% ^6Li >0.2% ^6Li	Reactor $\bar{\nu}$; excellent PSD Reactor $\bar{\nu}$; super PSD with improved optics
Boron	>0.5%	Dark Matter veto, reactor $\bar{\nu}$
Potassium	>1%	Calibration for LS detectors
Iron, Strontium	ppm to 1%	Nuclear waste management, environmental tracers
Gadolinium	0.1% Gd	Dark matter veto Reactor monitoring Reactor $\bar{\nu}$ oscillations
High-Z elements	10-15% Pb	Solar ν Calorimeters Medical QA/AC

Table 2: Examples of metallic targets loaded in Liquid Scintillator and Water-based Liquid Scintillator with projected applications

3.2.2 Te Loading in Liquid Scintillator for $0\nu\beta\beta$

A method for loading tellurium into organic liquid scintillator has been developed based on the formation of soluble organic compounds derived from telluric acid ($\text{Te}(\text{OH})_6$, hereafter TeA) and 1,2-butanediol (BD) in conjunction with N,N-dimethyldodecylamine (DDA), which acts as a stabilisation/solubilisation agent. The chemicals involved can all be purified to high levels, have high flash points and are relatively safe to work with in underground environments. The loading process results in acceptable optical absorbance and light output in larger detectors for loading levels up to several percent Te by weight. Stability of the loading has been demonstrated to be at least on the timescale of years.

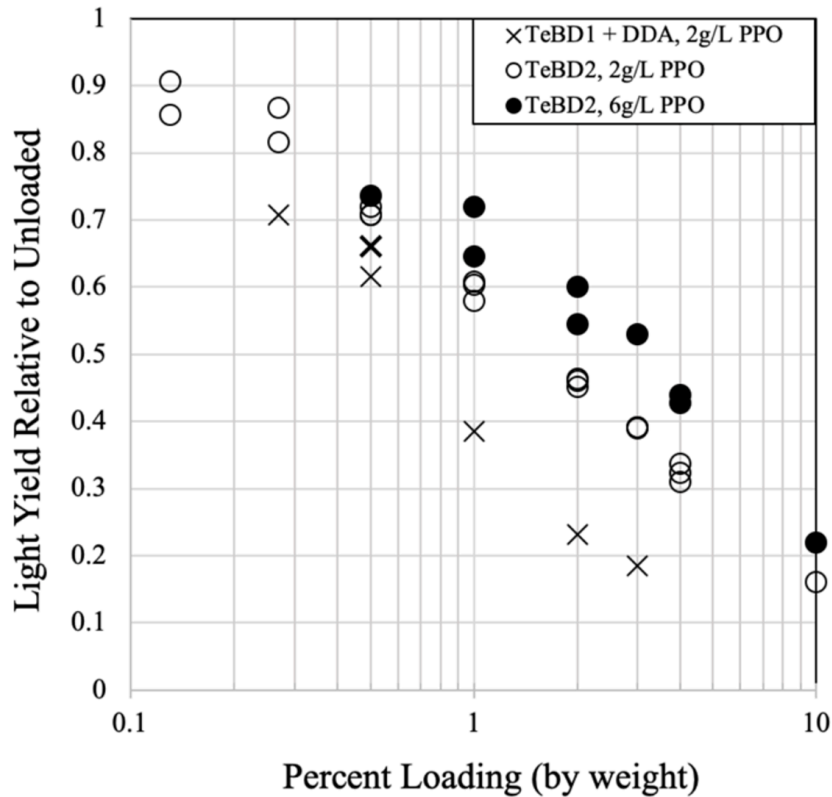


Figure 19: Relative light levels as a function of percent Te loading for two variants of the technique: TeBD1 (heated solubilization) and TeBD2 (DDA-induced solubilization).

This is an important advance that opens the door to a highly scalable and economical approach for neutrinoless double beta decay. Further advances in Te loading and associated purification techniques could provide a practical path to realising sensitivity to the non-degenerate normal mass ordering.

3.2.3 ^6Li Loading in Plastic Scintillator

Plastic scintillators are comprised of dopants entrained in a polymer matrix. In some cases, the scintillation signal from these dopants can be used to discriminate between particle types, e.g. electromagnetic depositions vs those from heavy ions, via “Pulse Shape Discrimination” (PSD) [99]. Further particle discrimination can be enabled by other dopants that have specific neutron capture reactions, which can also be identified via a combination of energy gating and PSD. For example, when loaded with lithium-6 and high amounts of a primary dye and secondary dye, plastic scintillators can use PSD to distinguish between electrons or positrons, neutrons, and thermalized neutron captures [100, 101]. At the current stage of development these plastics have broadly similar performance in terms of light

yield, optical attenuation, and PSD separation to liquids (e.g. Fig. 20). Elements have been produced with greater than 50-cm length and 7.5-cm width, and a commercial vendor is developing a production process (Fig. 21).

A key challenge to the production of these ^6Li -doped PSD plastics is the balance between scintillation properties and solubility of the dopants in the polymer matrix and the polymer precursors (i.e., monomers). One option to improve the solubility of these lithium-6 salts is to incorporate a comonomer with styrene that can dissolve the lithium-6 salts. Methacrylic acid is one possible comonomer that has polar substituents that can solubilize the lithium-6 salts [102,103]. Another option for soluble lithium-6 salts is to use organic salts with aromatic organic groups that have good solubility in primary dyes like PPO. Overall, the balance of scintillation properties and solubility of dopants that enable multiple modes of PSD remains an interesting challenge to investigate and solve.

Plastic scintillators with PSD and ^6Li -doping provide the same capabilities as the PSD ^6Li -doped liquid scintillator used for PROSPECT that is described in Sec. 3.2.1. As described in a recent LOI [104], the new solid form makes self-supporting fine-grained segmentation on a large scale possible, enables light guiding approaches based on air gaps, and eliminates the need for containment vessels and supporting infrastructure. Several detector implementations are proposed and under development using ^6Li -doped PSD plastics. The SANDD concept (Fig. 21) has implemented mm-scale segmentation to study reactor antineutrino directionality and cosmogenic background rejection [105,106]. Segmentation at the 5–10-cm scale in 2D bar geometries is being developed for efficient, aboveground reactor antineutrino detection (e.g. ROADSTR [107]) with the goal of a mobile system appropriate for monitoring applications and measurements at multiple reactors with correlated systematics.

3.2.4 Quantum Dots

In recent years new methods for the production of metal loaded LS in neutrino physics were studied involving semiconducting nanocrystals, which are known as “quantum dots”. The optical and electrical properties of the quantum dots are directly proportional to their size, which is typically in the order of few nanometers. The emission band consists of a narrow resonance around the characteristic wavelength of the dot. Since the dot size can be controlled to high precision in the synthesis, the absorption and re-emission spectrum of the dots can be tuned and optimized for a respective application. In some synthesis methods the quantum dots are already delivered in colloidal suspension with the aromatic solvent toluene at concentrations of several grams per liter.

The most commonly used quantum dot cores are binary alloys such as CdS, CdSe, CdTe, and ZnS. Alternatively, there are also phosphor-based rare-earth dots. Therefore, quantum dots provide a method to dope scintillator with various metals and rare-earth elements. For a cadmium (Cd) based LS there are two different applications in the field of neutrino physics: neutron-enhanced isotopes (^{113}Cd) and $\beta\beta$ -decay candidates ($^{106,116}\text{Cd}$). Also Se, Te, and Zn, which are present in common quantum dot cores, have $\beta\beta$ -decay candidates. There is also a possibility to tune the scintillator emission spectrum in a way that allows to separate scintillation from Cherenkov light by narrowing scintillation emission from the quantum dots separated from the Cerenkov contribution.

The basic limitations of quantum-dot-doped liquid scintillator in use for particle physics detectors are probably cost and availability in large quantity (\sim ton). The stability tests on typical solutions of quantum dots in concentration at few g/l indicate that larger particles are formed by aggregation in the concentrated solutions over long time scales. This could explain the fact that filtering improves

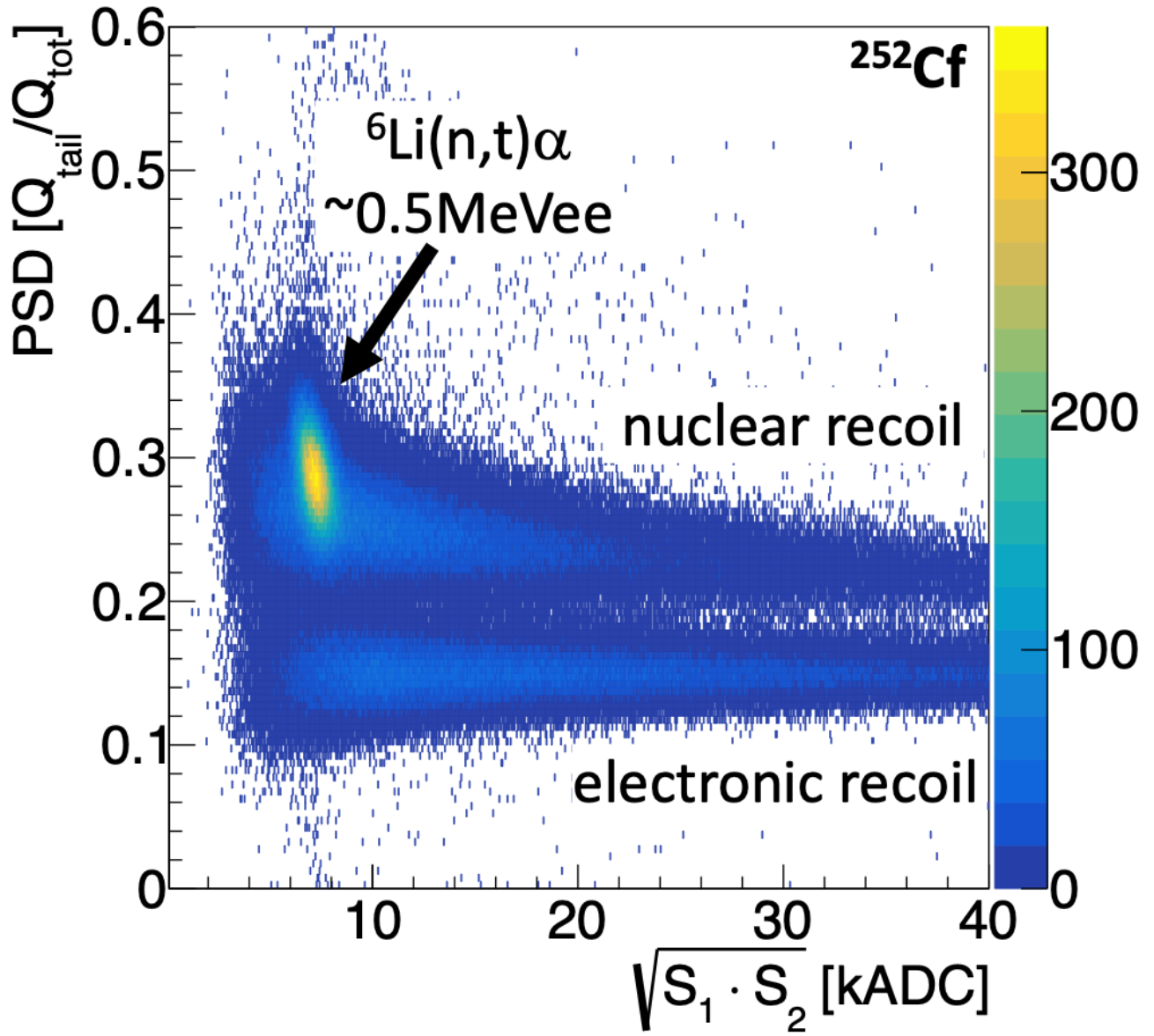


Figure 20: Pulse Shape Discrimination performance of the $5.5 \text{ cm} \times 5.5 \text{ cm} \times 50 \text{ cm}$ ^6Li -doped PSD plastic scintillator shown in panel (b) under ^{252}Cf flood-field illumination, in terms of uncalibrated ADC units. A clear neutron capture feature is observed at about 0.5 MeV_{ee} , along with electronic and nuclear recoil separation.

the attenuation length as well as the observation of transparency degradation after several weeks. However, there is room for optimization on the stability and optical performance by improvements in the loading process of quantum dots in scintillator solution. Instead of suspension, incorporating chelating agents or WbLS surface active agents into the mixing procedures could load the quantum dots in organic solvents homogeneously with lengthy stability.

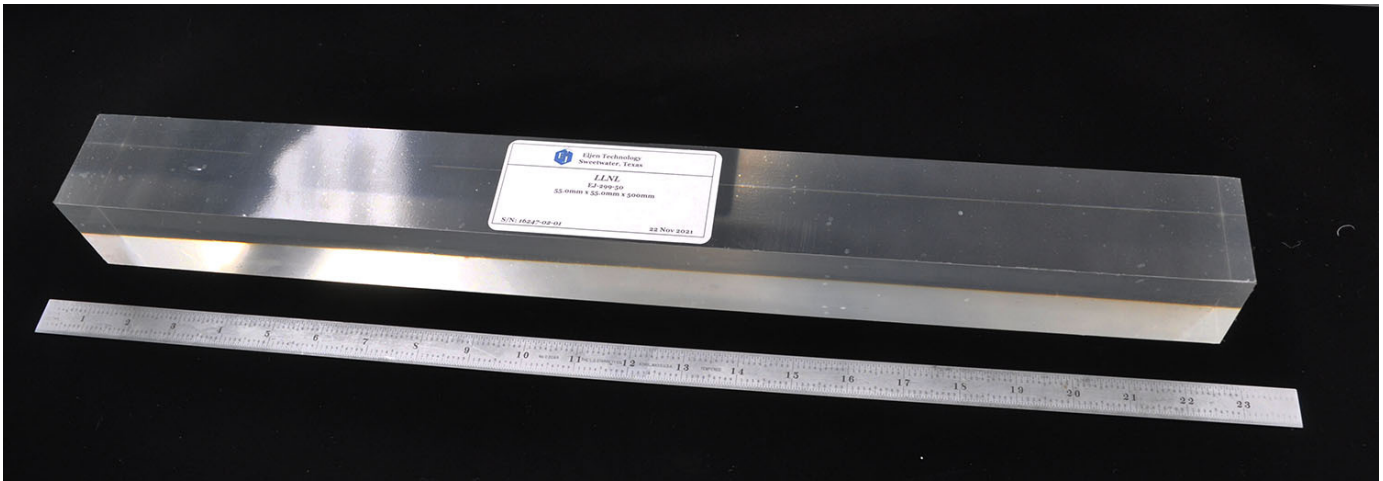


Figure 21: A 5.5 cm \times 5.5 cm \times 50 cm bar produced by Eljen Technology.

3.3 Improvements in Simulation and Analysis

The ever-increasing desire for more precise detectors models and better background rejection has led to development of many new approaches to simulation and analysis. There are far too many to include all of them here, but we have focused on a few that were represented in relevant LOIs to NF10.

3.3.1 GPU-Accelerated Photon Ray Tracing (*Chroma*)

As large-scale neutrino detectors become ever larger, photon coverage becomes higher, and photon sensor technology becomes more complex with devices like the ARAPUCA [108], the dichroicon [91], or distributed imaging [109], a major bottleneck in both simulation and reconstruction of physics events is the propagation of photons through the detector geometry. Originally created for the water Cherenkov option for the LBNE experiment, a fast photon ray-tracer was developed by Stan Seibert and Anthony LaTorre [110] that improved photon simulation speeds by a factor of 200 over what GEANT4 itself could do. In order to achieve such high performance, *Chroma* combines techniques from 3D rendering algorithms with the massively parallel calculation hardware inside GPUs. A high-end GPU costs approximately \$5000 (twice the cost of a fast consumer-grade CPU), yet provides forty times the raw floating point performance and ten times the memory bandwidth. *Chroma* uses the CUDA toolkit, provided by NVIDIA, to directly access the GPU resources and perform all major calculations. CUDA-compatible GPUs are being used more and more in the construction of large supercomputing clusters, which will make it easier in the future for the work on next-generation neutrino detectors such as THEIA [93] to use *Chroma*.

Nearly all fast 3D rendering systems represent the world geometry using a mesh of triangles. Triangle meshes are very simple to represent, and can be used to approximate any surface shape, limited by how much memory can be devoted to triangle storage. With only one surface primitive, there is only code path to optimize. In particular, we have adopted the Bounding Volume Hierarchy (BVH) technique from the graphics world to speed up ray intersection tests with triangle meshes. A BVH is a data structure that organizes a spatial arrangement of shapes (triangles in our case) into a tree of nested boxes. Rather than test for ray intersection with every triangle in a geometry, the photon propagator tests for intersection with boxes in the BVH. If the ray does not intersect the box, then all of the children of that box can be skipped, leading to a large reduction in the number of intersection tests required. For example, a model of a large, 200 kton water Cherenkov detector consists of 62

million triangles, but the BVH reduces a typical propagation step for a photon to 130 box intersection tests and only 2 triangle intersection tests.

One collateral bonus of *Chroma's* speed is that it provides remarkably beautiful, *realtime* detector displays. It is quite easy to “fly through” a detector and see it rendered in all of its detailed geometry, exactly the way the photons themselves will see the detector. Fig. 22 shows on the left a rendering of the SNO+ [85] detector which, in a static pdf document like this proposal cannot be examined dynamically in realtime, but was created from that realtime fly-through and simply captured by screen-shot. The rendering is in fact a 3D image; with red-blue glasses one can see the relief in the image.

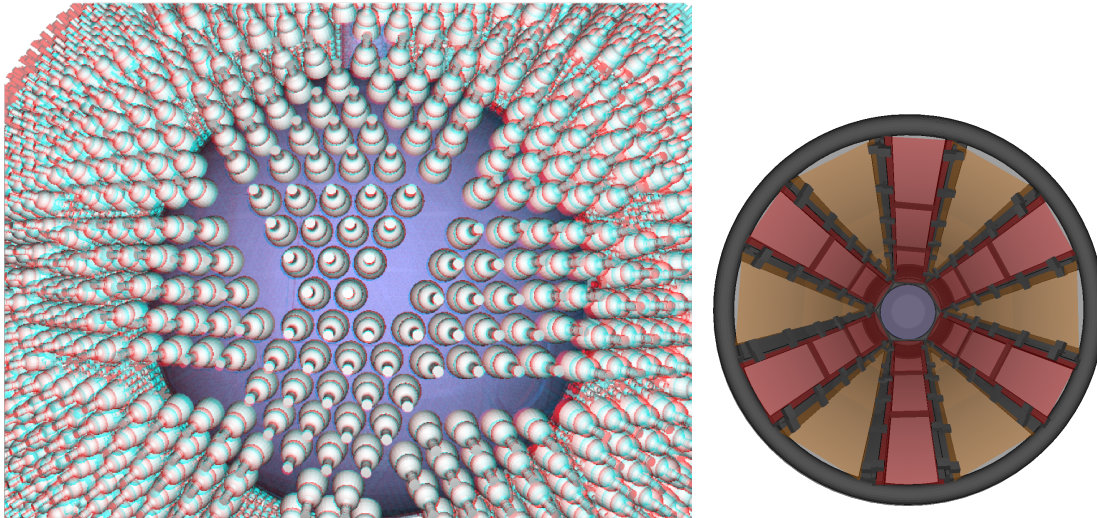


Figure 22: Left: A screen capture from a realtime, three-dimensional “movie” of the SNO+ [85] detector created with *Chroma*, which is best viewed with red-blue 3D glasses. The model shown is exactly the model used by *Chroma's* physics simulation, albeit with false-color optics for the display rather than the complete physics the simulation uses. The PMTs are fully rendered, including their Winston-cone light concentrators. Right: The CAD drawing for the 3D-printed dichroic filter holder for the dichroicon [91] was directly imported into *Chroma*, and used to accurately simulate the orientations of the dichroic filters (shown in red and orange) with respect to the benchtop experiment.

The choice of representing geometries in *Chroma* as triangle mesh makes it straightforward to import CAD drawings into the optical simulation, as shown in Figure 22. All that is required is that the triangles on the mesh have optical properties assigned to them, which is a trivial operation in the case of a CAD model with uniform properties over its entire surface, but allows for fine-grained position dependent control of material properties as well. This allows anyone with CAD experience to quickly create an arbitrarily complicated simulation without having to learn a new way to represent geometries. The ability to rapidly prototype designs makes *Chroma* well suited for benchtop studies as well, and with easy scaling up from there to very large detectors, as shown in 23, which includes 3D Large Area Picosecond Photodetectors (LAPPD) [97] mixed with standard PMTs in a *Chroma* model of the THEIA25 [93] detector.

3.3.2 GEANT4-based toolkits *RAT-PAC*

RAT-PAC is an open-source GEANT4-based toolkit that offers both micro-physical simulation capabilities and analysis tools for high-precision event modeling, evaluation, and characterization, from

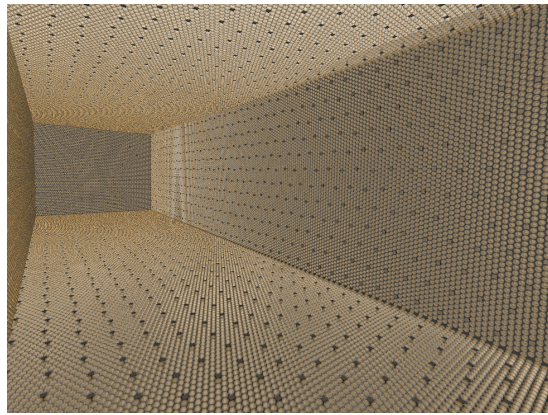


Figure 23: Next-generation photon detectors like LAPDs [97] are straightforward to simulate and include in larger geometries, as shown in this internal view of a THEIA25 [93] model made with *Chroma*, which has mixed PMTs and LAPDs for detecting photons. The *Chroma* framework makes it quick and easy to explore new detector geometries and photon detecting devices.

benchtop test stands to large-scale detectors.

The RAT-PAC Monte Carlo simulation and analysis suite [111] is a free and open-source version of the RAT toolkit. RAT was first written for the Braidwood reactor experiment [112], and is now the official simulation and analysis package for SNO+ [85], DEAP, and MiniCLEAN experiments, thus benefiting from shared efforts in development and verification. A GEANT4-based package [113], RAT-PAC (standing for “RAT Plus Additional Code”) was branched off from the core RAT development some years ago, to form an open-source version of the code, available for public use. RAT-PAC forms the basis of the official software for the THEIA collaboration [93], the proposed third phase of ANNIE [114], and for the WATCHMAN collaboration, who are developing a design for the NEO detector to be located at the AIT facility in the UK [115].

One of the great advantages of the RAT-PAC approach is that its procedural geometry description allows the same code to be used to simulate or analyze data from a large-scale experiment and a small benchtop test-stand. Figure 24 shows the detailed geometry of the full ktonne-scale SNO+ detector, and the even larger THEIA detector, and Fig. 25 shows the much smaller CHESSE detector at UC Berkeley/LBNL [95]. In addition to the flexible geometry descriptions, RAT-PAC takes a micro-physical approach, relying on physical, rather than phenomenological models. For example, individual photons are simulated hitting photon sensors and the resulting timing and charge are evaluated photon-by-photon, rather than by application of a phenomenological risetime correction. Therefore, simulating both benchtop test stands and large-scale detectors with the same micro-physical detail and the same code means that parameter measurements made by the benchtop are more easily translated into the larger-scale detector. A measurement of, for example, the light yield of a scintillator cocktail performed in a small-scale setup can be straightforwardly propagated to predict performance in large detectors, complete with systematics associated with optical models or even data acquisition approaches. Comparisons between simulations of Cherenkov and scintillation light generated using RAT-PAC and data from test stands, such as at Penn, CHESSE at LBNL, and FlatDot at MIT, show good agreement. An example from FlatDot is shown in Fig. 25 [116].

RAT(-PAC) is based on GEANT4.10 [113] and the GLG4Sim package written by Glenn Horton-Smith, with custom code for scintillation and neutron absorption processes as well as a complete model of

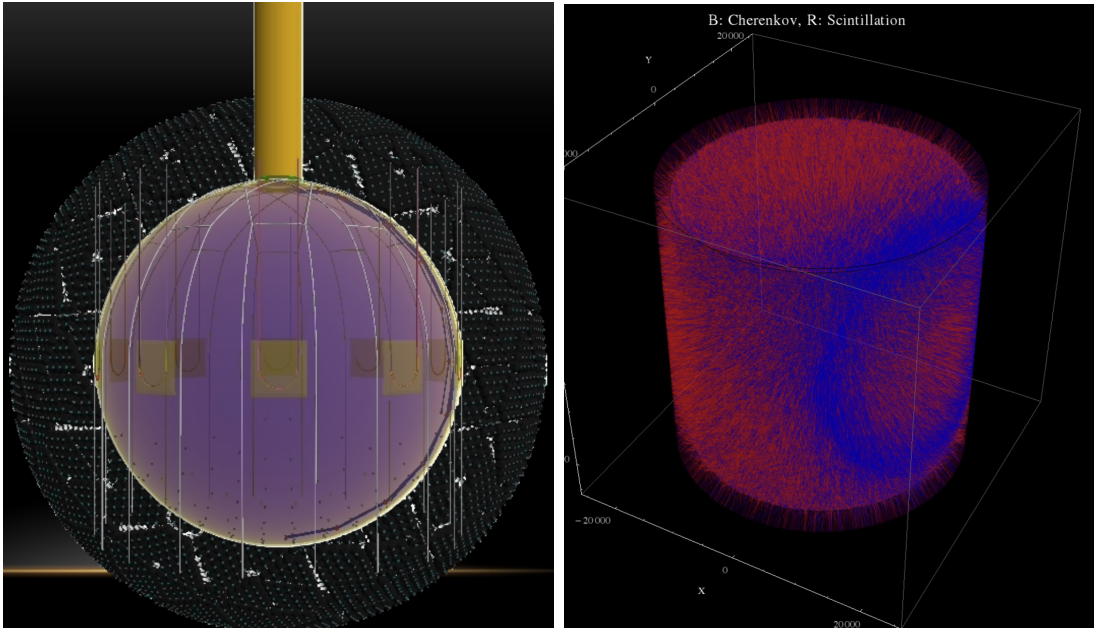


Figure 24: (Left) RAT-PAC generated image of the ktonne-scale SNO+ detector. (Right) RAT-PAC simulation of a high-energy (GeV) electron in the 50-ktonne THEIA detector, including full photon tracking. Blue shows Cherenkov photon track and red shows scintillation.

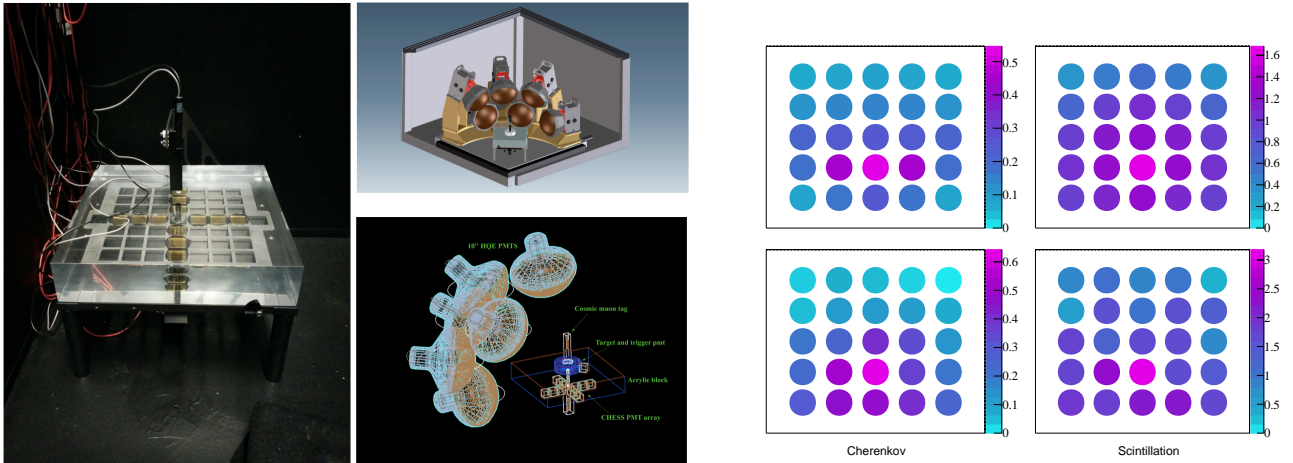


Figure 25: (Left) Photograph of the CHES PMT array. (Top centre) CAD image of the full CHES detector. (Bottom centre) RAT-PAC generated image of the full CHES detector. (Right) RAT-PAC simulations of both Cherenkov (*left*) and scintillation (*right*) signals show good agreement with data from the FlatDot experiment (*bottom*), up to a normalization factor reflecting the absolute light yield of the liquid scintillator.

PMT optics. RAT(-PAC) handles all stages of event simulation: from the propagation of primary particles; production of optical photons via Cherenkov and scintillation processes; individual photon propagation, including a full optical model of all detector materials; photon detection at the single PE level, including individual photon detector charge and timing response; and data acquisition including full customizable simulation of front end electronics, trigger systems, and event builders. It also allows root-formatted data to be used as input, and provides simple analysis tools and ways to include many more, as well as a macro command structure for control. Lastly, RAT-PAC also includes the ability to dynamically generate detector configurations via an external database. Thus, RAT-PAC is a complete

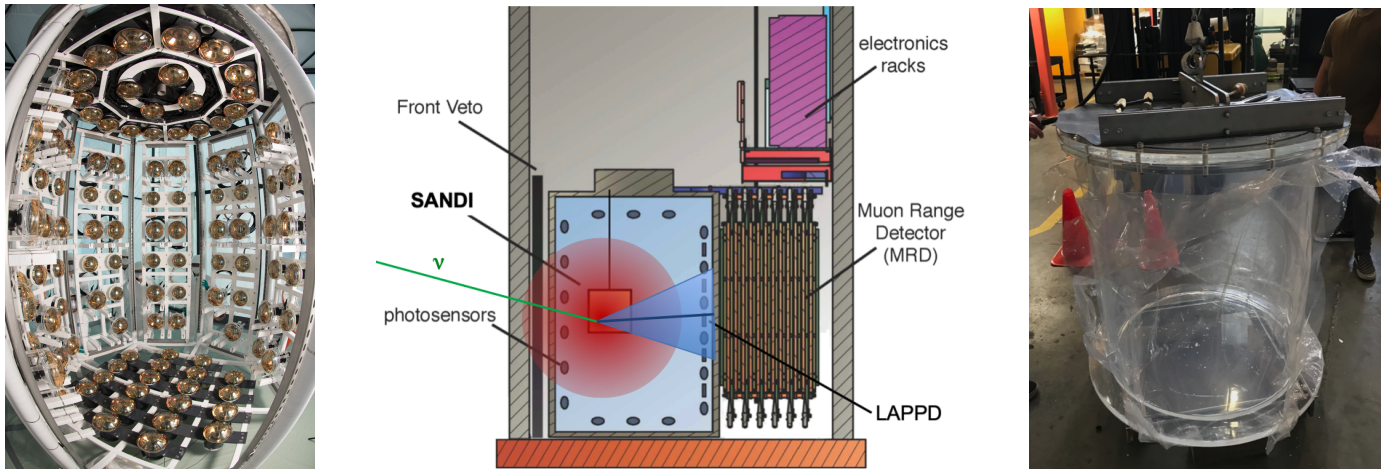


Figure 26: (left) NTT before installation. The rails allow LAPPDs to be inserted between the PMTs. (center) ANNIE detector setup with envisaged SANDI vessel containing 350 kg of GdWbLS. (right) Test of SANDI acrylic vessel wrapped in protective plastics at UC Davis.

package that can be used with small modifications for entire experiments.

3.3.3 Machine Learning Approaches

The applications of machine learning approaches to neutrino detectors in general, and to photon-based neutrino detectors in particular, is enormous. For photon detectors, these approaches fall into two primary classes: those that are used to create fast simulations, and those that are used for particle ID and background rejection.

3.4 Prototypes and Large-Scale R&D Platforms

3.4.1 ANNIE

The ANNIE (Accelerator Neutrino Neutron Interaction Experiment) [114, 117, 118] is located in the Booster Neutrino Beam at Fermilab. This beam is about 93% pure ν_μ in neutrino mode and has a spectrum that peaks at about 700 MeV, an energy scale of great interest to current and future neutrino oscillation experiments. While ANNIE's current Phase 2 investigates the combination of a Gd-loaded water target read out by ultrafast LAPPDs, a first insertion of a small WbLS-filled vessel (SANDI) is planned for the upcoming summer break, adding scintillation to the Cherenkov signal at the neutrino interaction vertex. In an eventual Phase 3, the full detection volume is to be filled with WbLS, making ANNIE the first experiment exploring the benefits of the new hybrid detection technique in the reconstruction of GeV-scale beam neutrinos.

ANNIE program with Gd-water target: The two main goals of the current ANNIE Phase 2 are the precision measurements of the neutron yield from neutrino interactions at the 1 GeV scale, and a test of the effectiveness of Large Area Picosecond PhotoDetectors (LAPPDs) in a realistic physics environment (Sec. 3.1.3). As illustrated by Figure 26, the current setup of the ANNIE detector comprises a 26-ton Neutrino Target Tank (NTT) equipped with 128 conventional PMTs, a Front Muon Veto (FMV) to reject “dirt” muons, and a Muon Range Detector (MRD) to track and range out muons. The water of the NTT was loaded with a mass fraction of 0.1% of gadolinium (GdS) in early 2019. In January 2021, ANNIE started to take physics data in this basic configuration, while

the deployment of first LAPPDs is foreseen for early 2022. The aim is to install in total five LAPPDs before the end of Phase 2 to evaluate their impact on the reconstruction of CC interaction final states as well as vertex reconstruction of the low-energy signals of neutron capture on gadolinium. The conventional PMT array provides a vertex reconstruction of $\Delta r = 38$ cm for CC final-state muons. The full configuration including the LAPPDs and their sub-nanosecond timing is expected to substantially improve this vertex resolution to about $\Delta r = 12$ cm.

Scintillator for ANNIE Neutron Detection Improvement (SANDI): From simulation studies, we know that – even in the presence of LAPPDs – the vertex resolution suffers from the need to image the ring edge with the conventional PMT array. There is a timing degeneracy in single track particles that makes the vertex location parallel to the track entirely dependent on ring edge imaging. One way to improve on this is to use a slightly scintillating material as neutrino target, resulting in a comparatively small amount of isotropic light emitted from the vertex that can be separated from Cherenkov light by timing and topology.

To explore the potential benefit for event reconstruction, ANNIE plans to insert a 3'×3' cylindrical vessel (SANDI) containing about 350 kg of gadolinium-loaded Water-based Liquid Scintillator (GdWbLS) into the center of the NTT water volume (Figure 26). In addition, one or more of the five LAPPDs may be moved to the backward hemisphere. A deployment of several weeks will allow us to confirm models for track reconstruction and to identify additional scintillation light emitted by the hadronic recoil at the vertex. First simulation studies show that the inclusion of this signal will indeed lead to an improvement in reconstruction capability. While the muon energy reconstruction is dominated by the information from the (unchanged) MRD, the additional information from the GdWbLS volume improves the neutrino energy reconstruction from ($\Delta E/E \sim 15\%$ to 11%).

Future full GdWbLS phase: Following a successful SANDI test, ANNIE plans to propose a Phase 3 that features a complete replacement of the Gd-water with GdWbLS. Neutron captures in GdWbLS feature a substantially increased light output (factor ~ 3) compared to Gd-water, greatly improving neutron detection efficiency ($\rightarrow \geq 90\%$) and spatial resolution for the capture vertex ($\rightarrow \sim 40$ cm). This will enhance not only the precision of neutron multiplicity measurements but also bears the chance to reconstruct the neutron energy spectrum by their capture position relative to the production vertex. A full calorimetric measurement of the cross-section (including vertex hadronic energy) may also be possible.

With these ambitious goals in mind, ANNIE is investigating the possibility to reconstruct the inner part of the NTT to make it compatible with WbLS, including encapsulation of PMTs and other components, in addition to the first-ever deployment of a WbLS liquid recirculation system. Systems based on nanofiltration and phase separation technology are being developed for Eos and Theia (Sects. 3.4.3 and 3.5.1). ANNIE Phase 3 will be a significant step towards realization of hybrid optical detectors in addition to making neutron-inclusive neutrino cross-section measurements of unprecedented scope and quality.

3.4.2 NuDOT

NuDot is a mid-scale prototype designed to demonstrate timing-based Cherenkov/scintillation separation in a realistic experimental geometry, focusing on techniques applicable to searches for neutrinoless double-beta decay ($0\nu\beta\beta$). It builds on the successful demonstration of this approach in the FlatDot test stand [116]. It is currently undergoing detector commissioning, with its initial physics data-taking campaign expected to begin by Summer 2022.

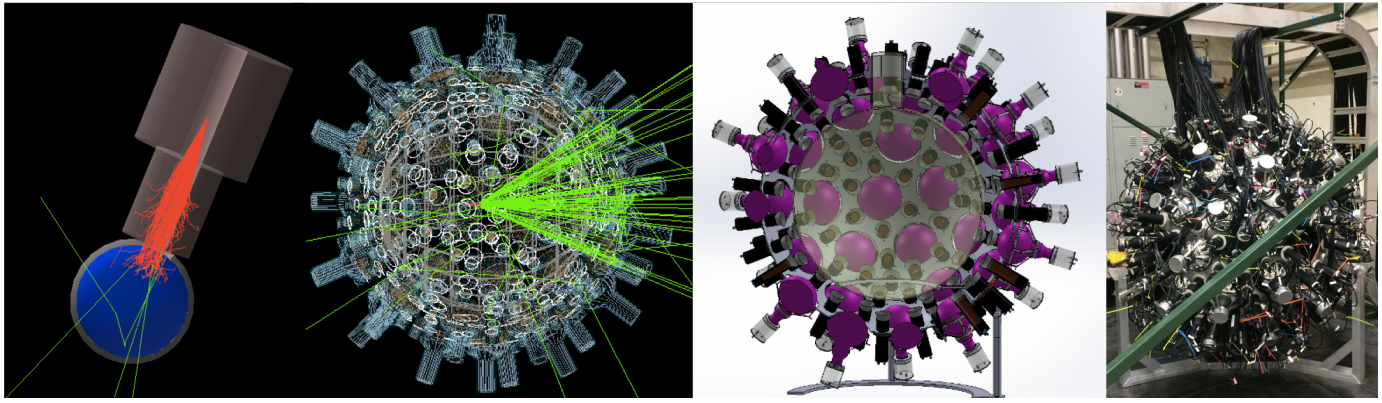


Figure 27: *From left to right:* A RAT-PAC simulation of electron tracks in the collimated β source and coupled liquid scintillator cuvette used for “dry” surface data-taking; a RAT-PAC simulation of Cherenkov light tracks for a 1 MeV β in NuDot; a rendering of a section view of the NuDot detector; a photo of NuDot, before the calibration system was deployed and the sphere was made light-tight for commissioning runs.

The NuDot design, shown in Fig. 27, relies on a combination of 59 8"-diameter PMTs (primarily a combination of EMI Model D642 and Hamamatsu Model R1408 PMTs previously used by the MACRO experiment) and 151 2"-diameter PMTs (Hamamatsu Module R13089, with an average transit time spread of 200 ps) to achieve high light collection efficiency and fast-timing capability. These detectors surround a 36"-diameter acrylic sphere that will be filled with a LAB-based liquid scintillator cocktail, with the entire assembly immersed in a mineral oil tank to provide shielding and optical coupling. Detector calibration and the first two phases of data-taking will be conducted using a remotely-controlled 4π calibration system with 3 independent axes of motion. In addition to an LED source used for gain and pulse-shape calibrations, this system holds a collimated β -emitting ^{90}Sr needle source that can be adjusted to shine on any point on the NuDot sphere from any point along the sphere diameter, allowing tests of the NuDot Cherenkov/scintillation separation capability as a function of position and direction.

NuDot has 3 planned phases of operation, the first two of which are conducted prior to underground deployment:

1. “Dry” runs at Bates Research and Engineering Center: a small cuvette of liquid is coupled directly to the collimated source, allowing for calibration of the PMT timing response and pulse shape with water Cherenkov data, followed by C/s separation tests with a variety of liquid scintillator cocktails.
2. Liquid scintillator- and mineral-oil-filled runs at Triangle Universities Nuclear Laboratories: following the completion of phase 1 data taking, NuDot will be moved to TUNL for any needed detector upgrades and liquid-filling. The goal of this phase is to demonstrate NuDot’s C/s separation and energy reconstruction capability in the final operational configuration using the calibration system.
3. Underground proof-of-concept measurement: in phase 3, NuDot will be re-deployed underground for a proof-of-concept measurement. The current baseline is to conduct a $2\nu\beta\beta$ decay measurement, but alternatives like $\beta+/\text{EC}$ searches are under consideration.

The isotope and isotope-loading technique that will be used in phase 3 has not yet been selected. The NuDot Collaboration is currently conducting R&D measurements of quantum-dot-loaded liquid scintillator cocktails that use perovskite wavelength shifters (see Ref. [119]), but is also considering high-concentration Te loading and pressurized Xe loading options.

3.4.3 Eos

Successful detection of Cherenkov light from highly scintillating media has been achieved in CHESSE, and complemented with an extensive characterisation program at LBNL, BNL, LLNL, and Davis. These measurements inform large-scale Monte Carlo models, which are used to predict performance in kton-scale detectors. Ton-scale deployments of novel scintillators (ANNIE, BNL) are planned to test production, deployment, and recirculation.

While bench-top measurements have been, and will continue to be used to measure microphysical properties of novel scintillators and photon detection technology, all demonstrations of event reconstruction and the resulting background rejection capabilities are purely Monte Carlo driven. Data-driven demonstrations of the event imaging capabilities of hybrid detector technology is a critical step to realising a large detector for both fundamental physics and nonproliferation applications.

The proposed EOS prototype is a few-ton scale detector, designed to hold a range of novel scintillators, coupled with an array of photon detection options and the ability to deploy a range of low-energy calibration sources. EOS will be constructed, calibrated and tested in Berkeley. Assuming a successful surface deployment, EOS could later be re-deployed underground, for example at SURF or SNOLAB, or at an alternative off-site location such as a reactor or test beam for further characterization of detector response to a range of particle interactions. EOS represents significant risk reduction for a large-scale deployment of (Wb)LS and novel detection technology.

EOS will be sufficiently large to use time-of-flight based reconstruction, and to fully contain a range of low-energy events (α , β , γ , n) for detailed event-level characterisation. EOS represents a balance of sufficient size for full event characterization, complemented with economy of scale, and flexibility to adapt for multiple target materials and photon detection options.

The primary goal of EOS is to validate performance predictions for large-scale hybrid neutrino detectors by performing a data-driven demonstration of low-energy event reconstruction leveraging both Cherenkov and scintillation light simultaneously. By comparing data to model predictions, and allowing certain detector configuration parameters to vary – such as the fraction of LS in a WbLS target cocktail, or by using PMTs with differing TTS, or deployment of dichroicons – the predictive power of the model can be validated. This validated microphysical model of hybrid neutrino detectors can then be used by the neutrino community for design optimization of next-generation hybrid detectors.

EOS will provide an important test bed to the community, for testing alternative target media, photon detectors, and readout technology and methodology, and assessing the impact of these novel developments on detector performance.

After the conclusion of operations at LBNL, EOS could be redeployed at an off-site location. This would take place after the end of the primary project period, and successful completion of the project objective. Options include:

- Underground deployment, for example at SURF or SNOLAB, where scintillator handling procedures are well vetted and understood, and we have relationships of long standing. This would allow more precise measurements in a low-background environment.
- Deployment at a reactor for low-energy neutrino reconstruction. This provides a near-field demonstration of the remote reactor monitoring concept.
- Deployment at a test beam for hadronic event reconstruction, or a neutron source such as the Spallation Neutron Source at ORNL for neutron studies, useful for advanced event identification and background characterization.

3.5 Large-Scale Detector Ideas

3.5.1 Theia

New developments in liquid scintillators, high-efficiency, fast photon detectors, and chromatic photon sorting have opened up the possibility for building a large-scale detector that can discriminate between Cherenkov and scintillation signals. Such a detector could exploit these two distinct signals to observe particle direction and species using Cherenkov light while also having the excellent energy resolution and low threshold of a scintillator detector. Situated in a deep underground laboratory, and utilizing new techniques in computing and reconstruction techniques, such a detector could achieve unprecedented levels of background rejection, thus enabling a rich physics program that would span topics in nuclear, high-energy, and astrophysics, and across a dynamic range from hundreds of keV to many GeV. The scientific program would include observations of low- and high-energy solar neutrinos, determination of neutrino mass ordering and measurement of the neutrino CP violating phase δ , observations of diffuse supernova neutrinos and neutrinos from a supernova burst, sensitive searches for nucleon decay and, ultimately, a search for NeutrinoLess Double Beta Decay (NLDBD) with sensitivity reaching the normal ordering regime of neutrino mass phase space.

THEIA is a detector concept that incorporates these new technologies in a practical and affordable way to accomplish the science goals described above. We consider two scenarios, one in which THEIA would reside in a cavern the size and shape of the caverns intended to be excavated for the Deep Underground Neutrino Experiment (DUNE) which we call THEIA -25, and a larger 100 ktonne version (THEIA -100) that could achieve an even broader and more sensitive scientific program.

In the THEIA reference design, the target material would be water-based liquid scintillator (WbLS) described in Section 3.1.1, which has an advantage for a big detector in its long attenuation lengths. For much of the low-energy program of THEIA, the WbLS would need to be made radiopure at levels not far from what can be done in an organic scintillator.

The broadband neutrino beam being built for the Long Baseline Neutrino Facility (LBNF) [120] and the Deep Underground Neutrino Experiment (DUNE) [121] offers an opportunity for world-leading long-baseline neutrino oscillation measurements. Due to advances in Cherenkov ring reconstruction techniques, a THEIA detector in the LBNF beam would have good sensitivity to neutrino oscillation parameters, including CP violation (CPV), with a relatively modestly-sized detector. In addition to this long-baseline neutrino program, THEIA will also contribute to atmospheric neutrino measurements and searches for nucleon decay, particularly in the difficult $p \rightarrow K^+ + \bar{\nu}$ and $N \rightarrow 3\nu$ modes.

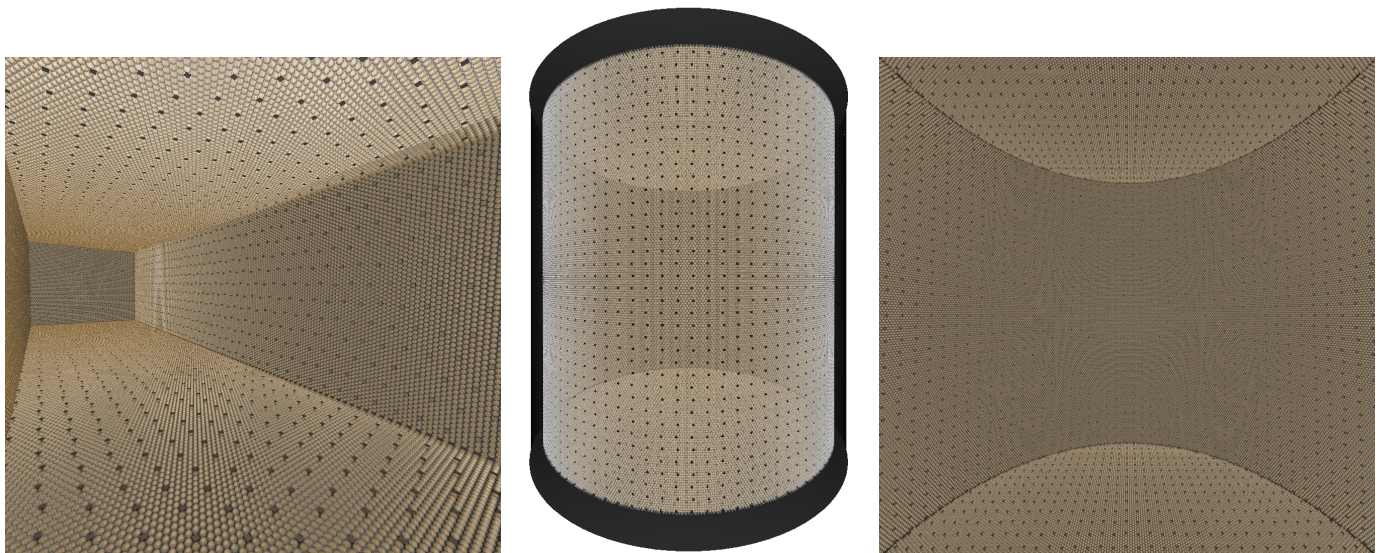
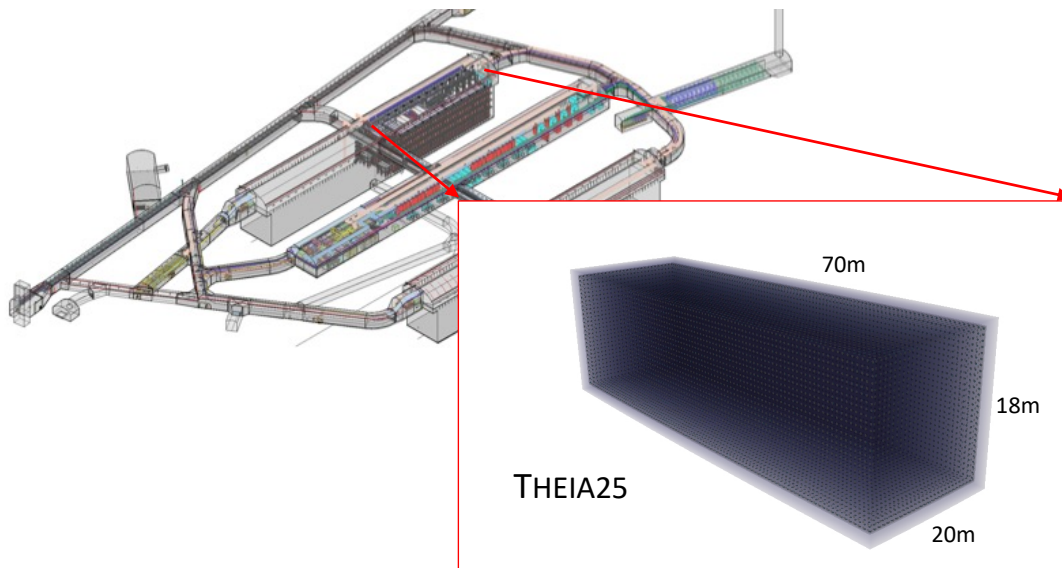


Figure 28: The THEIA detector. *Top panel:* THEIA -25 sited in the planned fourth DUNE cavern; *Lower left panel:* an interior view of THEIA -25 modeled using the Chroma optical simulation package [110]; *Lower middle panel:* exterior view of THEIA -100 in Chroma; *Lower right panel:* an interior view of THEIA -100 in Chroma. In all cases, THEIA has been modelled with 86% coverage using standard 10-inch PMTs, and 4% coverage with LAPPDs, uniformly distributed, for illustrative purposes. Taken from [93].

THEIA will also make a definitive measurement of the solar CNO neutrinos, which have recently been detected exclusively by Borexino [122], but without enough precision to distinguish between competing models of the Sun’s metallicity. THEIA will also provide a high-statistics, low-threshold (~ 3 MeV) measurement of the shape of the ^8B solar neutrinos and thus search for new physics in the MSW-vacuum transition region [123,124]. Antineutrinos produced in the crust and mantle of the Earth will be measured precisely by THEIA with statistical uncertainty far exceeding all detectors to date.

Should a supernova occur during THEIA operations, a high-statistics detection of the $\bar{\nu}_e$ flux will be made—literally complementary to the detection of the ν_e flux in the DUNE liquid argon detectors. The simultaneous detection of both messengers—and detection of an optical, x-ray, or gamma ray component will enable a great wealth of neutrino physics and supernova astrophysics. With a very deep location and with the detection of a combination of scintillation and Cherenkov light, THEIA will have world-leading sensitivity to make a detection of the Diffuse Supernova Neutrino Background (DSNB) antineutrino flux. The most ambitious goal, which would likely come in a future phase, is a search for Neutrinoless double beta decay (NLDBD), with a total isotopic mass of 10 tonnes or more, and with decay lifetime sensitivity in excess of 10^{28} years [93,125].

THEIA is able to achieve this broad range of physics by exploiting new technologies to act simultaneously as a (low-energy) scintillation detector and a (high-energy) Cherenkov detector. Scintillation light provides the energy resolution necessary to get above the majority of radioactive backgrounds and provides the ability to see slow-moving recoils; Cherenkov light enables event direction reconstruction which provides particle ID at high energies and background discrimination at low-energies. Thus, the scientific program benefits in many cases on the ability of THEIA to discriminate efficiently and precisely between the “scintons” (scintillator photons) and “chertons” (Cherenkov photons).

A major advantage of THEIA is that the target can be modified in a phased program to address the science priorities. In addition, since a major cost of THEIA is expected to be photosensors, investments in THEIA25 instrumentation can be transferred directly over to THEIA100. Thus, THEIA can be realized in phases, with an initial phase consisting of lightly-doped scintillator and very fast photosensors, followed by a second phase with enhanced photon detection to enable a very low energy solar neutrino program, followed by a third phase that could include doping with a $0\nu\beta\beta$ isotope and perhaps an internal containment vessel.

3.5.2 LiquidO

LiquidO is a new approach to detecting neutrinos that, in contrast with conventional liquid scintillator detectors, relies on using an opaque scintillator medium as the primary neutrino target [126]. The scintillators that can be best used by LiquidO have a short scattering length and a medium to long absorption length, an example of which has already been successfully produced [127]. In such a medium, the photons produced by the opaque scintillator undergo a random walk process near their creation point and are trapped in so-called *light balls* around each energy deposition point. The light is collected by a dense array of wavelength-shifting fibres that traverses the volume and that is readout by photo-sensors in the periphery. Silicon photomultipliers (SiPMs) are well-suited to this purpose given their affordable price, high efficiency, and excellent time resolution.

A full description of LiquidO, its expected performance, first experimental demonstration, and potential applications, can be found in Ref. [126]. Fig. 29 illustrates LiquidO’s performance using a

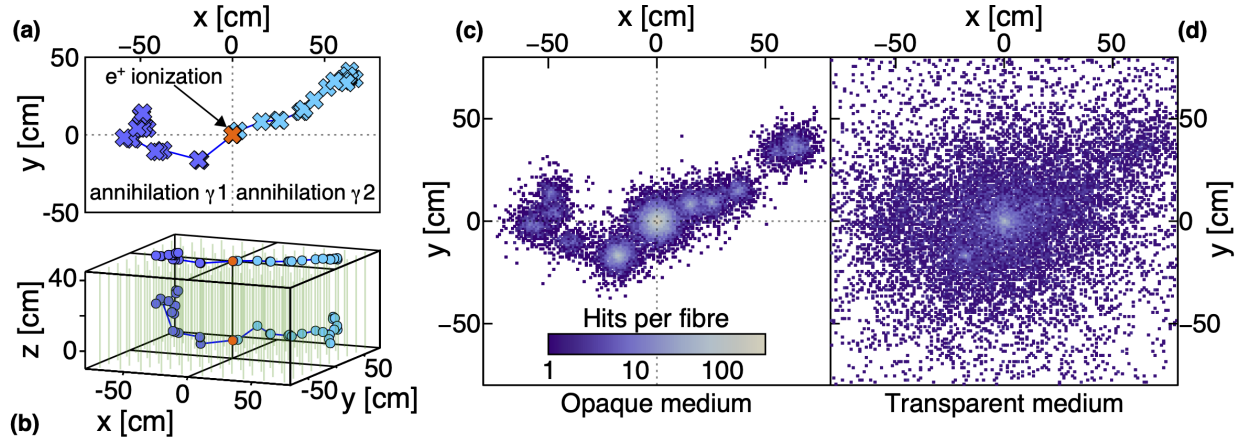


Figure 29: Left: energy depositions of a simulated 1 MeV kinetic energy positron in a LiquidO detector with a regular 1 cm fibre pitch running along the z direction. Panel (a) shows the x - y projection, while panel (b) shows the full three-dimensional extent. The fibres are represented in green. Right: true number of photons hitting the fibres, each of which is represented by a pixel, in the opaque and transparent scintillator scenarios. In the former case, the scintillator is assumed to have a 5 mm scattering length and a 5 m absorption length. Figure obtained from Ref. [126].

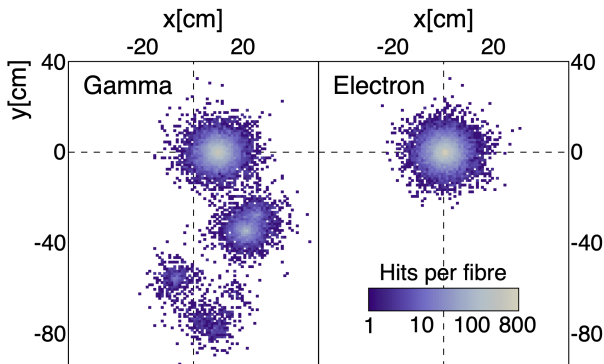


Figure 30: Simulated 2 MeV gamma (left) and electron (right) in the same detector configuration of Fig. 29. Figure obtained from Ref. [126].

simulated positron with 1 MeV of kinetic energy. Here, the simplest configuration with fibres running only along one direction (z) is assumed. The true energy depositions of the positron are shown on the left panels, with (a) showing the x - y projection and (b) the full three-dimensional extent. Panel (c) shows the number of true photons hitting each fibre in a 1-cm-pitch lattice when a scintillator with a 5 mm scattering length is used. The positron's loss of kinetic energy produces a light-ball at the vertex of the event. The two back-to-back gamma-rays resulting from its annihilation lose energy via Compton scattering, leaving two trails of smaller light balls that detach from the central one. A comparison is made in panel (d) of the light pattern collected by the same fibre array when using a transparent scintillator. Despite the use of fibres, the event topology is almost entirely washed out, illustrating the key role played by the scintillator's opacity in self-segmenting the detector.

The clear event topology of \sim MeV positrons in LiquidO stands in contrast with that of other events, as illustrated in Fig. 30. At these energies, gammas lose their energy primarily via the Compton effect and produce trails of light balls over many tens of cm, whereas electrons produce single light balls. At higher energies (more than ~ 10 MeV for electrons), charged particles have enough kinetic energy to travel several cm or more in the detector, producing sequences of point-like energy depositions that form clear tracks. As a result, many other interactions, from cosmic ray muons to charged and neutral current neutrino interactions of various energies, could also be precisely reconstructed in LiquidO. In this way, this detector technology combines some of the advantages of conventional liquid scintillator detectors with those of tracking detectors.

3.5.3 SLIPs

The construction of large-scale liquid scintillator detectors is complicated by the need to separate the scintillation region from photomultiplier tubes (PMTs) due to their intrinsic radioactivity. This is generally done using acrylic and/or nylon barriers, whose own intrinsic activity can also lead to substantial cuts to the fiducial detection volume for a number of low energy (MeV) studies. Such barrier constructions also become increasingly difficult and expensive for larger detector volumes, with JUNO already pushing the boundaries of what might be achievable. The SLIPS concept is to do away with such physical barriers entirely by instead mounting PMTs on the bottom of a wide cavity and covering them with a distillable, lipophobic liquid, above which a less dense scintillator is layered. Liquids such as various ethylene glycols are good candidates for the bottom layer as they provide a good refractive index match to a number of liquid scintillator solvents. Thin, opaque and highly reflective ($>90\%$) surfaces are used near the top and side areas of the detector to provide a buffer region against radioactivity from the walls and to reflect scintillation light back to the bottom PMT array, where the time-separated reflected signals are used to reconstruct the 3D vertex position as well as the event energy. A conceptual design can be seen in Figure 31. Initial simulation studies indicate that good position and energy reconstruction can be achieved with this approach. The notion is to use a shallow layer of scintillator relative to the cavity width, where the vertical depth of scintillator is chosen to be much less than the optical absorption length and can be optimised to balance fiducial volume, light level and reconstruction accuracy.

Initial simulations have been carried out assuming a densely packed array of R5912-100 HQE PMTs in a pillbox-shaped detector with a diameter of 50m, an ethylene glycol layer extending 2m above the PMTs, a scintillator layer composed of LAB + 2g/L PPO, and 90% specular reflective surfaces. Figure 32 shows the resulting number of detected photons from a 1 MeV electron as a function of event position for vertical scintillator heights of both 5m and 10m. These correspond to fiducial volumes of $\sim 8\text{kT}$ and 16kT , respectively.

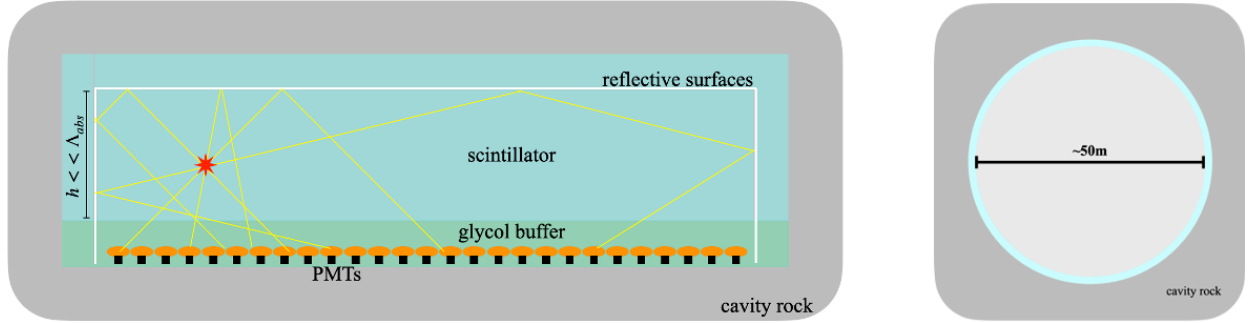


Figure 31: SLIPS design. Left - cross-sectional side view; right - top view.

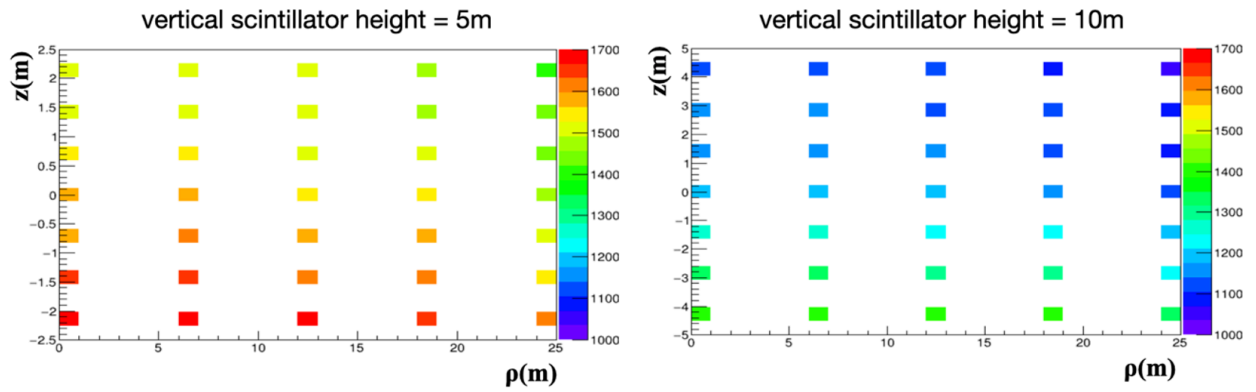


Figure 32: Detected number of photoelectrons for a 1 MeV electron for the simulated configuration as a function of ρ (cylindrical radius from the centre of the detector) and z (vertical height relative to the centre of the scintillator layer). The left plot is for a scintillator layer height of 5m and the right is for a height of 10m.

4 Low-Threshold Neutrino Detectors

Low-threshold neutrino detectors are opening up new avenues in low-energy neutrino physics. This section summarizes the ongoing and planned projects as well as their enabling detector technologies. Recent breakthroughs in lowering the nuclear-recoil thresholds all the way down to the 10 eV regime enables the exploration of coherent elastic neutrino-nucleus scattering (CE ν NS), which is a new portal to fundamental physics within and beyond the Standard Model of Particle Physics. The U.S.-based COHERENT experiment has set a milestone in 2017 with the first observation of CE ν NS and has triggered numerous experiments and extensive R&D programs worldwide. Those have the potential to fully exploit CE ν NS at spallation sources and at nuclear reactors within the next decade. The efforts will also lead to technological advances and potentially enable detector applications in science, industry and homeland security. Table 3 summarizes the many ongoing CE ν NS detectors and their enabling technologies.

Experiment	Enabling technology	$E_{th}(\text{NR})$	target material	mass	status	ν source
MINER [128]	phonon detectors	$\mathcal{O}(100\text{eV})$	Ge, Al ₂ O ₃	$\mathcal{O}(100\text{g})$	D/C	R
NUCLEUS [129–131]	phonon detectors	$\mathcal{O}(10\text{eV})$	CaWO ₄ , Al ₂ O ₃	$\mathcal{O}(10\text{g})$	D/C	R
RICOCHET [132]	phonon detectors	$\mathcal{O}(10\text{eV})$	Ge, Zn	$\mathcal{O}(1\text{kg})$	D/C	R
BULLKID [133]	phonon detectors	$\mathcal{O}(10\text{eV})$	Si	$\mathcal{O}(10\text{g})$	R&D	-
CONNIE [134]	CCD sensors	$\mathcal{O}(100\text{eV})$	Si	$\mathcal{O}(100\text{g})$	run	R
COHERENT [135]	cryog. scintillator	$\mathcal{O}(1\text{keV})$	CsI	$\mathcal{O}(10\text{kg})$	D/C	S
COHERENT [135]	HPGe	$\mathcal{O}(1\text{keV})$	Ge	$\mathcal{O}(10\text{kg})$	D/C	S
COHERENT [135]	scintillator	$\mathcal{O}(1\text{keV})$	NaI	$\mathcal{O}(1\text{ton})$	D/C	S
CONUS [136]	HPGe	$\mathcal{O}(1\text{keV})$	Ge	$\mathcal{O}(1\text{kg})$	run	R
Dresden [137]	HPGe	$\mathcal{O}(1\text{keV})$	Ge	$\mathcal{O}(1\text{kg})$	run	R
nuGen [138]	HPGe	$\mathcal{O}(1\text{keV})$	Ge	$\mathcal{O}(1\text{kg})$	run	R
TEXONO [139]	HPGe	$\mathcal{O}(1\text{keV})$	Ge	$\mathcal{O}(1\text{kg})$	run	R
NEON [140]	scintillator	$\mathcal{O}(1\text{keV})$	Ge	$\mathcal{O}(10\text{kg})$	run	R
SBC [141]	bubble	$\mathcal{O}(100\text{eV})$	lAr(Xe)	$\mathcal{O}(10\text{kg})$	R&D	R
NEWS-G [142]	gaseous	$\mathcal{O}(100\text{eV})$	Ne, CH ₄	$\mathcal{O}(100\text{g})$	run	-
COHERENT [143]	liquid noble	$\mathcal{O}(1\text{keV})$	lAr	$\mathcal{O}(10\text{kg})$	run	S
RED100 [144]	liquid noble	$\mathcal{O}(1\text{keV})$	lXe	$\mathcal{O}(100\text{kg})$	run	R
CHILLAX [145]	liquid noble	$\mathcal{O}(100\text{eV})$	lAr, lXe	$\mathcal{O}(10\text{kg})$	R&D	R/S
NUXE [146]	liquid noble	$\mathcal{O}(100\text{eV})$	lAr, lXe	$\mathcal{O}(10\text{kg})$	R&D	R

Table 3: Proposed detectors and enabling technologies for the exploration of CE ν NS. The order of magnitude of the projected or demonstrated nuclear recoil energy threshold $E_{th}(\text{NR})$ and the envisioned total target mass ("mass") are listed. The status is indicated as "R&D" (R&D phase), "D/C" (design or commissioning phase) and "run" (running experiment). If the project has a clear choice for the (anti)neutrino source, it is tagged by "PR" (power reactor), "RR" (research reactor) and "S" (spallation neutron source).

There are significant technological synergies of CE ν NS detectors with high-resolution detectors for direct neutrino mass measurements [147–149] in particular for multiplexed readout, see e.g. [150]. Furthermore, this section covers plenty of new ideas on future detector ideas to advance low-energy neutrino measurements by accessing new neutrino sources [151, 152], by entirely new detector concepts [153, 154], by exploiting new laboratories [155] and by establishing directional sensitivity [156, 157].

Furthermore, the striking mutual synergies of Dark Matter (DM) direct detection (Cosmic Frontier) and neutrino low-threshold detectors should be emphasized: on the one hand, the detector technology

currently been used or considered for $\text{CE}\nu\text{NS}$ measurements widely relies on the expertise gathered within the last decades in direct DM detection – both fields will highly profit from the currently blooming R&D efforts for $\text{CE}\nu\text{NS}$. On the other hand, a laboratory measurement of the $\text{CE}\nu\text{NS}$ cross-section will be essential to study solar neutrinos with future DM detector as well as to overcome the so-called neutrino-floor [158]. Successful laboratory $\text{CE}\nu\text{NS}$ experiments will further be an important tool to verify (“calibrate”) the DM detector technology by measuring a (fairly well) known neutrino signal.

4.1 Common challenges of low-energy neutrino detectors

To reach the ambitious physics goals of the next decade in low-energy neutrino physics, the enabling detector technology has to be continuously improved. The common technological and scientific challenges of low-threshold neutrino detectors can be summarized as follows:

- **Improving resolution and threshold:** one of the highest priority of current R&D effort is improving the performance of the individual devices, since low thresholds in the 100 eV (or even 10 eV and below) and sub-eV resolutions are a prerequisite for $\text{CE}\nu\text{NS}$ and direct neutrino mass measurements, respectively. What concerns cryogenic detectors there is extensive R&D on the optimization of transition-edge-sensors, the improvement of NTD phonon sensor readout and increasing the sensitivity of charge readout electronics. There has been enormous progress in lowering the thresholds of HPGe detectors and R&D programs to further improve the charge collection and the low-noise readout electronics are ongoing. Scintillation detectors, liquid noble gas detectors and bubble chambers profit from advanced photon sensors and imaging techniques, as well as detector material with improved light yield and improved light collection efficiencies.
- **Increasing detector mass:** Within the next decade low-threshold detector technology will enable precision physics at low energies, which requires larger detector masses. Typical phase1 $\text{CE}\nu\text{NS}$ experiments will need to be scaled up in mass by factors of 10-100. This implies either increasing the target mass at same performance (requires improved sensor technology, see above), or increasing the number of detectors significantly. Usually, parallelizing the readout by “simply” multiplying the number of single electronic readout channels is not feasible, independent of the respective detector technology. However, the multiplexing technology has become mature in recent years, under leadership of U.S. institutes finds application in TES arrays e.g. in astronomy. This technology is a promising tool for next generation $\text{CE}\nu\text{NS}$ experiments as well as for large scale direct neutrino mass experiments based on cryogenic detectors.
- **Reduction of backgrounds:** Since most of the low-threshold $\text{CE}\nu\text{NS}$ detectors for will be located at shallow depths, or even above ground as well as at radiogenically challenging environments (e.g. at reactors, accelerators), advanced background suppression and rejection techniques are needed. Promising techniques are: 1) Particle discrimination via 2-channel readout schemes (e.g. phonon-charge), pulse-shape discrimination, dual-phase TPCs or the different event topologies in bubble chambers and CCDs, 2) Passive shielding arrangements to moderate gamma and - in particular relevant at lowest energies - neutron radiation, 3) Active veto detectors that will act as large volume anti-coincidence detectors (e.g. HPGe detectors, liquid-scintillator) of instrumented detector holders that might veto stress-related events (in case of cryogenic detectors), 4) Highly-efficient muon vetos surrounding the setups, 5) Pulsed neutrino sources that provide a timing signal to increase signal-to-background, and - ultimately - 6) Directional sensitivity to specially separate the sources for background and signal. In this context, it should be empha-

sized that the sensitivity of most of the CE ν NS experiments is currently limited by the so-called low-energy Excess background [159]. A community-wide effort to understand and mitigate the Excess is absolutely required to reach the physics goals in the next decade.

- **Understanding the low-energy detector response:** In recent years energy reach of neutrino detectors has been lowered by more than one order of magnitude, however the energy range of 10eV to 1KeV is lacking robust and precise calibration, in particular what concerns nuclear recoils. Several calibration methods have been proposed: X-ray fluorescence sources, LED calibration, identification of low-energetic Compton edges, as well as low-energy neutrino scattering and exploiting neutron-capture reaction. Fundamental measurements to understand the detector signals at lowest energies are absolutely required and should be conducted as a community-wide effort with high priority.
- **Increase level of automatization** of experimental equipment for future applications of neutrino detectors in science, industry, and for society (e.g. reactor monitoring for nuclear proliferation via CE ν NS).

4.2 The eV frontier of neutrino detectors

4.2.1 Cryogenic particle detectors for CE ν NS

MINER: The Mitchell Institute Neutrino Experiment at Reactor (MI ν ER) experiment was launched to use cryogenic germanium and silicon detectors with a low nuclear recoil energy thresholds to register nuclear recoils of coherent elastic neutrino-nucleus scattering (CE ν NS) at a TRIGA research nuclear reactor at the Texas A&M University [128]. This reactor has a movable core (1 m to 10 m) that will allow precision studies of very short baseline neutrino oscillation by comparing rates as a function of distance and largely eliminating reactor flux uncertainties. Close proximity of the detector to the reactor core, combined with multiple low threshold detectors with event-by-event discrimination between the dominant electromagnetic background and the nuclear recoil signal provides sensitivity to BSM physics, sterile neutrinos that oscillate away on a few-meter scale, and above all a highly sensitive probe for applied reactor monitoring for safeguards and non-proliferation. Planned deployment of the MIN ν ER experimental set up at the South Texas Project (3 GW) power reactor will provide significant further improvement in measurement sensitivity.

NUCLEUS: The NUCLEUS experiment aims for a detection of CE ν NS using CaWO₄ cryogenic calorimeters with nuclear recoil thresholds around 20 eV. This unique feature demonstrated in an early prototype [129–131] will allow observation of the majority of tungsten recoils induced by reactor antineutrinos by accessing unprecedentedly low energies, taking full advantage of the coherent cross-section boost. The first experimental phase will deploy a 10 g cryogenic target [160] composed of approximately 6 g CaWO₄ and 4 g Al₂O₃ in a new experimental location [161] at the Chooz nuclear power plant in France. The two target materials feature widely different CE ν NS cross-sections but a comparable neutron response, useful for in-situ measurement of potentially dangerous nuclear-recoil backgrounds.

The experimental setup will consist of a dry dilution refrigerator, a compact passive shielding made of neutron moderators and lead, active muon [162] and gamma anticoincidence veto detectors as well as an integrated LED-based calibration system. The setup is under construction for commissioning in Munich in 2022 before deployment at the reactor site planned from 2023 on.

Ricochet: The Ricochet neutrino experiment aims to measure neutrinos produced from nuclear reactors by using cryogenic bolometers to identify the signature nuclear recoil from $\text{CE}\nu\text{NS}$ [132]. In order to overcome the high level of electromagnetic background present at low energies, Ricochet will make use of particle identification in order to discriminate between electron and nuclear recoils. The future Ricochet experiment will be deployed at the ILL-H7 site in Grenoble, France. The H7 site starts at about 8 m from the ILL reactor core that provides a nominal nuclear power of 58.3 MW, leading to a neutrino flux at the Ricochet detectors 8.8 m from the reactor core of about $1.2 \times 10^{12} \text{ cm}^{-2}\text{s}^{-1}$. The experiment will make use of two detector technologies/targets. The CryoCube will consist of an array of 27 ($3 \times 3 \times 3$) high purity germanium crystal detectors, encapsulated in a radio-pure infrared-tight copper box suspended below a lead shield inside the cryostat [163]. Q-Array – the complimentary detector array within Ricochet – will consist of 9 cubes of superconducting zinc cubes, each with a mass of about 35 g, as its target. Using superconductors as the primary detector is a novel technology which is expected to provide detection sensitivity theoretically down to the Cooper pair binding energy. The expected discrimination mechanism begins with the different efficiency of quasiparticle (QP) production (breaking Cooper pairs) by electron recoils (higher QP production) vs. nuclear recoils (lower QP production). Ricochet is currently scheduled to see “first light” in 2023.

BULLKID is a R&D project on cryogenic detectors for $\text{CE}\nu\text{NS}$ and light Dark Matter [133]. By exploiting the high multiplexing levels of kinetic inductance detectors, goal of BULLKID is to create a monolithic and highly-segmented array of silicon targets with energy threshold on nuclear recoils around 100 eV and total mass of 30-60 g. In future experiments several arrays would be produced and stacked to obtain target masses exceeding 1 kg.

Cryogenic Carbon Detectors have various advantages: They have good isotopic purity, outstanding radiation hardness, and excellent phonon properties and dynamics due to the particularly strong carbon bonds. In their tetrahedral forms have the highest sound speeds and most energetic optical phonons of any known crystals. These properties are expected to yield a significant improvement in energy sensitivity relative to more conventional semiconductors, thus enabling detection thresholds in the meV to eV energy range [164, 165]. Finally, much of the thin-film phonon-readout technology developed for germanium and silicon can be applied to diamond with minimal modification. Initial work on diamond and SiC particle detectors is promising, and a Transition Edge Sensor (TES) readout on a diamond sample was recently demonstrated with comparable performance to sapphire [166].

Phonon-mediated KIDs Athermal (meV-scale) phonons in sub-Kelvin target materials can be produced by such small energy depositions, and superconducting kinetic inductance detectors (KIDs) can sense these meV phonons, with long-term potential for even single-phonon sensitivity. The inherent multiplexability of KIDs also makes them ideal for recovering position information from phonons. Different architectures are appropriate for different applications. In the case of low-mass dark matter (sub-GeV nuclear- and electron-scattering particles and sub-eV dark photons and axion-like particles (ALPs)), thresholds at the meV scale are eventually needed, motivating small individual detectors with a single KID sensor, exploiting the energy resolution potential of KIDs. For coherent elastic neutrino-nucleus scattering of solar and reactor neutrinos, information about recoil type (nucleus or electron) and position are as important as energy resolution, motivating larger individual detectors instrumented with many KIDs.

4.2.2 CCD-based detectors for CE ν NS

CONNIE: The Coherent Neutrino-Nucleus Interaction Experiment (CONNIE) uses low-noise fully depleted charge-coupled devices (CCDs) with the goal of measuring low-energy recoils from CE ν NS of reactor antineutrinos with silicon nuclei [134]. The CCD detectors can operate at a electron recoil threshold of approximately 30 eV, where the conversion from electron equivalent to silicon recoil energy is given by the so-called quenching factor, from which measurements at low energies (≈ 0.7 keV) and new theoretical approaches are used [167–169]. CONNIE has reported results from its analysis with a detector array of 8 CCDs with a fiducial mass of 36.2 g, and a total exposure of 2.2 kg-days. In an analysis of the difference between the reactor-on and reactor-off spectra, no excess events are found at low energies, yielding upper limits at 95% confidence level on the CE ν NS rate. In the lowest-energy range analyzed by CONNIE, 50 – 180 eV, the expected limit is 34 (39) times the standard model prediction, depending on the assumed quenching factor.

ν IOLETA is a future experiment [170] that will measure reactor antineutrinos and their physical properties through two channels: neutrino-electronic interaction and Elastic Coherent Neutrino Nucleus interaction. This experiment will use the new Skipper-CCD technology that achieves sub-electronic readout noise and a detection threshold in the eV range. Two positions were identified to place ν IOLETA within the Atucha II Nuclear Power Plant in Argentina, 8 and 12 meters away from the center of the reactor core.

4.2.3 Detectors for neutrino mass

Project8 is an experiment designed to measure the absolute neutrino mass using cyclotron radiation emission spectroscopy (CRES) [147]. In addition to probing the electron-weighted neutrino mass through endpoint investigations, beta-decay spectrum measurements can also be used to study other neutrino properties that affect the spectrum shape. The Project 8 experiment plans to improve on the existing tritium beta-decay measurements in two different ways: by measuring beta-decay of atomic tritium and by using the CRES technique for spectrum measurement. The former reduces the systematic effects associated with the decay of molecular tritium [2], while the latter allows for a high-statistics differential spectrum measurement with excellent energy resolution over a range of energies. Leveraging these unique capabilities, Project 8 is projected to achieve m_β sensitivity of ~ 0.040 eV (90% C.L.). The advantages of the CRES method and the use of atomic tritium generally also extend to the rest of the measured spectrum, equipping Project 8 with unique access to other secondary physics capabilities.

Future large-scale ^{163}Ho experiment: The electron capture decay of ^{163}Ho provides an attractive system for kinematic measurements of the electron neutrino mass. When ^{163}Ho is embedded in a calorimetric sensor, each decay deposits energy in the sensor equal to the Q-value of the reaction minus the energy of the departing neutrino. The rest mass of the neutrino is manifested as a deficit of events in the region of the decay spectrum near the Q-value. ^{163}Ho is particularly attractive because of its low Q-value of 2.833 keV and its reasonable half-life of 4570 years [171]. The ECHO collaboration has demonstrated decay spectra with 275,000 counts using a small array of magnetic microcalorimeters [148] and is presently analyzing data corresponding to a spectrum with about 10^8 counts. The HOLMES collaboration is developing multiplexed transition-edge-sensors (TESs) for this purpose [149]. An international collaboration between groups in the US and Europe is an attractive path to execute a large-scale ^{163}Ho experiment. While work on ^{163}Ho in Europe is presently more

mature than in the U.S., the U.S. community is leading on multiplexed readout [150] and has excellent facilities for fabricating cryogenic detectors and SQUID multiplexers. This technology has large synergies with the CEvNS R&D program and will enable an up-scaling of the detector mass of cryogenic detectors using TES sensors.

4.2.4 Future detectors for relic neutrinos

PTOLEMY is designed to be the first instrument to detect neutrinos created in the early moments of the Big Bang based on the concept of neutrino capture on β -decay nuclei as a detection method for the Cosmic Neutrino Background (CNB). An experimental realization of the concept for CNB detection was proposed based on PTOLEMY [151] in 2013. The parameters for a relic neutrino experiment require 100 grams of weakly-bound atomic tritium, sub-eV energy resolution commensurate with the most massive neutrinos with electron-flavor content, and below microHertz of background rate in a narrow energy window above the tritium endpoint. The PTOLEMY experiment aims to achieve these goals through a combination of a large area surface-deposition tritium target, MAC-E filter methods, cryogenic calorimetry, and RF tracking and time-of-flight systems.

4.2.5 New detector concepts

Paleo-detectors use the nuclear damage tracks recorded in natural minerals over geological time-scales to detect weakly-interacting particles over exposures much larger than what is feasible in conventional terrestrial detectors [153, 172]. Unlike conventional experiments which measure nuclear recoils in real time, paleo-detectors measure the number of events integrated over the age of the mineral, reaching up to a billion years for minerals routinely found on Earth. The sources of the keV-scale nuclear recoils which can be recovered as tracks is rich, including atmospheric neutrinos [173], solar neutrinos [174], supernova neutrinos [175], as well as dark matter [176, 177]. Low-energy neutrino and dark matter tracks are initiated dominantly via CE ν NS (quasi-elastic charged-current interactions are more applicable for high-energy neutrinos).

PALEOCCENE: This concept [154, 178] aims to exploit the crystal defects caused by nuclear recoil by using an optical readout scheme based on the imaging of individual color centers. The resulting detectors would be room-temperature, passive devices with recoil thresholds close to the threshold damage energy of the detector material of 100 eV or less. The project is in the early stages of R&D.

Neutrino Spacecraft: The idea of new Science using a neutrino detector spacecraft [155], which is of interest to NASA and DOE elementary particle physics, is discussed in the context of two physics scenarios: the detection of solar neutrinos at close distance to the Sun, and the search for dark matter at the outskirts of the Solar system. It is possible to detect far more solar neutrinos by going closer to the Sun and at 7 solar radii distance the solar neutrino flux would be 1000x that on Earth and at 3 solar radii 10,000x that on Earth. This would result in the need for a smaller detector to do the same things that large detectors on earth do and a 1 ton detector need only be 1 kg at 7 solar radii. Other science that can be done with a spacecraft capable of detecting neutrinos in space are that solar neutrino backgrounds in dark matter searches go down as the detector goes away from the Sun and at Jupiter a 10x reduction is expected and 100x reduction at Uranus. Furthermore, there are ideas to study the gravitational focus of the sun for neutrinos to image exoplanets. The feasibility of the physics scenarios mentioned above depend crucially on the ability to operate detectors in unshielded space.

Snowball detectors: A new detector technology proposed, the so-called “Snowball Chamber,” is based on the phase transition (of liquid to solid) for metastable fluids. A water-based supercooled detector [179] has the potential to move past the Neutrino Floor, and extend the reach of direct detection dark matter experiments and has also applications within CEvNS.

4.3 Optimized conventional detectors to exploit CEvNS

4.3.1 HPGe detectors

COHERENT-HPGe: Continued development over the past decade of P-type Point-Contact (PPC) High-Purity Germanium (HPGe) detectors has resulted in devices with masses in excess of 2 kg each and sub-keV energy resolution and thresholds [180]. Combined with the well-understood systematics and measured quenching factors, the resolution allowed by PPC detectors enables precision measurements of spectral shape distortions due to nuclear form factors or new physics. The drawbacks of these detectors are primarily in their relatively high cost to manufacture, and in the case of SNS operation, the limited timing resolution afforded due to the wide range of drift times in larger mass detectors (up to $\sim 2\mu\text{sec}$). Currently, the COHERENT Collaboration is deploying an array of 8 PPC germanium detectors with a total mass in excess of 16 kg. To enable a next-generation effort, we propose the development of new classes of PPC detectors with larger masses and a narrower range of drift lengths, while maintaining reasonable depletion/operating voltages and the low-noise performance that enables excellent energy resolution and low thresholds.

CONUS: The CONUS (COherent elastic Neutrino nUcleus Scattering) experiment employs four 1 kg low energy threshold high-purity point-contact Germanium detectors to look for CE ν NS. The experiment is located at the commercial nuclear power plant of Brokdorf, Germany, in a distance of 17.1 m from the reactor core with a maximum thermal power of 3.9 GW. With the electrically cooled spectrometers an energy resolution of 150-160 eV (ionization energy, full width at half maximum ionization energy) at the 10.4 keV K-shell X-ray of $^{71}\text{Ge}/^{68}\text{Ge}$ is achieved [181]. The energy threshold is $\leq 1.875\text{ keV}$ for nuclear recoils. With the onion-like shield consisting of layers of lead, borated polyethylene and a muon anti-coincidence veto a background level of $\sim 10\text{ counts/kg/d}$ below 1 keV ionization energy is achieved at reactor site [182]. With the data collected in 2018 and 2019 an upper limit on CE ν NS was derived in dependence of the quenching factor (ratio between detected ionization energy and recoil energy) in germanium [136]. For a quenching factor of $k=0.16$, this corresponds to a limit of 0.34 kgd^{-1} at 90% confidence level (factor 17 above the standard model prediction). The quenching factor for germanium at low recoil energies is not well known and large discrepancies between the existing measurements persist. Recently, the CONUS collaboration carried out an own quenching measurement [183] to significantly reduce this major systematic uncertainty.

Dresden: The experiment consists of a low-noise 3 kg p-type point contact germanium detector which has been installed and operated at the Dresden-II power reactor, near Chicago, at about 10 meters from its 2.96 GW_{th} core [137]. The detector are enclosed by a compact shielding made of several layers of active vetos and passive shielding material. The results from an upgraded setup suggest a preference for a CE ν NS component in the data, when being compared to a background only model [184].

nuGen: The nuGEN experiment aims at the detection of CE ν NS with low-background, low-threshold HPGe detectors installed at a distance of $\sim 10\text{ m}$ to one of the 3.1 GW_{th} reactors at the Kalinin Nuclear

Power Plant (KNPP) in Russia. The detectors are surrounded by a compact passive shielding and an active muon veto, which are installed on a movable platform to modify the distance to the reactor core. nuGEN has been installed on-site in 2019 and preliminary data from first science runs have been presented [138].

TEXONO: The TEXONO collaboration has been studying neutrino physics with sub-keV germanium detectors at the Kuo-Sheng Reactor Neutrino Laboratory (KSNL) in Taiwan [139]. There is a national policy of de-commissioning nuclear power in Taiwan, and the Kuo-Sheng Reactor will be phased out by 2023. As a result, there are no plans on expansion or new projects to the KSNL program. The collaboration would seek to continue the studies via collaboration with other existing reactor laboratories. Data taking and R&D program are conducted with electro-cooled (EC) point-contact germanium detectors (PCGe). As of summer 2020, detector mass up to 1.43 kg are built and threshold as low as 200 eV ee is achieved. The data would also bring improved sensitivities to the searches on various Beyond Standard Model (BSM) physics channels, such as neutrino magnetic moments [185] and milli-charged neutrinos [186]. Active theory program is being pursued in parallel, with focuses on atomic corrections to νN (and χN for dark matter) cross-sections [186], as well as BSM searches.

4.3.2 Photon-based low-threshold detectors

COHERENT-CsI: The COHERENT collaboration is performing R&D towards optimizing low threshold cryogenic scintillators. The most serious limitation in reducing the energy threshold of the COHERENT CsI(Na) detector was the Cherenkov radiation originated from its PMT quartz window by natural radiation and cosmic rays, which can be eliminated by replacing PMTs with SiPM arrays. Cryogenic operation is needed to reduce the dark count rate of SiPM arrays, which also calls for the replacement of doped crystals with undoped ones due to much higher intrinsic light yield of the latter. The light yield of such a combination is expected to be at least 4 times higher than that of the CsI(Na) detector, and the energy threshold would be at least three times lower. With such a low threshold, even a ~ 10 kg prototype can detect a thousand CEvNS events annually.

NEON: The Neutrino Elastic-scattering Observation on NaI(Tl) (NEON) experiment uses high-light yield NaI(Tl) crystals to observe the CE ν NS events at a distance of 24 m from the core of the Hanbit nuclear reactor in Korea. This experiment utilized the previous experiences of the NaI(Tl) crystal detectors for the COSINE-100 dark matter search experiments [187,188]. The NaI(Tl) detector used in the COSINE-100 experiments showed a light yield of 15-photoelectrons/keV [189], and a multivariate machine learning technique was used to effectively remove the noise event caused by PMT to reach a low energy threshold of 1 keV [190]. Preliminary studies to lower the energy threshold achieved 0.5 keV energy event access with 80% selection efficiency and 25% noise contamination level. In addition, a novel encapsulation method of the NaI(Tl) crystals with improved light collection efficiency up to 22 photoelectrons/keV [191] has been developed. Energy thresholds of less than 0.3 keV can be achieved with these detectors. The first phase NEON experiment (NEON-pilot) was built with a 2×3 array of 6 detectors with a total mass of 15 kg using the commercial quality crystals while the next phase experiment (NEON-1) may use up to 100 kg of the low-background NaI(Tl) crystals [192]. The NEON-pilot crystals were immersed in an 800-L liquid scintillator. It was shielded with 10-cm-thick leads and 30-cm-thick polyethylene. The shields and DAQ systems closely follows the COSINE-100 dark matter experiment [189,193].

COHERENT-NaI: The COHERENT collaboration is currently constructing a multi-tonne modular array of re-purposed thallium-doped, 7.7 kg NaI crystals [135]. Each module of 63 crystals provides

485 kg of detector mass. The current phase consists of the sectional deployment of 5 modules for a 2.4 tonne detector designed using dual-gain bases on the photomultiplier tubes to measure the low-energy CEvNS signal ($\sim 3\text{--}25\text{ keV}_{ee}$) simultaneously with the high-energy (10–50 MeV) charged-current signal on ^{137}I . Background studies with the NaIvE-185 detector array of 24 crystals deployed in Neutrino Alley since 2016, indicates that environmental and intrinsic backgrounds are sufficiently low for a successful CEvNS measurement. Recent quenching-factor measurements and a calibration scheme will address nonlinearity issues for low-energy signals. Initial charged-current studies with the NaIvE-185 detector will inform the analysis of the NaI Tonne-scale Experiment (NaIvETe) neutrino scattering measurement on ^{127}I . The future deployment of an additional two modules will bring the NaIvETe mass total to 3.4 tonnes.

COHERENT-D2O: One of the dominant systematics of the COHERENT measurements are neutrino flux uncertainties. To benchmark the neutrino flux, COHERENT plans to construct a 1300-kg D_2O detector in two modules. Its operation is based on detecting Cherenkov light from CC electron neutrino reactions with d. Each module will consist of an upright cylinder, with D_2O contained inside a central acrylic cylinder, contained inside a steel tank with 10 cm of H_2O tail catcher. Twelve PMTs view the volume from above. With the theoretical cross section known at the 2–3% level [194], it has the potential to significantly improve the overall systematic uncertainties of the experiment. More than 500 CC neutrino-deuterium events per module per SNS beam-year are anticipated.

4.3.3 Bubble chambers

SBC: The SBC (Scintillating Bubble Chamber) Collaboration is developing novel liquid-argon bubble chambers for GeV-scale dark matter and CEvNS physics [141,195]. The first detector, SBC-Fermilab, with 10-kg active mass, is currently under construction for characterization and calibration in the NuMI tunnel at Fermilab, aiming to reach a threshold for nuclear recoils of 100 eV. The detector consists of a quartz jar filled with superheated liquid argon, which is spiked with ppm levels of xenon acting as a wavelength shifter. Cameras are used to image bubbles, silicon photo-multipliers detect scintillation, and piezo-acoustic sensors listen for bubble formation. A duplicate detector constructed with low-background components, SBC-SNOLAB, will follow for a search for 0.7–7 GeV dark matter. Following this initial program, a deployment of one of these detectors after ~ 2024 at a nuclear reactor could make a high signal-to-background measurement of reactor neutrino CEvNS. Sensitivity to the weak mixing angle, neutrino magnetic moment, and a Z' gauge boson mediator have been calculated for deployments at both a 1 MW research reactor and a 2 GW power reactor [196]. Background characterizations are ongoing at the 1 MW TRIGA Mark III research reactor located at the National Institute for Nuclear Research (ININ) near Mexico City for a potential first reactor deployment 3 m from the core.

4.3.4 Gaseous detectors

NEWS-G is a direct dark matter detection experiment, sensitive to light Dark Matter (DM) between 0.1 and 10 GeV/c^2 . NEWS-G uses a spherical gaseous detector, the Spherical Proportional Counter (SPC) [142]. The SPC's features that make it ideal for light DM searches make it also appealing for the detection of neutrinos through CEvNS. The study of CEvNS with a sub-keV energy threshold detector, like the SPC, allows for a rich physics program and opens a window to physics beyond the Standard Model that will appear as deviations from the expected recoil spectra predicted by SM interactions [197]. The detector is composed of a spherical shell made of radio-pure copper, acting as the cathode, and a read-out sensor at the center with either a single anode [198] or multiple

anodes [199, 200]. The detector is versatile and can operate with a wide variety of gas mixtures. The SPC exhibits several features, such as: simple, few component build; very low energy threshold (single ionization electron level) independent of detector size [201]; and fiducialization and event discrimination through pulse shape analysis. NEWS-G plans to construct a 60 cm diameter sphere made of ultra-pure copper for CE ν NS studies. The detector will be encased in a shielding inspired from the GIOVE [202] and CONUS [203] experiments. A muon veto will complete the shielding apparatus. The experimental setup will be installed at Queen’s University, Kingston, Canada, to assess the environmental and cosmogenic backgrounds and to establish if any alterations are required for operations in the proximity of a reactor. The construction of the shield will start in fall 2020 and commissioning at Queen’s University is expected to take place by summer 2021.

ArgonTPC: This R&D program intends to study the feasibility of, and help achieve the measurement of nuclear recoil (NR) directionality by tracking their ionization signatures in gaseous argon TPCs. The goal is to develop detectors capable of tracking the O(10-100) μm ionization tracks produced by O(10-100) keV NRs from CE ν NS interactions in gaseous argon employing high-granularity GEM-based GAr TPCs. Such a detector would enable a broad range of physics measurements in focused neutrino beams of O(100) MeV neutrinos as well as high-intensity stopped pion neutrino sources which are currently available or will be operational in the coming years at facilities such as the SNS at Oak Ridge National Lab and in Fermilab’s next-generation neutrino beamline. A particularly interesting scenario would envision augmenting, through this effort, a DUNE-like GAr TPC detector in order to measure CE ν NS interactions from sub-100 MeV neutrinos in a future underground near-detector experimental hall at Fermilab.

4.3.5 Liquid noble gas detectors

COHERENT-LAr: The COHERENT collaboration is developing Liquid argon (LAr) detectors, with focus on reducing energy thresholds and understanding the LAr detector response to make the technology ready for CE ν NS measurements. COHERENT has performed detailed studies of the 24 kg fiducial mass CENNS-10 LAr scintillator detector [143] and performed the first detection of CE ν NS in a light nucleus, advancing the understanding of neutrino-nucleus interactions and constraining non-standard interactions. Detailed background studies and lowering the scintillation threshold were crucial for these results, laying the groundwork for the 610 kg fiducial mass CENNS-750 detector [204]. The CENNS-750 detector will provide precision measurements of the CE ν NS cross section on argon. Novel techniques are pursued, including the study of high-efficiency PMTs and SiPMs to reduce thresholds, and explore highly-segmented photodetector geometries to improve event selection and particle ID.

RED-100: RED-100 is a two-phase xenon emission detector built to observe the coherent elastic scattering of reactor electron antineutrinos off xenon atomic nuclei [144]. The mass of the detector medium is 160 kg in the sensitive volume, and about 100 kg in the fiducial volume — the largest value among detectors developed for CE ν NS observations at reactors. The capability of detector full-scale operation in the background conditions caused by cosmic radiation has been demonstrated in a ground-level laboratory [205]. The detector was deployed at the Kalinin NPP in 2021 at 19 m distance under the 3 GW reactor core (50 m.w.e. overburden) and acquired both reactor on and off data in January and February of 2022 with an energy threshold of about 1 keV $_{nr}$.

CHILLAX: The CoHerent Ionization Limit in Liquid Argon and Xenon (CHILLAX) project is an experimental effort to develop a xenon-doped argon ionization detector that can enjoy the benefits of both argon and xenon [145]. Thanks to the relatively small atomic mass, an argon atom can pick up more kinetic energy from neutrino scatters than heavier elements can, and by doping it with xenon – which has lower excitation/ionization energy and faster scintillation than argon does – the detector can be more efficient in producing ionization electrons from CE ν NS interactions and also generate detectable light signals with long wavelength and fast decays. Combining an argon target with a xenon detector-like performance, CHILLAX aims to develop the ideal large-mass noble liquid CE ν NS detector. With an expected energy threshold of 200-300eV, CHILLAX may detect a few times less CE ν NS interaction signal per kilogram than what is possible in eV-threshold detectors, but thanks to the scalability of the noble liquid technology CHILLAX can easily achieve an active mass of tens of kilogram and be a leading competitor in rate-oriented CE ν NS applications. CHILLAX is currently focusing on developing the first generation prototype detector. Once the xenon-doping benefits and low-energy sensitivity are experimentally demonstrated, we plan to build a ~ 50 kg detector to deploy either at the SNS (for BSM physics studies) or near a reactor (for sterile neutrino search and reactor monitoring demonstrations).

NUXE: The NUXE experiment will use a liquid xenon detector to observe reactor neutrino CE ν NS events down to single ionization electron signals [146]. The experiment is currently under development at UC San Diego with a 30-kg liquid xenon target in an electron counting chamber (ECC). Major effort is reducing the background down to the single electrons, corresponding to a nuclear recoil energy threshold of ~ 300 eV [206].

4.4 Dark Matter detectors for next-generation neutrino measurements

Neutrinos from the astrophysical sources like the Sun and supernovae as well as from the atmospheric cosmic-ray-showers produce nuclear recoils via CE ν NS, leading to signals in future dark matter detectors (see [207]). The eventual presence of an unshieldable background in multiton-scale dark matter detectors has been anticipated for some time [208–214], and is thought to present a major obstacle for improving the sensitivity of these experiments. The central problem is that for many of the most commonly sought-after dark matter models produce nuclear recoil signals that look remarkably similar to the CE ν NS recoil energy spectra generated by natural neutrino sources. Due to the finite systematic uncertainty on the fluxes of those sources eventually a feeble-enough DM signal could disappear under the expected variation in the neutrino event rate, and because its signal would not be distinct enough from the background no positive identification of dark matter would be possible. Naively this implies that there is a “floor” to the sensitivity of direct detection experiments [158].

Since the dark matter and CE ν NS signals are not exactly identical— it is not impossible to search for dark matter in the presence of a CE ν NS background, but it does entail significant reduction in experiment’s sensitivity. This observation has been called “neutrino fog” [215]. Neutrino floor considerations play an important role when considering the feasibility of future experiments, as decreased sensitivity to DM signals in vicinity of neutrino background also hinder the increase in experimental sensitivity with scaling in detector exposure (e.g. [214, 216]). There are several approaches for circumventing the neutrino floor if an experiment can access additional information to further discriminate the dark matter signal and neutrino background, including the use of annual modulation [217], target complementarity [214, 218–220], and directionality [156, 221–227].

4.4.1 Multi-ton liquid noble detectors

XENON: The XENON1T experiment operated a dual-phase time projection chamber (TPC) filled with 3.2 tonnes of ultra-pure liquid xenon (LXe). The TPC contained 2.0 tonnes of LXe that is sensitive to ionization electrons (S2) and scintillation photons (S1) produced by interactions therein. In a fiducial volume with 1.0 tonnes of LXe, a background level down to (76 ± 2) events/(tonne \times year \times keV) has been achieved. A WIMP dark matter search lasted from December 2017 to February 2018. Using this data, the XENON collaboration has performed a first sensitive search for solar ^8B neutrinos through nuclear recoils from the $\text{CE}\nu\text{NS}$ process [69]. ^8B $\text{CE}\nu\text{NS}$ leads to an average nuclear recoil energy of ~ 1 keV, requiring unprecedented low energy thresholds in identifying scintillation and ionization signals. In this analysis, the threshold in ionization and scintillation signals was lowered down to 4 electrons and 2 photon-electrons, respectively. With an exposure of 0.6 tonne \times year, the expected $\text{CE}\nu\text{NS}$ signal is 2.1 events with a background expectation of 5.4 events, dominated by the accidental pileup of isolated-S1 and isolated-S2 signals. The mean discovery power of ^8B $\text{CE}\nu\text{NS}$ is 2σ , limited by the exposure of this experiment. No significant excess from ^8B $\text{CE}\nu\text{NS}$ is found in XENON1T.

LUX-ZEPLIN: LUX-ZEPLIN (LZ) is a dual-phase xenon TPC with a 7-tonne active mass located 1 mile underground at the Sanford Underground Research Facility (SURF) in Lead, South Dakota. The LZ detector was designed to search for interactions of particle dark matter in the mass range from 1 GeV/ c^2 to 10 TeV/ c^2 . Because the $\text{CE}\nu\text{NS}$ process can produce low-energy nuclear recoil signals similar to those produced by low-mass WIMPs, LZ will also be sensitive to astrophysical sources of neutrinos such as solar ^8B neutrinos and atmospheric neutrinos. Over the full 15.34 tonne-year exposure, LZ is expected to observe 0.65 events from atmospheric neutrinos and 36 events from ^8B neutrino in its WIMP search campaigns [228]. A positive detection of ^8B $\text{CE}\nu\text{NS}$ signals will be an unambiguous confirmation of LZ's low-mass WIMP sensitivity. As the $\text{CE}\nu\text{NS}$ mechanism is insensitive to neutrino flavors, LZ's measured flux provides a data point complementary to large solar neutrino experiments that rely on charge-current interactions. The observable rate of ^8B $\text{CE}\nu\text{NS}$ in LZ depends strongly on the detector energy threshold. LZ relies on the detection of scintillation and ionization signals produced by particle interactions in the active liquid volume.

DARWIN: DARWIN (DARK matter WImp search with liquid xenoN) is a proposed next-generation dark matter experiment that will operate 50 t (40 t active) of xenon in a cylindrical time projection chamber with 2.6 m in diameter and height [71]. The TPC will be placed in a double-walled cryostat vessel surrounded by neutron and muon vetoes. While DARWIN's primary goal is to observe particle dark matter in the ~ 1 GeV-100 TeV mass range, it will also be able to measure the solar ^8B neutrino flux, as well as atmospheric and supernovae neutrinos via $\text{CE}\nu\text{NS}$. The expected ^8B neutrino rate is ~ 90 events/(tyr) [229, 230], depending on the achieved energy threshold. The measurement of the atmospheric neutrino flux requires a large exposure of about 700 t yr [231]. A DARWIN-like detector would be able to observe astrophysical neutrinos of all flavours from core-collapse [232], as well as failed core-collapse and thermonuclear runaway fusion [233] supernovae. Typically, about 100 events are expected from a core-collapse supernova at a distance of 10 kpc and a $27 M_\odot$ progenitor mass [232]. The detection of neutrinos from failed core-collapse supernovae would deliver the time when the proto-neutron star collapses into a black hole [233] and, in conjunction with the detection of gravitational waves, would identify the progenitor of a failed supernova. Finally, a large xenon detector such as DARWIN would dramatically improve the sensitivity to the diffuse supernova neutrino background

(DSNB) in the ν_x channel, where $\nu_x \subset (\nu_\mu, \nu_\tau, \bar{\nu}_\mu, \bar{\nu}_\tau)$ [234]. While there are strong upper limits on the $\bar{\nu}_e$ flux from Super-Kamiokande, of $2.7 \text{ cm}^{-2}\text{s}^{-1}$, the limits on ν_x are about three orders of magnitude weaker. DARWIN would be able to reach a sensitivity of $\sim 10 \text{ cm}^{-2}\text{s}^{-1}$ per flavour. While this is not sufficient for a detection, such a constraint would exclude many DSNB scenarios with new astrophysics or physics [234].

4.4.2 Large-scale cryogenic detectors

SuperCDMS SNOLAB: SuperCDMS SNOLAB is a dark matter search focused on the 0.5–5 GeV mass range [235, 236]. It will use two kinds of cryogenic solid-state detectors. The first type, iZIP detectors, will have the capacity to discriminate nuclear recoils from electron recoils via measurement of athermal phonons and ionization production down to 1–2 keV recoil energy. The second type, HV detectors, will use a high drift field to transduce the charge signal into athermal phonons, provide a recoil energy threshold about $10\times$ lower, though without the ability to discriminate nuclear recoils. These thresholds should enable the detection of ^8B neutrino CEvNS in a solid-state detector for the first time, albeit with low statistics. The experiment is currently under construction at SNOLAB and anticipates beginning to acquire data in late 2023.

Going forward, the SuperCDMS Collaboration anticipates extending its scientific reach for dark matter with the SNOLAB facility primarily through detector improvements that will provide access to much lower energy recoils [236]. (Modest background upgrades will also be implemented.) This work will provide sufficiently low threshold to detect CEvNS of solar neutrinos from the CNO, *pep*, ^7Be , and even *pp* reaction chains, going well past the ^8B neutrinos detectable in SuperCDMS SNOLAB. In particular, with the 0.5 eV threshold anticipated for 25-gram Si detectors operated with phonon-only readout at 0V bias (i.e., neither iZIP nor HV, and smaller in mass than the kg-scale SuperCDMS SNOLAB detectors), the rate of solar neutrino events will be roughly 0.01/kg-day. With anticipated exposures of 12–240 kg-yr, there will be the potential to detect tens to hundreds of *pp* chain CEvNS events. These events will compete with a background of coherent photonuclear scattering, which can be modeled well based on measurements of Compton scattering at high energies, and with environmental backgrounds such as vibrations, RF noise, infrared and blackbody radiation, etc., which will be explored and better understood during SuperCDMS SNOLAB.

RES-NOVA: RES-NOVA is a newly proposed experiment for the detection of neutrinos from astrophysical sources [152]. RES-NOVA will employ an array of archaeological Pb-based cryogenic detectors sensitive to SN neutrino emission from the entire Milky Way Galaxy. Its modular design will be suited for the detection of nearby SN explosions ($<3 \text{ kpc}$) [237].

4.4.3 Directional detectors

DRIFT: The goal of the Directional Recoil Identification From Tracks (DRIFT) collaboration was the detection of a directional signal from Weakly Interacting Massive Particle (WIMP), halo, dark matter [238]. In order to accomplish this goal a unique, low-pressure, Negative Ion Time Projection Chamber (NITPC) technology was developed. The negative-ion drift allowed DRIFT NITPCs to have the lowest energy threshold and best inherent directional sensitivity of any limit-setting, directional dark matter detector. With its unique directional and background rejection capabilities, the DRIFT NITPC technology is ideally suited to search for nuclear recoils in beam dump experiments (BDX-DRIFT). A 1 m^3 $\nu\text{BDX-DRIFT}$ detector run for one year in the DUNE Near Detector Complex is

estimated to detect several $\text{CE}\nu\text{NS}$ events. In the near term a 1 m^3 $\nu\text{BDX-DRIFT}$ detector is available to be deployed in the NuMI beam at Fermilab on a year or two timescale [157].

CYGNUS is a proposed modular and multi-site network of large-scale gas time projection chambers [156]. The primary goal of the CYGNUS experiment is to perform a direction-dependent search for dark matter, which has been shown to be one of the only ways to convincingly prove the galactic origin of a detected signal [223, 226]. Directionality is also the best means of circumventing the neutrino fog [221, 222], but requires that good performance can be achieved at the sub-10-keV nuclear recoil energies where the majority of $\text{CE}\nu\text{NS}$ events coming from solar neutrinos would lie. A nuclear recoil threshold of 8 keV has already been shown to be feasible in the 755:5 He:SF₆ atmospheric pressure gas mixture suggested by Ref. [156]. This could be lowered to 3–5 keV with further gas/readout optimisation, and the development of specialized track-fitting techniques to improve particle identification at low energies. This would enable a CYGNUS-1000 m^3 detector to see between 30–50 $\text{CE}\nu\text{NS}$ events over a few years.

5 High- and Ultra-High-Energy Neutrino Detectors

Neutrinos at energies of TeV and beyond are interesting in part because they come to us from astrophysical and cosmic sources, such as active galactic nuclei or perhaps even neutron-star mergers. They are also interesting because as they pass through the Earth their propagation is very sensitive to non-standard interactions. Precision measurements of standard model neutrino interactions at the TeV scale will provide a new opportunity to search for physics beyond the standard model, while interactions in the PeV-ZeV regime probe nucleon structure in a way that cannot be done at terrestrial accelerators. The detectors at these ultra-high energies vary widely; neutrino telescopes need very large masses to deal with the rarity of such

5.1 Advanced High- and Ultra-High-Energy Neutrino Telescopes

Neutrino telescopes aimed at looking at neutrinos from TeV scales and beyond have been extremely successful in both uncovering new astrophysical sources of neutrinos, and on searching for neutrino physics beyond the standard model. Detection techniques are heavily dependent on neutrino energy. In the TeV-PeV (“high-energy”) regime, Earth’s opacity is high but neutrinos may still travel thousands of kilometers; beyond this regime detected neutrinos are either in regions surrounding large detectors, in dense media such as the lunar regolith, or by looking at air showers created by Earth-skimming ν_τ s.

A detailed SNOWMASS white paper [239] provides a comprehensive view of this very exciting and challenging area. In keeping with the NF10 scope, we focus here primarily on future ideas that are not already at the technical design stage, with an emphasis on new enabling technologies. Interestingly, in many cases the “enabling technology” is a particular piece of geography, whether it is polar ice or a mountain range.

A summary of sensitivities of some current and proposed experiments to 1000 s bursts and to diffuse high-energy neutrino sources can be found in Figures 33 and 34, respectively, taken from Ref. [239].

Table 4 summarizes the many ideas and their enabling technologies for high-energy and ultra-high energy natural-source neutrino detection.

5.1.1 Detector Requirements

There are four important observables measured by neutrino telescopes to search for new physics and probe astrophysics: energy spectrum, distribution of arrival directions, flavor composition, and arrival times. A summary of how detector requirements flow from physics goals can be found in Figure 35, taken from Ref. [239]. Next-generation detectors aim for ever larger sizes to be sensitive to the very small fluxes of possible ultra-high energy sources, with goals of an order of magnitude in flux for HE sources and two orders of magnitude for UHE sources. Energy resolutions of 0.1 in $\log_{10}(E/\text{GeV})$ at the HE scale, and in half-decade energy binning, are sufficient to resolve bumps and dips that may indicate new physics [266–272] while also distinguishing among models of astrophysical neutrino production [273, 274]. In EeV energy scale, next-generation detectors will need tens of events to measure the cross section to within an order of magnitude.

Measuring the arrival times of neutrinos is important for both time-domain transient and multi-messenger astrophysics, but also to search for evidence for new physics that would cause photons,

Proposed Detector	Basic Approach	Energy Range	Enabling Technology
P-ONE	Water Cherenkov	$> \text{TeV}$	Scale, telecomm fibers
ICECUBE-Gen2 (optical)	Ice Cherenkov	TeV-PeV	Scale, multi-PMTs
Trinity	Air-shower Cherenkov	$10\text{-}1000 \text{ PeV}$	60° FOV optics
RET	Radar reflection off ionization	$> 10 \text{ PeV}$	In-ice radar reflection
TAMBO	(Air-shower) water Cherenkov tanks	$1\text{-}100 \text{ PeV}$	Mountain/valley geography
RNO-G	Askaryan emission in ice	$> \text{PeV}$	Greenland ice, solar+wind power autonomous radio detectors
ICECUBE-Gen2 (radio)	Radio array	PeV-EeV	Omni-directional cylindrical antennas
BEACON	Radio air-shower detection	100 PeV-EeV	Mountain geometry, interferometric phased arrays
GRAND	Geomagnetic air-shower radio	$> \text{PeV}$	Very large-scale radio array
POEMMA	Space-based optical air-shower	$10 \text{ PeV-}40 \text{ EeV}$	Wide-FOV Schmidt telescopes, Cherenkov camera
PUEO	Balloon-based radio in ice and air	$> \text{EeV}$	Realtime interferometric beamforming,
GCOS	Nested water Cherenkov tanks +radio	$> 10 \text{ EeV}$	Xilinx RFSoc TBD

Table 4: Proposed detectors and enabling technologies for high-energy and ultra-high-energy neutrino detection. Only those experiments not yet past the technical design phase are included.

neutrinos, and gravitational waves to arrive at Earth at different times [275–277]. Being able to capture the transient behavior of sources requires the ability for instruments to send and respond to real-time alerts. Continuous operation is ideal for detecting transient events and improving overall flux sensitivity.

Flavor and $\nu/\bar{\nu}$ ratios provide complementary probes of new neutrino physics and neutrino production mechanisms. Large event statistics and complementary flavor-specific detection techniques are needed to identify flavor-specific signals and to measure the flavor composition statistically in a sample of collected events. Future directions should explore new techniques to improve flavor separation, like muon and neutron echoes [278]. In the EeV range, some instruments will be sensitive only to certain flavors, while others will be sensitive to all flavors. A comprehensive approach may allow flavor information across multiple experiments to be combined.

Sub-degree pointing resolution is needed to resolve the neutrino sky [279–283] while also reducing the systematic uncertainties on cross section [284–288] and inelasticity measurements [289]. Resolving the neutrino sky will be important to search for BSM physics that causes anisotropies.

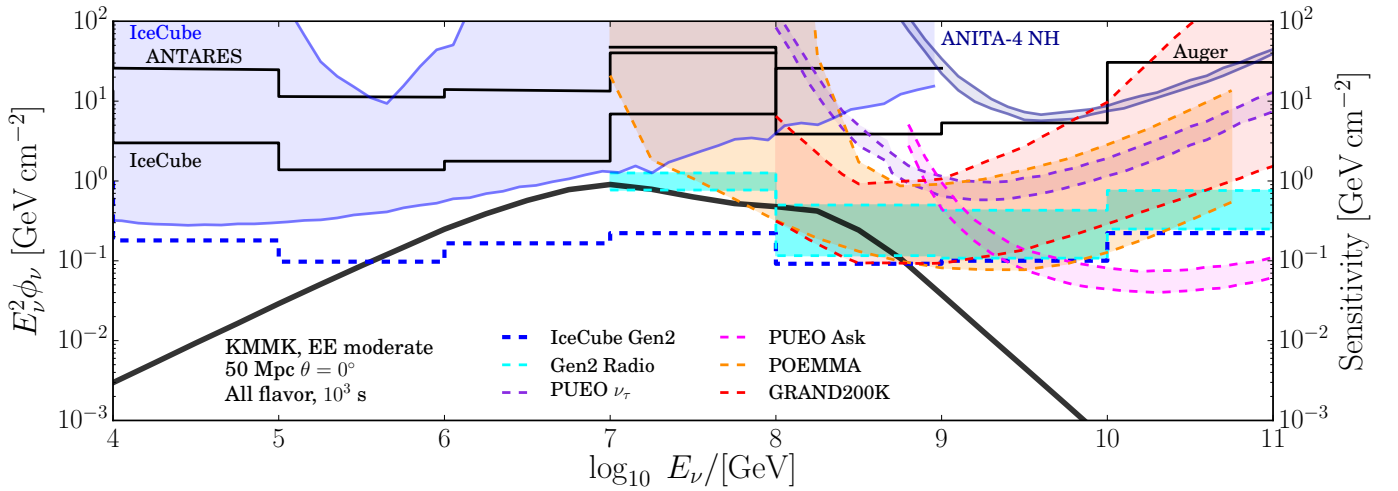


Figure 33: Sensitivity to short (1000 s) burst all-flavor neutrino plus antineutrino spectral fluence for some current and future detectors. The ANTARES, IceCube and Auger limits are 90% confidence level limits in a ± 500 s window around the gravitational wave event from GW170817 [240]. The dashed blue histogram shows IceCube-Gen2’s projected sensitivity for such an event [241], including IceCube-Gen2 radio [242] (shown for a range of declination with cyan). The blue shaded band comes from IceCube’s all-sky point-source effective area values tabulated for 2012 with 86 strings [243, 244]. The ANITA-4 NH limit is shown with the solid purple curves, and projected all-flavor sensitivities for PUEO [245] from ν_τ -sourced and Askaryan signals are shown with purple and magenta dashed curves, for POEMMA (orange) [246] and for GRAND200K (red) [247]. The Kimura et al. [248] extended emission short gamma ray burst fluence for on-axis viewing ($\theta = 0^\circ$) [248] from 50 Mpc is shown with the solid black curve. Taken from Ref. [239].

5.1.2 Optical Cherenkov Approaches

Experiments of this type typically look for tracks of secondary leptons produced by charged-current neutrino interactions or cascades produced by neutral-current and charged-current neutrino interactions. Track events have excellent angular resolution due to the long lever arm left by a final-state muon track, while cascade events have superior energy resolution. Typically, astrophysical purity increases with energy as the backgrounds from atmospheric neutrinos and muons fall more steeply with energy than the astrophysical neutrino flux. At UHE energies, these detectors are also sensitive to neutrinos that cascaded from EeV ν_τ to PeV energies [290]. To get detectors large enough to see the very small fluxes, either polar ice or sea water typically need to be instrumented. Future plans to improve HE sensitivity and broaden energy coverage are to expand detector volumes of optical arrays in the Northern Hemisphere, e.g., KM3NeT [291], Baikal-GVD [292], and P-ONE [293]. The primary enabling technology for these experiments is *scale* and accessibility of the target volume (e.g., availability of clear water or ice).

5.1.3 Radio Detection in Ice

In dense media like ice, compact electromagnetic showers generated after UHE neutrino interactions emit coherent Askaryan radiation at the Cherenkov angle. Askaryan radiation—fast, coherent radio-frequency impulses—is due to the excess negative charge in the shower [294]. The long attenuation length at radio frequencies allows the signal to propagate over kilometer-long distances. In-ice radio experiments are sensitive to all three flavors [295, 296], and may have the power to discriminate flavors based on different event topologies [296, 297], such as the stretching of electromagnetic showers due to the Landau-Pomeranchuk-Migdal (LPM) effect [298]. In ARA [299] and ARIANNA [300, 301], radio

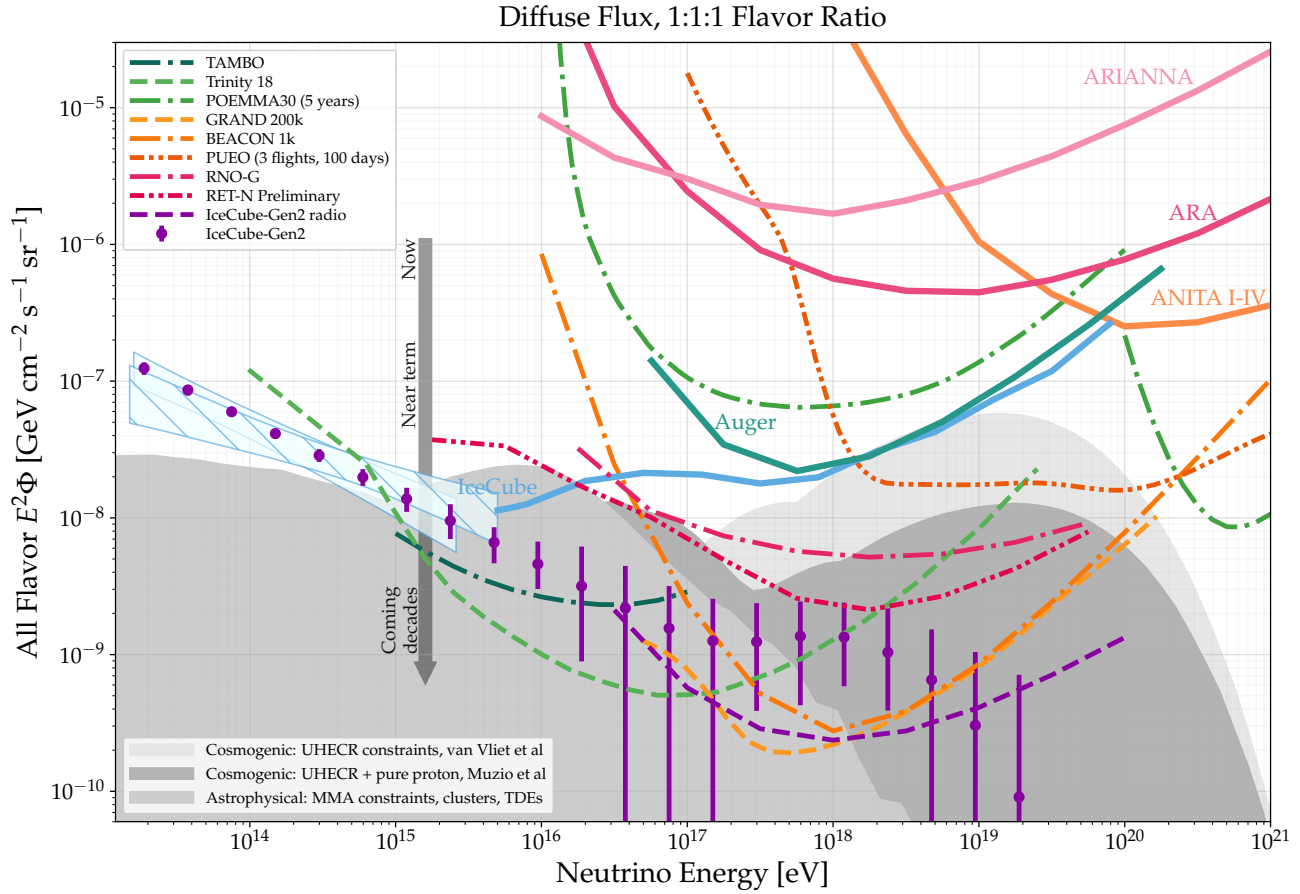


Figure 34: The expected differential 90% C.L. sensitivities for a variety of experiments to an all-flavor diffuse neutrino flux computed in decade-wide energy bins and assuming a ten-year integration (unless otherwise noted in the legend). The measurements and sensitivities are compared with a range of cosmogenic neutrino models [249, 250] and astrophysical neutrino models [250–252]. The blue bordered bands show the astrophysical neutrino flux measured by IceCube using tracks (ν_μ [253]) in hatch and using cascade-like events (ν_e and ν_τ [254]) in solid band. The solid lines show experimental upper limits at higher energies from the Pierre Auger Observatory [255], ARA [256], ARIANNA [257], ANITA I-IV [258], and IceCube [259]. The dashed lines show the sensitivities of a selection of proposed experiments currently in various design and prototyping stages (GRAND with 200,000 stations [247], BEACON with 1000 stations [260], TAMBO with 22,000 detectors [261], Trinity with 18 stations [262], RET-N with 10 stations [263], POEMMA30 [264]) and under construction (RNO-G [265], PUEO [245]). Experiments using the same detection technique are grouped into similar colors (orange, Earth-skimming radio (GRAND, BEACON); dark teal, particle showers (TAMBO); light green, Earth-skimming optical Cherenkov and fluorescence (Trinity, POEMMA30); pink, in-ice radio (ARIANNA, ARA, PUEO, RNO-G, RET-N (radar); blue, in-ice optical Cherenkov (IceCube)). Sensitivity from IceCube-Gen2 (dashed purple) is computed using radio and PUEO (dashed orange) uses both in-ice and Earth-skimming radio techniques. Auger (teal) uses particle showers and fluorescence and its upgrade, AugerPrime, will employ radio. The expected measurement of the diffuse astrophysical neutrino flux by IceCube-Gen2 in 10 years is shown with the purple points assuming a continuous single-power-law spectrum with an additional cosmogenic flux at the highest energies [241]. The grey downward-pointing arrow is a reminder that experimental sensitivities improve not only as exposure increases with time, but also as new experimental techniques and analysis methods are both demonstrated and scaled to larger detection volumes. Taken from Ref. [239].

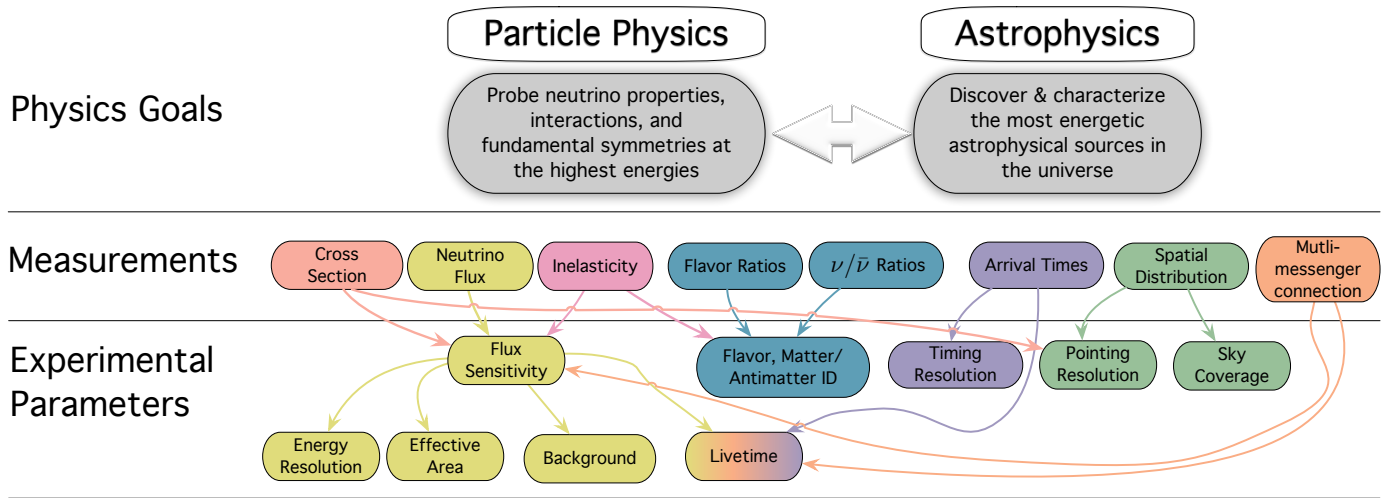


Figure 35: Flow of several neutrino telescope physics and astrophysics goals into detector requirements. Taken from Ref. [239].

antennas are buried in the Antarctic ice. RNO-G, based on a similar concept, is a radio detector under construction in Greenland [302]. The experience gained in these experiments will directly feed into the design of the expansive, sparse radio array of IceCube-Gen2 [241]. Radar signals reflecting off in-ice showers is also being explored as a detection method [263, 303, 304].

5.1.4 Air-shower detection techniques for UHE ν_τ s

CC interactions of ν_τ s produce tau leptons that at UHE energies typically decay over tens to hundreds of kilometers. If the geometry of the experimental setting is right, the neutrino interacts inside the Earth and the tau emerges and decays in the atmosphere. The decay initiates an extensive air shower, which can be detected with particle, air-shower imaging, or radio detectors [305]. But even in cases where a ν_τ interacts deep underground and the tau decays before reaching the surface, a new ν_τ is produced in the decay which can again interact in the Earth and generate a tau emerging from the surface. This “ ν_τ regeneration” increases the chances of Earth-skimming ν_τ reaching the detector. Earth-skimming neutrino fluxes have the added advantage of being unaffected by atmospheric neutrinos and only mildly affected by atmospheric muons [296].

The Pierre Auger Observatory (Auger) is a long-running large-scale array of surface water tanks that detect the Cherenkov light from air-shower particles passing through them. Auger is designed to detect UHECRs, but it has been used to search for horizontal showers initiated by UHE neutrinos in the atmosphere [255]. The Telescope Array (TA) [306] and HAWC [307] experiments have used a similar detection strategy, but have a more limited sensitivity. TAMBO is a planned array of water tanks to be located on one side of an Andean canyon, designed to detect the showers initiated by UHE taus emerging from the opposite side [261].

5.1.5 Air-shower radio detection

Radio-detection of Earth-skimming tau neutrinos is a promising method due to the long attenuation lengths of radio waves in air. As with in-ice radio detection, sparse arrays can be used to instrument large areas. Radio emission is generated in air showers initiated by tau decays, via the geomagnetic effect, due to charge separation in the magnetic field of Earth as the air showers progress through the atmosphere. Moreover, the narrow Cherenkov cone and fast radio imaging enables sub-degree

angular resolution. BEACON [260], in its prototype phase, TAROGE [308], and TAROGE-M [309] are compact antenna arrays in elevated locations that aim to detect UHE ν_τ emerging upwards via the radio emission of the air showers that they trigger. ANITA [310] and PUEO [310] are also sensitive to upgoing ν_τ , from a higher elevation. GRAND [247] is a planned experiment that will cover large areas with a sparse antenna array to detect the radio emission from air showers triggered by UHE ν_τ , cosmic rays, and gamma rays.

5.1.6 Air-shower imaging

Several air-shower imaging instruments, although optimized for cosmic-ray and gamma-ray detection, have demonstrated that the imaging of air showers via the Cherenkov and fluorescence light radiated by shower particles is a viable detection method of UHE ν_τ [311–313, 313–315]. Air-shower imaging allows the reconstruction of the air-shower arrival direction with arcminute resolution and the shower energy within a few tens of percent of uncertainty. These excellent reconstruction characteristics are why the very-high-energy gamma-ray and UHECR communities have been using air-shower imaging for quite some time [316]. Two planned instruments optimized for the detection of UHE neutrinos from the ground are Trinity [317] and Ashra NTA [318]. POEMMA is designed to detect the Cherenkov light of UHE ν_τ -initiated showers from a satellite. A unique feature of POEMMA is its ability to rapidly reposition to target transient multi-messenger events [246, 264]. EUSO-SPB2 is a telescope mounted on a super-pressure balloon which will fly at high altitudes and serve as a pathfinder for POEMMA [319].

5.2 Detectors for the Forward Physics Facility at the LHC

The Forward Physics Facility (FPF) will be a new underground cavern at the Large Hadron Collider (LHC) to host a suite of far-forward experiments during the High-Luminosity LHC era. The existing large LHC detectors do not cover particles beyond pseudorapidity range of $|\eta| \leq 4.5$ [320], and so they miss the physics opportunities provided by the enormous flux of particles produced in the far-forward direction. The FPF will realize this physics potential. In the following we will briefly summarize the physics considerations for FPF detectors, the technical challenges, and novel approaches to these detectors.

5.2.1 Detector Requirements

The FPF will need a diverse set of experiments, each optimized for particular physics goals. Details of the physics reach can be obtained in [321, 322].

FASER2, a magnetic spectrometer and tracker, will search for light and weakly-interacting states, including long-lived particles, new force carriers, axion-like particles, light neutralinos, and dark sector particles. FASER2 will increase sensitivity by many orders of magnitude beyond the FASER experiment [323, 324] by increasing the acceptance and the length of the magnetic spectrometer. FASER ν 2 and Advanced SND are proposed emulsion and electronic neutrino detectors, respectively. They are both in the several ton scale. FLArE is a proposed 10-tonne-scale noble liquid detector. These detectors will detect neutrinos and also search for light dark matter. They will each detect $\sim 10^6$ neutrinos and anti-neutrinos at energies ranging from 100 GeV to few TeV. Each is expected to detect $\sim 10^3$ tau neutrinos also at very high energies. Laboratory experiments have not detected neutrinos in this high energy range in the past. The detection, reconstruction, energy measurement, and particle identification present unique challenges to existing instrumentation. Detection of tau particles either by explicit identification of decays near the vertex (in emulsion) or by kinematics (in electronic detectors)

in a high energy charged current tau neutrino interaction particularly presents unique challenges. Collecting a large sample of well identified tau neutrino interactions is a unique capability of the FPF. This capability will be fully utilized by multiple detectors with very different technical approaches. Lastly, it is of great interest that these same detectors have low thresholds ($< \text{few hundred MeV}$) for detection of light dark matter scattering.

Finally, the FORMOSA detector is composed of scintillating bars. These bars are arranged to measure charge deposition from straight-through millicharged particles and other very weakly-interacting particles across a large range of masses.

5.3 Technical Considerations

The most important technical issue is finding a location along the line of sight (LOS) at an appropriate distance and with features that include access, safety, and the ability to have a large space to house multiple detectors and their infrastructure. During 2021-2022, in a series of workshops [325] informed by the CERN civil engineering team and accelerator advisory body, the location 617-682 m west of the ATLAS interaction point (IP) has been selected. This location is about ~ 80 m deep and shielded from the ATLAS IP by over 200 m of concrete and rock, providing an ideal location to search for rare processes and very weakly-interacting particles. A dedicated shaft will provide access to the underground hall, and the construction of both the facility and detectors can be substantially decoupled from HL-LHC construction and activities; this will make planning, scheduling, as well as safety aspects easier for the FPF.

Despite the shielding from the IP due to LHC magnets, concrete and rock, there is a substantial flux of high energy μ^-/μ^+ particles directly from the IP as well as produced in the various LHC accelerator structures. Studies are progressing to reduce this flux to $< 1 \text{ Hz/cm}^2$ during the HL-LHC running (with nominal luminosity of $\sim 5 \times 10^{34}/\text{cm}^2/\text{sec}$) using sweeping magnets with momentum kick of ~ 7 Tesla-meter in a location ~ 350 m from the IP. Given the many uncertainties including the maximum luminosity in the planned long running of the HL-LHC (until 2040) detectors at the FPF should be designed to operate with an expected high energy muon flux in the range of $\sim 1 \text{ Hz/cm}^2$. For comparison, the neutrino event rate will be approximately 50 charged current events per day per ton of detector with 45 ν_μ CC, 5 ν_e CC, and $\sim 0.2 \nu_\tau$ CC.

5.3.1 Experimental Technologies

The proposed experiments vary in their technological readiness. While they are conceptually similar to previous efforts, many of them require scaling up of hardware and software technologies to a new level. And some will require focused R&D efforts to tackle specific issues. Two such efforts will be the ability to trigger the detectors in the presence of considerable muon backgrounds, and the ability to track and reconstruct neutrino vertices with high multiplicities due to the very high energies of the events.

FASE2: The experiment proposes a large superconducting spectrometer magnet of 2 to 3 meter diameter and decay volume length of 10-20 meters. The very high energies of expected tracks from decays of long lived particles implies that for reasonably large magnetic fields (1 T), the spectrometer will require charged particle resolution exceeding ~ 1 mm in large area tracking detectors. The detector will also need to include a fine grained EM calorimeter and a muon identification system. A sophisticated trigger system to select LLP decays in the spectrometer volume in the presence of

background muons will be needed.

FASERnu2: This will be a $\times 10$ scaled up version of the current FASERnu (1.2 ton) detector composed of emulsion and tungsten stacks. A pilot run of this technology has already yielded 6 candidate neutrino events from the LHC [326]. The scaled up version for the FPF presents two issues that need to be solved. The HL-LHC presents much high muon rate for this kind of detector which has no trigger capability; the emulsion detectors need to be changed regularly because of the muon radiation. The increased size and frequency of replacement will mean over two orders of magnitude greater production and handling of emulsion films with correspondingly larger analysis effort for FASERnu2. The experience from FASERnu, however, will prove to be extremely valuable to automate much of this process.

Electronic Neutrino Detectors:

Advanced-SND is conceived to be an electronic fine grained detector with a magnetic muon spectrometer. The neutrino target is nominally expected to be a few tons. The technology is still under development with several choices including a detector with silicon tracking detectors sandwiched with passive neutrino target material. Such a silicon readout will require further development.

FLArE will be a noble liquid tracking time projection chamber with a hadronic calorimeter to capture particles escaping from the downstream end, as well as a muon tagger. The default fill is considered to be liquid argon, although liquid krypton is also under consideration. The nominal size of the detector is approximately 2m wide, 2m high, and 7m long for the TPC and an additional few meters for the hadronic calorimeter and muon tagging system. The key technical challenges for the detector are the installation of the cryostat and cryogenic systems, the TPC design to obtain the highest spatial resolution for tracks near the vertex, and the scintillation photon system to trigger on neutrino and dark matter events with sufficiently low threshold. This detector benefits enormously from the last decade of R&D investment into DUNE [327] technologies, however the needed tracking resolution and trigger capability is unique for FLArE and will require dedicated R&D.

FORMOSA: The technologies for FORMOSA are standard with scintillation counters and readout of photo-multiplier pulses, however care has to be exercised in limiting backgrounds from muons and instrumental effects. Much will be learned from a prototype experiment, expected to be built and run during the upcoming Run-3 of the LHC.

All detectors will require intelligent flexible trigger systems that can capture interesting events and associate them across detector systems. Requirements for such triggers to cooperate across detector systems as well as with the collider detector at the IP are in consideration.

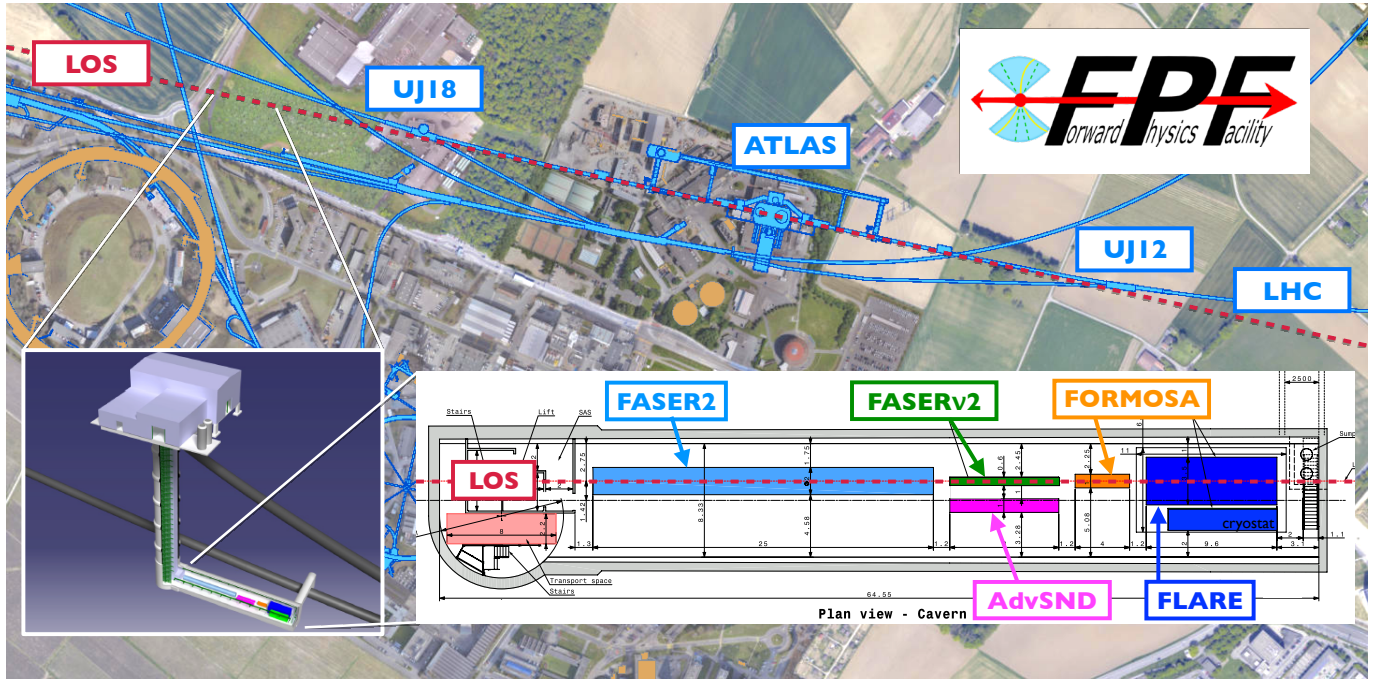


Figure 36: The preferred location for the Forward Physics Facility, a proposed new cavern for the High-Luminosity era. The FPF will be 65 m-long and 8.5 m-wide and will house a diverse set of experiments along the line of sight (LOS) to explore the many physics opportunities in the far-forward region.

Technology	FASER2	FASERnu2	Adv-SND	FLArE	FORMOSA
Large aperture SC magnet	x				
High resolution tracking	x		x	x	
Large scale emulsion		x			
Silicon tracking			x		
High purity noble liquids				x	
Low noise cold electronics				x	
Scintillation				x	x
Optical materials				x	x
Cold SiPM				x	
Picosec synchronization			x	x	x
Intelligent Trigger	x		x	x	x

Table 5: Enabling technologies for the detectors and systems of the far forward physics facility.

6 Additional Detector Ideas

6.1 Hydrogen and Deuterium Detectors

Understanding neutrino interactions at the nucleon-level will require a new generation of precision experiments. These measurements are simplest on the lightest of nuclei—hydrogen and deuterium. Yet the available neutrino data on hydrogen or light nuclei come from bubble-chamber experiments of the 1970s and 1980s [328–332]. These data have served the community well but they have essential shortcomings. They have poor statistical precision, coming from the relatively low-intensity neutrino beams of an earlier era, and they have poorly-constrained systematic uncertainties associated with hand-scanning of events and poorly known fluxes. Moreover, in most cases, event-level data have been lost, and information exists only as one-dimensional projections in publications. Using the published bubble-chamber data in subsequent work involves making assumptions about the details of the analysis, such as whether or not efficiency corrections have been applied to event rate distributions [333].

While these experiments were pioneering in their age, and probed qualitative features of neutrino interactions that helped establish our modern Standard Model (SM) of the strong and electroweak forces, they were not designed to underpin the ambitious neutrino oscillation experiments of the current precision era. It is clear that new and better data are needed.

Detector options to make these measurements include using DUNE’s SAND detector’s hydrocarbon $(\text{CH}_2)^n$ radiators as a source of hydrogen. Pure carbon radiators and precise primary vertex location will allow the separate measurement of neutrino interactions on the hydrocarbon and carbon. Subtraction of the carbon measurements from the hydrocarbon measurements in the same beam yields estimates of the interaction rates on pure hydrogen. The use of transverse kinematic imbalance (TKI) variables further improves the signal-to-background ratio before the subtraction and allows for side-band control of important backgrounds. Unfortunately, the measurements cannot be extended to deuterium in this way as deuterated plastics are prohibitively expensive.

Another option is to include a hydrogen-rich gas in the ND-GAr subdetector. ND-GAr, with its full solid-angle acceptance and MeV-level proton tracking threshold, is ideal for performing exclusive final-state measurements. One unique advantage of the ND-GAr, compared to other DUNE ND components, is its flexibility to use various gas mixtures as interaction targets. Possible hydrogen-rich mixtures include binary systems such as He-Alkane. For example, in terms of the ratio between the numbers of neutrino-interacting free protons and bound protons, a mixture of 90% He + 10% CH_4 equals to polystyrene (CH), and 75% He + 25% CH_4 equals to polypropylene (CH_2); at 50%, CH_4 provides the same target mass as pure hydrogen gas (H_2)—higher concentration will not only further improve the event purity, but also increase the free-proton target mass.

With the help of the superb tracking of ND-GAr, a successful search for a safe and hydrogen-rich gas mixture would enable measurements of event-by-event neutrino-hydrogen interactions [334, 335]. The idea was that beamed neutrinos interacting on hydrogen could be selected out of those on the heavier targets via Transverse Kinematic Imbalance (TKI) once sufficient momentum resolution is achieved: with perfect tracking, interactions on hydrogen would have balanced final-state transverse momenta (that is, zero TKI), while the TKI on heavier nuclei is irreducibly wide due to nuclear effects such as Fermi motion and final-state interactions.

A separate hall can be constructed upstream of the DUNE Near Detector hall to house large, hydrogen

or deuterium target detectors. Two choices exist for an active-target liquid hydrogen detector – a TPC that collects drifting electrons from ionized hydrogen molecules and a liquid hydrogen bubble chamber that is read out optically on each spill. Both a TPC and bubble chamber would need auxiliary devices and detectors to perform high-precision cross section studies. Both detectors would require a strong magnet for charge separation as well as the measurement of charged particle momentum. Depending on their size and shape, both detectors could contribute complementary calorimetric measurements for short-lived particles, but heavier particles and those with higher lifetimes would require calorimetry and a muon chamber.

A liquid hydrogen TPC presents several challenges in design, construction and operation. The very slow electron drift velocity in liquid hydrogen [336,337] presents pileup and background issues, which will need to be evaluated in the context of detector design. Furthermore, extremely long free-electron lifetimes (of order seconds) will be required in order to collect charge after a long drift distance. A time-projection chamber can be built with crossed wire planes similar to the single-phase liquid-argon TPC design of the DUNE Far Detector, or it could have pixel readout, similar to the LArTPC near detector design. This would yield a resolution of around 4 mm [338]. The presence of high-voltage electrodes in contact with hydrogen will require careful attention to safety, such as the removal of all oxidizers in the hall.

While bubble chambers have many similar safety concerns, they offer several advantages over a similarly-sized hydrogen TPC and have a strong history of successful use in particle physics. Spatial resolutions of about 100 microns and momentum resolutions of 2% were standard for historic devices using traditional cameras and relatively weak magnets [339]. Also, the use of special holographic optical techniques can reduce spatial resolutions down to less than 10 microns [340].

The prospect of measuring neutrino cross sections on a polarized target is very exciting. It has never been done before, and the inherent polarization of neutrinos in the Standard Model and the parity-violating nature of the weak interactions result in very large polarization asymmetries. A polarized target would have to be scaled up in size relative to existing ones in order to provide event rates high enough to make useful measurements. A polarized target would require very low temperatures, of order 1 K, a strong magnetic field, and RF applied so that dynamical nuclear polarization can be used. The very intense LBNF neutrino beam provides opportunities for even small targets to produce enough data over time to make an impact in this previously unexplored domain.

The requirement for such detectors of having both high nuclear target polarization and high heat load simultaneously is achievable through dynamic nuclear polarization (DNP) of solid-state targets. These systems contain a high-powered microwave generator, a superconducting magnet (~ 5 T) to produce the Zeeman splitting, and a high-cooling-power evaporation refrigerator used to hold the target at 1 K despite the heat load from the beam, the microwaves, the integrated particle detection, and external heat leaks [341,342]. The technology of these targets is quite mature and it is now possible to polarize nucleons and other nuclei in any orientation required for beams of photons, muons, electrons, protons, and mesons.

Due to the negligible heat load from high-intensity neutrino beams, either an evaporation or a frozen spin target could be used. Both of these systems can also be scaled up longitudinally along the beam line to increase the exposure. There are, however, limits to the width of the target as both require a strong polarizing magnetic field with high field homogeneity. It is also possible to increase the target's overall diameter as well but the limiting factor is the size of bore of the magnet [343] and the expense

of building a polarizing magnet on the desired scale (more than a meter). Polarizing solenoids can be built to have much larger warm bores but to keep the desired homogeneity usually the field strength will need to decrease to keep the magnet construction expenses reasonable. Using a 1.5 T magnet to polarize materials such as NH_3 is still practical assuming that the nuclei are polarized at a much lower temperature. The DNP process will then take significantly longer to reach optimal polarization enhancement.

The detector must be integrated with the target due to the low energies of the outgoing production particles and the very small interaction cross section of neutrinos on nuclei. Historically this type of constraint has been addressed using active targets where the target material also acts as a detector of the low-energy decay products. For nitroxyl radicals such as TEMPO, DTBN and oxo-TEMPO, the unpaired electron is localized predominately in the N-O bond and is surrounded and shielded by four methyl groups [344]. This molecular structure allows the dopant to be chemically mixed without losing the free electron. These free radicals can be combined with materials like polymethyl methacrylate (PMMA) and polystyrene which can also be used as scintillating detectors. Such approaches provide active targets for experiments that require a polarized target combined with particle detection very close to the polarized target nucleus [344–346].

An initial design consists of a scintillator mesh with 1 mm strips running both longitudinally and transversely to provide pixel and cluster reconstruction information. These strips are connected to wavelength shifting fiber inside the mixing chamber volume of a large scale $^3\text{He}/^4\text{He}$ dilution refrigerator. In the insulating vacuum space, these fibers interface and optically connect to a set of Multi-Pixel Photon Counter (MPPC), also known as silicon photomultiplier (SiPM), a solid state photomultiplier comprised of a high density matrix of Geiger-mode-operated avalanche photodiodes. Routing the optical fibers outside of the mK volume distances the heat source of the SiPMs and associated electronics from the cold target.

The suggested system could be built to house a target with diameter of 25 cm with a length of several meters. The system could be polarized with a long solenoid magnet (2.5 T) that could move back and forth to polarize different sections and the two different spin states of the long sections of target. A separate large Helmholtz holding coil (0.3 T) could be positioned outside of the cryostat on the section not being actively polarized with the solenoid. This holding field would preserve the polarization during the frozen spin state. In this system, the dilution refrigerator is static but the magnets can move on a track in the longitudinal direction to polarize different sections of the target.

Acknowledgements

We thank the editors of the Snowmass Whitepaper ‘Coherent elastic neutrino-nucleus scattering: Terrestrial and astrophysical applications’, L. Strigari, P. Barbeau and R. Strauss for important input to this report. We also acknowledge the many authors of the Snowmass Whitepaper, “Future Advances in Photon-based Neutrino Detectors,” along with the many participants in the Photon-based Neutrino Detector Workshop; we have relied heavily in several sections on these. We also thank the many authors of the Snowmass Whitepaper, “High-Energy and Ultra-High Energy Neutrinos,” which we have used as the basis for many of the relevant sections in this report. We also thank the authors of the Snowmass Whitepaper, “Neutrino Scattering Measurements on Hydrogen and Deuterium: A Snowmass Whitepaper.” We would also like to thank Diego Garcia Gamez, Ettore Segreto, and Andrzej Szelc for very helpful input.

References

- [1] P. Agnes *et al.*, “Low-Mass Dark Matter Search with the DarkSide-50 Experiment,” *Phys. Rev. Lett.*, vol. 121, no. 8, p. 081307, 2018.
- [2] DEAP-3600 Collaboration, P. A. Amaudruz *et al.*, “Design and Construction of the DEAP-3600 Dark Matter Detector,” *Astropart. Phys.*, vol. 108, pp. 1–23, 2019.
- [3] LZ Collaboration, D. S. Akerib *et al.*, “LUX-ZEPLIN (LZ) Conceptual Design Report,” 9 2015.
- [4] EXO-200 Collaboration, M. Auger *et al.*, “Search for Neutrinoless Double-Beta Decay in ^{136}Xe with EXO-200,” *Phys. Rev. Lett.*, vol. 109, p. 032505, 2012.
- [5] MicroBooNE, LAr1-ND, ICARUS-WA104 Collaboration, M. Antonello *et al.*, “A Proposal for a Three Detector Short-Baseline Neutrino Oscillation Program in the Fermilab Booster Neutrino Beam,” arXiv:1503.01520 [physics.ins-det].
- [6] DUNE Collaboration, B. Abi *et al.*, “Deep Underground Neutrino Experiment (DUNE), Far Detector Technical Design Report, Volume I Introduction to DUNE,” *JINST*, vol. 15, no. 08, p. T08008, arXiv:2002.02967 [physics.ins-det].
- [7] nEXO Collaboration, J. B. Albert *et al.*, “Sensitivity and Discovery Potential of nEXO to Neutrinoless Double Beta Decay,” *Phys. Rev. C*, vol. 97, no. 6, p. 065503, 2018.
- [8] X. Qian and others, “Development of lartpc vertical drift solutions with pcb anode readouts for dune,” 2020. Snowmass 2022 Letter of Interest.
- [9] D. Dwyer, M. Garcia-Sciveres, D. Gnani, C. Grace, S. Kohn, M. Kramer, A. Krieger, C. Lin, K. Luk, P. Madigan, C. Marshall, H. Steiner, and T. Stezelberger, “LArPix: demonstration of low-power 3d pixelated charge readout for liquid argon time projection chambers,” *Journal of Instrumentation*, vol. 13, pp. P10007–P10007, oct 2018.
- [10] D. Nygren and Y. Mei, “Q-Pix: Pixel-scale Signal Capture for Kiloton Liquid Argon TPC Detectors: Time-to-Charge Waveform Capture, Local Clocks, Dynamic Networks,” arXiv:1809.10213 [physics.ins-det].
- [11] C. Adams, M. D. Tutto, J. Asaadi, M. Bernstein, E. Church, R. Guenette, J. Rojas, H. Sullivan, and A. Tripathi, “Enhancing neutrino event reconstruction with pixel-based 3d readout for liquid argon time projection chambers,” *Journal of Instrumentation*, vol. 15, pp. P04009–P04009, apr 2020.
- [12] Q-Pix Collaboration, S. Kubota *et al.*, “Enhanced Low-Energy Supernova Burst Detection in Large Liquid Argon Time Projection Chambers Enabled by Q-Pix,” arXiv:2203.12109 [hep-ex].
- [13] D. Dwyer and others, “An r&d collaboration for scalable pixelated detector systems,” 2020. Snowmass 2022 Letter of Interest.
- [14] E. Gramellini and others, “Multi-modal pixels for noble element time projection chambers,” 2020. Snowmass 2022 Letter of Interest.
- [15] J. Asaadi, E. Gramellini, B. Jones, K. Kelly, P. Machado, “Dual-readout time projection chamber: exploring sub-millimeter pitch for directional dark matter and tau identification in ν_τ cc interactions,” 2020. Snowmass 2022 Letter of Interest.
- [16] M. Szydagis *et al.*, “A Review of Basic Energy Reconstruction Techniques in Liquid Xenon and Argon Detectors for Dark Matter and Neutrino Physics Using NEST,” *Instruments*, vol. 5, p. 13, arXiv:2102.10209 [hep-ex].
- [17] A. Mastbaum, F. Psihas, and J. Zennaro, “Xenon-Doped Liquid Argon TPCs as a Neutrinoless Double Beta Decay Platform,” arXiv:2203.14700 [physics.ins-det].
- [18] D. Caratelli *et al.*, “Low-Energy Physics in Neutrino LArTPCs,” arXiv:2203.00740 [physics.ins-det].
- [19] D. F. Anderson, “New Photosensitive Dopants for Liquid Argon,” *Nucl. Instrum. Meth. A*, vol. 245, p. 361, 1986.

- [20] P. Cennini *et al.*, “Improving the performance of the liquid argon tpc by doping with tetramethyl-germanium,” *Nuclear Instruments and Methods in Physics Research Section A: Accelerators, Spectrometers, Detectors and Associated Equipment*, vol. 355, no. 2, pp. 660 – 662, 1995.
- [21] E. D. Church, “LArSoft: A Software Package for Liquid Argon Time Projection Drift Chambers,” arXiv:1311.6774 [physics.ins-det].
- [22] Y. Nakajima, A. Goldshmidt, H. S. Matis, T. Miller, D. R. Nygren, C. A. B. Oliveira, and J. Renner, “Measurement of scintillation and ionization yield with high-pressure gaseous mixtures of Xe and TMA for improved neutrinoless double beta decay and dark matter searches,” *JINST*, vol. 11, no. 03, p. C03041, arXiv:1511.02257 [physics.ins-det].
- [23] D. Hollywood, K. Majumdar, K. Mavrokoridis, K. McCormick, B. Philippou, S. Powell, A. Roberts, N. Smith, G. Stavakis, C. Touramanis, and J. Vann, “ARIADNE—a novel optical LArTPC: technical design report and initial characterisation using a secondary beam from the CERN PS and cosmic muons,” *Journal of Instrumentation*, vol. 15, pp. P03003–P03003, mar 2020.
- [24] A. Roberts, P. Svihra, A. Al-Refaie, H. Graafsma, J. Küpper, K. Majumdar, K. Mavrokoridis, A. Nomerotski, D. Pennicard, B. Philippou, S. Trippel, C. Touramanis, and J. Vann, “First demonstration of 3d optical readout of a TPC using a single photon sensitive timepix3 based camera,” *Journal of Instrumentation*, vol. 14, pp. P06001–P06001, jun 2019.
- [25] A. Lowe, K. Majumdar, K. Mavrokoridis, B. Philippou, A. Roberts, C. Touramanis, and J. Vann, “Optical readout of the ariadne lartpc using a timepix3-based camera,” *Instruments*, vol. 4, no. 4, 2020.
- [26] P. Amedo and others, “Letter of intent: Large-scale demonstration of the ariadne lartpc optical readout system at the cern neutrino platform,” 2020. CERN Letter of Interest.
- [27] A. Lowe, K. Majumdar, K. Mavrokoridis, B. Philippou, A. Roberts, and C. Touramanis, “A novel manufacturing process for glass thgems and first characterisation in an optical gaseous argon tpc,” *Applied Sciences*, vol. 11, no. 20, 2021.
- [28] T. Doke, “Fundamental Properties of Liquid Argon, Krypton and Xenon as Radiation Detector Media,” *Portugal. Phys.*, vol. 12, pp. 9–48, 1981.
- [29] A. Machado and E. Segreto, “ARAPUCA a new device for liquid argon scintillation light detection,” *Journal of Instrumentation*, vol. 11, pp. C02004–C02004, feb 2016.
- [30] D. Collaboration, “First results on ProtoDUNE-SP liquid argon time projection chamber performance from a beam test at the CERN neutrino platform,” *Journal of Instrumentation*, vol. 15, pp. P12004–P12004, dec 2020.
- [31] vol. 13, pp. C04026–C04026, apr 2018.
- [32] H. Souza, E. Segreto, A. Machado, R. Sarmiento, M. Bazetto, L. Paulucci, F. Marinho, V. Pimentel, F. Demolin, G. de Souza, A. Fauth, and M. Ayala-Torres, “Liquid argon characterization of the x-ARAPUCA with alpha particles, gamma rays and cosmic muons,” *Journal of Instrumentation*, vol. 16, p. P11002, nov 2021.
- [33] C. Brizzolari, S. Brovelli, F. Bruni, P. Carniti, C. Cattadori, A. Falcone, C. Gotti, A. Machado, F. Meinardi, G. Pessina, E. Segreto, H. Souza, M. Spanu, F. Terranova, and M. Torti, “Enhancement of the x-arapuca photon detection device for the DUNE experiment,” *Journal of Instrumentation*, vol. 16, p. P09027, sep 2021.
- [34] DUNE Collaboration, N. Gallice, “Xenon doping of liquid argon in ProtoDUNE single phase,” *JINST*, vol. 17, no. 01, p. C01034, arXiv:2111.00347 [physics.ins-det].
- [35] M. Collaboration, “Design and construction of the MicroBooNE detector,” *Journal of Instrumentation*, vol. 12, pp. P02017–P02017, feb 2017.

- [36] D. Collaboration, “Design, construction and operation of the ProtoDUNE-SP liquid argon TPC,” *Journal of Instrumentation*, vol. 17, p. P01005, jan 2022.
- [37] I. Collaboration, “Study of electron recombination in liquid argon with the icarus tpc,” *Nuclear Instruments and Methods in Physics Research Section A: Accelerators, Spectrometers, Detectors and Associated Equipment*, vol. 523, no. 3, pp. 275–286, 2004.
- [38] M. Collaboration, “Reconstruction and measurement of o(100) MeV energy electromagnetic activity from $\pi^0 \rightarrow \gamma\gamma$ decays in the MicroBooNE LArTPC,” *Journal of Instrumentation*, vol. 15, pp. P02007–P02007, feb 2020.
- [39] M. Collaboration, “Study of space-charge effects in microboone,” *Public Note 1018*, 2016.
- [40] D. Collaboration, “First results on ProtoDUNE-SP liquid argon time projection chamber performance from a beam test at the CERN neutrino platform,” *Journal of Instrumentation*, vol. 15, pp. P12004–P12004, dec 2020.
- [41] D. Collaboration, “Volume IV. the DUNE far detector single-phase technology,” *Journal of Instrumentation*, vol. 15, pp. T08010–T08010, aug 2020.
- [42] H. Anderhub, M. Devereux, and P.-G. Seiler, “On a new method for testing and calibrating ionizing particle detectors,” *Nuclear Instruments and Methods*, vol. 166, no. 3, pp. 581–582, 1979.
- [43] J. Sun, D. Cao, and J. Dimmock, “Investigating laser-induced ionization of purified liquid argon in a time projection chamber,” *Nuclear Instruments and Methods in Physics Research Section A: Accelerators, Spectrometers, Detectors and Associated Equipment*, vol. 370, no. 2, pp. 372–376, 1996.
- [44] I. Badhrees, A. Ereditato, I. Kreslo, M. Messina, U. Moser, B. Rossi, M. S. Weber, M. Zeller, C. Altucci, S. Amoruso, R. Bruzzese, and R. Velotta, “Measurement of the two-photon absorption cross-section of liquid argon with a time projection chamber,” *New Journal of Physics*, vol. 12, p. 113024, nov 2010.
- [45] B. Rossi, I. Badhrees, A. Ereditato, S. Haug, R. Hänni, M. Hess, S. Jano  , F. Juget, I. Kreslo, S. Lehmann, P. Lutz, R. Mathieu, M. Messina, U. Moser, F. Nydegger, H. U. Sch  tz, M. S. Weber, and M. Zeller, “A prototype liquid argon time projection chamber for the study of UV laser multi-photon ionization,” *Journal of Instrumentation*, vol. 4, pp. P07011–P07011, jul 2009.
- [46] A. Ereditato, I. Kreslo, M. L  thi, C. R. von Rohr, M. Schenk, T. Strauss, M. Weber, and M. Zeller, “A steerable UV laser system for the calibration of liquid argon time projection chambers,” *Journal of Instrumentation*, vol. 9, pp. T11007–T11007, nov 2014.
- [47] M. Collaboration, “A method to determine the electric field of liquid argon time projection chambers using a UV laser system and its application in MicroBooNE,” *Journal of Instrumentation*, vol. 15, pp. P07010–P07010, jul 2020.
- [48] J. Maneira, “Techniques for tpc calibration: Application to liquid ar-tpcs,” *Particles*, vol. 5, no. 1, pp. 74–83, 2022.
- [49] ARTIE Collaboration Collaboration, V. Fischer, L. Pagani, L. Pickard, A. Couture, S. Gardiner, C. Grant, J. He, T. Johnson, E. Pantic, C. Prokop, R. Svoboda, J. Ullmann, and J. Wang, “Artie final results,” *Oral communication at the PANIC2021 conference*, 2021.
- [50] ACED Collaboration Collaboration, V. Fischer, L. Pagani, L. Pickard, A. Couture, S. Gardiner, C. Grant, J. He, T. Johnson, E. Pantic, C. Prokop, R. Svoboda, J. Ullmann, and J. Wang, “Measurement of the neutron capture cross section on argon,” *Phys. Rev. D*, vol. 99, p. 103021, May 2019.
- [51] A. A. Abud *et al.*, “Snowmass Neutrino Frontier: DUNE Physics Summary,” in *2022 Snowmass Summer Study*, 3 2022, 2203.06100.

- [52] A. A. Abud *et al.*, “A Gaseous Argon-Based Near Detector to Enhance the Physics Capabilities of DUNE,” in *2022 Snowmass Summer Study*, 3 2022, 2203.06281.
- [53] DUNE Collaboration, A. Abed Abud *et al.*, “Deep Underground Neutrino Experiment (DUNE) Near Detector Conceptual Design Report,” *Instruments*, vol. 5, no. 4, p. 31, arXiv:2103.13910 [physics.ins-det].
- [54] H. O. Back, W. Bonivento, M. Boulay, E. Church, S. R. Elliott, F. Gabriele, C. Galbiati, G. K. Giovanetti, C. Jackson, A. McDonald, A. Renshaw, R. Santorelli, K. Scholberg, M. Simeone, R. Tayloe, and R. Van de Water, “A Facility for Low-Radioactivity Underground Argon,” 2022. <https://arxiv.org/abs/2203.09734>.
- [55] T. Alexander, H. O. Back, W. Bonivento, M. Boulay, P. Collon, Z. Feng, M. Foxe, P. G. Abia, P. Giampa, C. Jackson, C. Johnson, E. Mace, P. Mueller, L. Palcsu, W. Pettus, R. Purtschert, A. Renshaw, R. Saldanha, K. Scholberg, M. Simeone, O. Šrámek, R. Tayloe, W. TeGrotenhuis, S. White, and R. Williams, “The low-radioactivity underground argon workshop: A workshop synopsis,” 2019.
- [56] A. Peurrung, T. Bowyer, R. Craig, and P. Reeder, “Expected atmospheric concentration of ^{42}Ar ,” *Nuclear Instruments and Methods in Physics Research Section A: Accelerators, Spectrometers, Detectors and Associated Equipment*, vol. 396, no. 3, pp. 425–426, 1997.
- [57] V. Ashitkov, A. Barabash, S. Belogurov, G. Carugno, S. Konovalov, I. Pilugin, G. Puglierin, R. Saakyan, V. Stekhanov, V. Umatov, and I. Vanushin, “New experimental limit on the ^{42}Ar content in the earth’s atmosphere,” *Nuclear Instruments and Methods in Physics Research Section A: Accelerators, Spectrometers, Detectors and Associated Equipment*, vol. 416, no. 1, pp. 179–181, 1998.
- [58] S. S. Poudel, “Low radioactivity argon for rare event searches,” Presented at Workshop on Low Radioactivity Technique (LRT 2022) (AAP 2018), 2022.
- [59] C. Zhang and D. Mei, “Evaluation of cosmogenic production of ^{39}Ar and ^{42}Ar for rare-event physics using underground argon,” *Astropart. Phys.*, vol. 142, p. 102733, arXiv:2202.06403 [physics.ins-det].
- [60] S. Para *et al.*, “SoLAr: Solar Neutrinos in Liquid Argon,” in *2022 Snowmass Summer Study*, 3 2022, 2203.07501.
- [61] A. Avasthi, T. Bezerra, A. Borkum, E. Church, J. Genovesi, J. Haiston, C. M. Jackson, I. Lazanu, B. Monreal, S. Munson, C. Ortiz, M. Parvu, S. J. M. Peeters, D. Pershey, S. S. Poudel, J. Reichenbacher, R. Saldanha, K. Scholberg, G. Sinev, J. Zennamo, H. O. Back, J. F. Beacom, F. Capozzi, C. Cuesta, Z. Djurcic, A. C. Ezeribe, I. Gil-Botella, S. W. Li, M. Mooney, M. Sore, and S. Westerdale, “Low Background kTon-Scale Liquid Argon Time Projection Chambers,” 2022. <https://arxiv.org/abs/2203.08821>.
- [62] Xin Qian, et al., “Snowmass 2021 Letter of Interest: “Development of LArTPC Vertical Drift Solutions with PCB Anode Readouts for DUNE”.”
- [63] G. Zhu, S. W. Li, and J. F. Beacom, “Developing the MeV potential of DUNE: Detailed considerations of muon-induced spallation and other backgrounds,” *Phys. Rev. C*, vol. 99, p. 055810, May 2019.
- [64] F. Capozzi, S. W. Li, G. Zhu, and J. F. Beacom, “DUNE as the Next-Generation Solar Neutrino Experiment,” *Phys. Rev. Lett.*, vol. 123, p. 131803, Sep 2019.
- [65] D. S. Akerib, C. W. Akerlof, D. Y. Akimov, A. Alqahtani, S. K. Alsum, T. J. Anderson, N. Angelides, H. M. Araújo, A. Arbuckle, J. E. Armstrong, M. Arthurs, H. Auyeung, S. Aviles, X. Bai, A. J. Bailey, J. Balajthy, S. Balashov, J. Bang, M. J. Barry, D. Bauer, P. Bauer, A. Baxter, J. Belle, P. Beltrame, J. Bensinger, T. Benson, E. P. Bernard, A. Bernstein, A. Bhatti, A. Biekert, T. P. Biesiadzinski, H. J. Birch, B. Birrittella, K. E. Boast, A. I. Bolozdynya, E. M. Boulton, B. Boxer, R. Bramante, S. Branson, P. Brás, M. Breidenbach, C. A. J. Brew, J. H. Buckley,

- V. V. Bugaev, R. Bunker, S. Burdin, J. K. Busenitz, R. Cabrita, J. S. Campbell, C. Carels, D. L. Carlsmith, B. Carlson, M. C. Carmona-Benitez, M. Cascella, C. Chan, J. J. Cherwinka, A. A. Chiller, C. Chiller, N. I. Chott, A. Cole, J. Coleman, D. Colling, R. A. Conley, A. Cottle, R. Coughlen, G. Cox, W. W. Craddock, D. Curran, A. Currie, J. E. Cutter, J. P. da Cunha, C. E. Dahl, S. Dardin, S. Dasu, J. Davis, T. J. R. Davison, L. de Viveiros, N. Decheine, A. Dobi, J. E. Y. Dobson, E. Druszkiewicz, A. Dushkin, T. K. Edberg, W. R. Edwards, B. N. Edwards, J. Edwards, M. M. Elnimr, W. T. Emmet, S. R. Eriksen, C. H. Faham, A. Fan, S. Fayer, S. Fiorucci, H. Flaecher, I. M. F. Florang, P. Ford, V. B. Francis, E. D. Fraser, F. Froborg, T. Fruth, R. J. Gaitskell, N. J. Gantos, D. Garcia, V. M. Gehman, R. Gelfand, J. Genovesi, R. M. Gerhard, C. Ghag, E. Gibson, M. G. D. Gilchriese, S. Gokhale, B. Gomber, T. G. Gonda, A. Greenall, S. Greenwood, G. Gregerson, M. G. D. van der Grinten, C. B. Gwilliam, C. R. Hall, D. Hamilton, S. Hans, K. Hanzel, T. Harrington, A. Harrison, J. Harrison, C. Hasselkus, S. J. Haselschwardt, D. Hemer, S. A. Hertel, J. Heise, S. Hillbrand, O. Hitchcock, C. Hjermfelt, M. D. Hoff, B. Holbrook, E. Holtom, J. Y.-K. Hor, M. Horn, D. Q. Huang, T. W. Hurteau, C. M. Ignarra, M. N. Irving, R. G. Jacobsen, O. Jahangir, S. N. Jeffery, W. Ji, M. Johnson, J. Johnson, P. Johnson, W. G. Jones, A. C. Kaboth, A. Kamaha, K. Kamdin, V. Kasey, K. Kazkaz, J. Keefner, D. Khaitan, M. Khaleeq, A. Khazov, A. V. Khromov, I. Khurana, Y. D. Kim, W. T. Kim, C. D. Kocher, D. Kodroff, A. M. Konovalov, L. Korley, E. V. Korolkova, M. Koyuncu, J. Kras, H. Kraus, S. W. Kravitz, H. J. Krebs, L. Kreczko, B. Krikler, V. A. Kudryavtsev, A. V. Kumpan, S. Kyre, A. R. Lambert, B. Landerud, N. A. Larsen, A. Laundrie, E. A. Leason, H. S. Lee, J. Lee, C. Lee, B. G. Lenardo, D. S. Leonard, R. Leonard, K. T. Lesko, C. Levy, J. Li, Y. Liu, J. Liao, F. T. Liao, J. Lin, A. Lindote, R. Linehan, W. H. Lippincott, R. Liu, X. Liu, C. Loniewski, M. I. Lopes, E. Lopez-Asamar, B. L. Paredes, W. Lorenzon, D. Lucero, S. Luitz, J. M. Lyle, C. Lynch, P. A. Majewski, J. Makkinje, D. C. Malling, A. Manalaysay, L. Manenti, R. L. Mannino, N. Marangou, D. J. Markley, P. MarrLaundrie, T. J. Martin, M. F. Marzioni, C. Maupin, C. T. McConnell, D. N. McKinsey, J. McLaughlin, D. M. Mei, Y. Meng, E. H. Miller, Z. J. Minaker, E. Mizrachi, J. Mock, D. Molash, A. Monte, M. E. Monzani, J. A. Morad, E. Morrison, B. J. Mount, A. S. J. Murphy, D. Naim, A. Naylor, C. Nedlik, C. Nehrkorn, H. N. Nelson, J. Nesbit, F. Neves, J. A. Nikkel, J. A. Nikoleyczik, A. Nilima, J. O'Dell, H. Oh, F. G. O'Neill, K. O'Sullivan, I. Olcina, M. A. Olevitch, K. C. Oliver-Mallory, L. Oxborough, A. Pagac, D. Pagenkopf, S. Pal, K. J. Palladino, V. M. Palmaccio, J. Palmer, M. Pangilinan, N. Parveen, S. J. Patton, E. K. Pease, B. P. Penning, G. Pereira, C. Pereira, I. B. Peterson, A. Piepke, S. Pierson, S. Powell, R. M. Preece, K. Pushkin, Y. Qie, M. Racine, B. N. Ratcliff, J. Reichenbacher, L. Reichhart, C. A. Rhyne, A. Richards, Q. Riffard, G. R. C. Rischbieter, J. P. Rodrigues, H. J. Rose, R. Rosero, P. Rossiter, R. Rucinski, G. Rutherford, J. S. Saba, L. Sabarots, D. Santone, M. Sarychev, A. B. M. R. Sazzad, R. W. Schnee, M. Schubnell, P. R. Scovell, M. Severson, and D. Seymour, "The LUX-ZEPLIN (LZ) radioactivity and cleanliness control programs," *The European Physical Journal C*, vol. 80, no. 11, p. 1044, 2020.
- [66] DEAP Collaboration Collaboration, R. Ajaj, P.-A. Amaudruz, G. R. Araujo, M. Baldwin, M. Batygov, B. Beltran, C. E. Bina, J. Bonatt, M. G. Boulay, B. Broerman, J. F. Bueno, P. M. Burghardt, A. Butcher, B. Cai, S. Cavuoti, M. Chen, Y. Chen, B. T. Cleveland, D. Cranshaw, K. Dering, J. DiGiuseffo, L. Doria, F. A. Duncan, M. Dunford, A. Erlandson, N. Fatemighomi, G. Fiorillo, S. Florian, A. Flower, R. J. Ford, R. Gagnon, D. Gallacher, E. A. Garcés, S. Garg, P. Giampa, D. Goeldi, V. V. Golovko, P. Gorel, K. Graham, D. R. Grant, A. L. Hallin, M. Hamstra, P. J. Harvey, C. Hearn, A. Joy, C. J. Jillings, O. Kamaev, G. Kaur, A. Kemp, I. Kochanek, M. Kuźniak, S. Langrock, F. La Zia, B. Lehnert, X. Li, J. Lidgard, T. Lindner, O. Litvinov, J. Lock, G. Longo, P. Majewski, A. B. McDonald, T. McElroy, T. McGinn, J. B. McLaughlin, R. Mehdiyev, C. Mielnichuk, J. Monroe, P. Nadeau, C. Nantais, C. Ng, A. J. Noble, E. O'Dwyer,

- C. Ouellet, P. Pasuthip, S. J. M. Peeters, M.-C. Piro, T. R. Pollmann, E. T. Rand, C. Rethmeier, F. Retière, N. Seeburn, K. Singh Rao, P. Skensved, B. Smith, N. J. T. Smith, T. Sonley, J. Soukup, R. Stainforth, C. Stone, V. Strickland, B. Sur, J. Tang, E. Vázquez-Jáuregui, L. Veloce, S. Viel, J. Walding, M. Waqar, M. Ward, S. Westerdale, J. Willis, and A. Zuñiga Reyes, “Search for dark matter with a 231-day exposure of liquid argon using DEAP-3600 at SNOLAB,” *Phys. Rev. D*, vol. 100, p. 022004, Jul 2019.
- [67] DarkSide Collaboration Collaboration, P. Agnes, L. Agostino, I. F. M. Albuquerque, T. Alexander, A. K. Alton, K. Arisaka, H. O. Back, B. Baldin, K. Biery, G. Bonfini, M. Bossa, B. Bottino, A. Brigatti, J. Brodsky, F. Budano, S. Bussino, M. Cadeddu, L. Cadonati, M. Cadoni, F. Calaprice, N. Canci, A. Candela, H. Cao, M. Cariello, M. Carlini, S. Catalanotti, P. Cavalcante, A. Chepurnov, A. G. Cocco, G. Covone, L. Crippa, D. D’Angelo, M. D’Incecco, S. Davini, S. De Cecco, M. De Deo, M. De Vincenzi, A. Derbin, A. Devoto, F. Di Eusanio, G. Di Pietro, E. Edkins, A. Empl, A. Fan, G. Fiorillo, K. Fomenko, G. Forster, D. Franco, F. Gabriele, C. Galbiati, C. Giganti, A. M. Goretti, F. Granato, L. Grandi, M. Gromov, M. Guan, Y. Guardincerri, B. R. Hackett, J. Hall, K. Herner, P. H. Humble, E. V. Hungerford, A. Ianni, A. Ianni, I. James, C. Jollet, K. Keeter, C. L. Kendziora, V. Kobychiev, G. Koh, D. Korablev, G. Korga, A. Kubankin, X. Li, M. Lissia, P. Lombardi, S. Luitz, Y. Ma, I. N. Machulin, A. Mandarano, S. M. Mari, J. Maricic, L. Marini, C. J. Martoff, A. Mereaglia, P. D. Meyers, T. Miletic, R. Milincic, D. Montanari, A. Monte, M. Montuschi, M. Monzani, P. Mosteiro, B. J. Mount, V. N. Muratova, P. Musico, J. Napolitano, A. Nelson, S. Odrowski, M. Orsini, F. Ortica, L. Paganini, M. Pallavicini, E. Pantic, S. Parmeggiano, K. Pelczar, N. Pelliccia, S. Perasso, A. Pocar, S. Pordes, D. A. Pugachev, H. Qian, K. Randle, G. Ranucci, A. Razeto, B. Reinhold, A. L. Renshaw, A. Romani, B. Rossi, N. Rossi, D. Rountree, D. Sablone, P. Saggese, R. Saldanha, W. Sands, S. Sangiorgio, C. Savarese, E. Segreto, D. A. Semenov, E. Shields, P. N. Singh, M. D. Skorokhvatov, O. Smirnov, A. Sotnikov, C. Stanford, Y. Suvorov, R. Tartaglia, J. Tatarowicz, G. Testera, A. Tonazzo, P. Trinchese, E. V. Unzhakov, A. Vishneva, B. Vogelaar, M. Wada, S. Walker, H. Wang, Y. Wang, A. W. Watson, S. Westerdale, J. Wilhelmi, M. M. Wojcik, X. Xiang, J. Xu, C. Yang, J. Yoo, S. Zavatarelli, A. Zec, W. Zhong, C. Zhu, and G. Zuzel, “Results from the first use of low radioactivity argon in a dark matter search,” *Phys. Rev. D*, vol. 93, p. 081101, Apr 2016.
- [68] E. Church, C. Jackson, and R. Saldanha, “Dark matter detection capabilities of a large multipurpose Liquid Argon Time Projection Chamber,” *Journal of Instrumentation*, vol. 15, p. P09026, Sep 2020.
- [69] XENON Collaboration, E. Aprile *et al.*, “Search for Coherent Elastic Scattering of Solar ^8B Neutrinos in the XENON1T Dark Matter Experiment,” *Phys. Rev. Lett.*, vol. 126, p. 091301, arXiv:2012.02846 [hep-ex].
- [70] LUX Collaboration, D. S. Akerib *et al.*, “Results from a search for dark matter in the complete LUX exposure,” *Phys. Rev. Lett.*, vol. 118, no. 2, p. 021303, arXiv:1608.07648 [astro-ph.CO].
- [71] J. Aalbers *et al.*, “A Next-Generation Liquid Xenon Observatory for Dark Matter and Neutrino Physics,” 3 2022.
- [72] Super-Kamiokande Collaboration, Y. Fukuda *et al.*, “Evidence for oscillation of atmospheric neutrinos,” *Phys. Rev. Lett.*, vol. 81, pp. 1562–1567, 1998.
- [73] SNO Collaboration, Q. R. Ahmad *et al.*, “Direct evidence for neutrino flavor transformation from neutral current interactions in the Sudbury Neutrino Observatory,” *Phys. Rev. Lett.*, vol. 89, p. 011301, 2002.
- [74] Daya Bay Collaboration, F. P. An *et al.*, “Observation of electron-antineutrino disappearance at Daya Bay,” *Phys. Rev. Lett.*, vol. 108, p. 171803, 2012.

- [75] KamLAND Collaboration, K. Eguchi *et al.*, “First results from KamLAND: Evidence for reactor anti-neutrino disappearance,” *Phys. Rev. Lett.*, vol. 90, p. 021802, 2003.
- [76] T2K Collaboration, K. Abe *et al.*, “Indication of Electron Neutrino Appearance from an Accelerator-produced Off-axis Muon Neutrino Beam,” *Phys. Rev. Lett.*, vol. 107, p. 041801, 2011.
- [77] Kamiokande-II Collaboration, K. Hirata *et al.*, “Observation of a Neutrino Burst from the Supernova SN 1987a,” *Phys. Rev. Lett.*, vol. 58, pp. 1490–1493, 1987.
- [78] IMB Collaboration, C. B. Bratton *et al.*, “Angular Distribution of Events From Sn1987a,” *Phys. Rev. D*, vol. 37, p. 3361, 1988.
- [79] Borexino Collaboration, C. Arpesella *et al.*, “Direct Measurement of the Be-7 Solar Neutrino Flux with 192 Days of Borexino Data,” *Phys. Rev. Lett.*, vol. 101, p. 091302, 2008.
- [80] Borexino Collaboration, G. Bellini *et al.*, “First evidence of pep solar neutrinos by direct detection in Borexino,” *Phys. Rev. Lett.*, vol. 108, p. 051302, 2012.
- [81] IceCube Collaboration, M. G. Aartsen *et al.*, “Evidence for High-Energy Extraterrestrial Neutrinos at the IceCube Detector,” *Science*, vol. 342, p. 1242856, 2013.
- [82] JUNO Collaboration, A. Abusleme *et al.*, “JUNO Physics and Detector,” 4 2021.
- [83] Hyper-Kamiokande Collaboration, K. Abe *et al.*, “Hyper-Kamiokande Design Report,” 5 2018.
- [84] DUNE Collaboration, D. Totani *et al.*, “A measurement of absolute efficiency of the ARAPUCA photon detector in liquid argon,” *JINST*, vol. 15, no. 06, p. T06003, 2020.
- [85] SNO+ Collaboration, V. Albanese *et al.*, “The SNO+ experiment,” *JINST*, vol. 16, no. 08, p. P08059, arXiv:2104.11687 [physics.ins-det].
- [86] BOREXINO Collaboration, M. Agostini *et al.*, “First Directional Measurement of Sub-MeV Solar Neutrinos with Borexino,” *Phys. Rev. Lett.*, vol. 128, no. 9, p. 091803, 2022.
- [87] J. R. Klein *et al.*, “Future Advances in Photon-Based Neutrino Detectors: A SNOWMASS White Paper,” arXiv:2203.07479 [physics.ins-det].
- [88] Super-Kamiokande Collaboration, K. Abe *et al.*, “Diffuse supernova neutrino background search at Super-Kamiokande,” *Phys. Rev. D*, vol. 104, no. 12, p. 122002, 2021.
- [89] R. Bonventre and G. D. Orebi Gann, “Sensitivity of a low threshold directional detector to CNO-cycle solar neutrinos,” *Eur. Phys. J. C*, vol. 78, no. 6, p. 435, 2018.
- [90] J. Sawatzki, M. Wurm, and D. Kresse, “Detecting the Diffuse Supernova Neutrino Background in the future Water-based Liquid Scintillator Detector Theia,” *Phys. Rev. D*, vol. 103, no. 2, p. 023021, 2021.
- [91] T. Kaptanoglu, M. Luo, B. Land, A. Bacon, and J. Klein, “Spectral Photon Sorting For Large-Scale Cherenkov and Scintillation Detectors,” *Phys. Rev. D*, vol. 101, no. 7, p. 072002, 2020.
- [92] M. Yeh, S. Hans, W. Beriguete, R. Rosero, L. Hu, R. L. Hahn, M. V. Diwan, D. E. Jaffe, S. H. Kettell, and L. Littenberg, “A new water-based liquid scintillator and potential applications,” *Nucl. Instrum. Meth. A*, vol. 660, pp. 51–56, 2011.
- [93] Theia Collaboration, M. Askins *et al.*, “THEIA: an advanced optical neutrino detector,” *Eur. Phys. J. C*, vol. 80, no. 5, p. 416, 2020.
- [94] T. Kaptanoglu, “Characterization of the Hamamatsu 8” R5912-MOD Photomultiplier Tube,” *Nucl. Instrum. Meth. A*, vol. 889, pp. 69–77, arXiv:1710.03334 [physics.ins-det].
- [95] J. Caravaca, F. B. Descamps, B. J. Land, J. Wallig, M. Yeh, and G. D. Orebi Gann, “Experiment to demonstrate separation of Cherenkov and scintillation signals,” *Phys. Rev. C*, vol. 95, no. 5, p. 055801, 2017.
- [96] J. L. Wiza, “Microchannel plate detectors,” *Nucl. Instrum. Meth.*, vol. 162, no. 1-3, pp. 587–601, 1979.
- [97] Adams, B. W. and Elagin, A. and Frisch, H. J. and Obaid, R. and Oberla, E. and Vostrikov, A. and Wagner, R. G. and Wang, J. and Wetstein, M., “Timing characteristics of Large Area

- Picosecond Photodetectors,” *Nuclear Instruments and Methods in Physics Research. Section A, Accelerators, Spectrometers, Detectors and Associated Equipment*, vol. 795, 9 2015.
- [98] B. J. Land, Z. Bagdasarian, J. Caravaca, M. Smiley, M. Yeh, and G. D. Orebi Gann, “MeV-scale performance of water-based and pure liquid scintillator detectors,” *Phys. Rev. D*, vol. 103, no. 5, p. 052004, 2021.
 - [99] N. Zaitseva *et al.*, “Plastic scintillators with efficient neutron/gamma pulse shape discrimination,” *Nucl. Instrum. Meth.*, vol. A668, pp. 88 – 93, 2012.
 - [100] N. Zaitseva *et al.*, “Pulse shape discrimination with lithium-containing organic scintillators,” *Nucl. Instrum. Meth.*, vol. A729, pp. 747 – 754, 2013.
 - [101] A. N. Mabe *et al.*, “Transparent plastic scintillators for neutron detection based on lithium salicylate,” *Nucl. Instrum. Meth.*, vol. A806, pp. 80 – 86, 2016.
 - [102] A. N. Mabe *et al.*, “Plastic scintillator materials development at llnl,” *Contribution to the Workshop on Applied Antineutrino Physics (AAP 2018)*, 12 2018.
 - [103] C. Frangville *et al.*, “Large solubility of lithium carboxylates reaching high rates of ^6Li incorporation in polystyrene-based plastic scintillators for fast/thermal neutron and gamma ray detection,” *Mater. Chem. Front.*, vol. 3, p. 1626, 2019.
 - [104] N. S. Bowden and H. P. Mumm, “Neutrino physics and nuclear security motivations for the continued development of organic scintillators with pulse shape discrimination capability and ^6Li -doping,” 2020. Snowmass 2022 Letter of Interest.
 - [105] V. A. Li *et al.*, “A prototype for SANDD: A highly-segmented pulse-shape-sensitive plastic scintillator detector incorporating silicon photomultiplier arrays,” *Nucl. Instrum. Meth. A*, vol. 942, p. 162334, arXiv:1903.11668 [physics.ins-det].
 - [106] F. Suto *et al.*, “SANDD: A directional antineutrino detector with segmented ^6Li -doped pulse-shape-sensitive plastic scintillator,” *Nucl. Instrum. Meth. A*, vol. 1006, p. 165409, arXiv:2105.00083 [physics.ins-det].
 - [107] ROADSTR Near-Field Working Group, “Roadstr: a mobile antineutrino detector platform for enabling multi-reactor spectrum, oscillation, and application measurements,” 2020. Snowmass 2022 Letter of Interest.
 - [108] G. Cancelo, F. Cavanna, C. O. Escobar, E. Kemp, A. A. Machado, A. Para, E. Segreto, D. Totani, and D. Warner, “Increasing the efficiency of photon collection in LArTPCs: the ARAPUCA light trap,” *JINST*, vol. 13, no. 03, p. C03040, arXiv:1802.09726 [physics.ins-det].
 - [109] J. Dalmasson, G. Gratta, A. Jamil, S. Kravitz, M. Malek, K. Wells, J. Bentley, S. Steven, and J. Su, “Distributed Imaging for Liquid Scintillation Detectors,” *Phys. Rev. D*, vol. 97, no. 5, p. 052006, arXiv:1711.09851 [physics.ins-det].
 - [110] S. Seibert and A. LaTorre, “Fast Optical Monte Carlo Simulation with Surface-based Geometries Using *Chroma*,” *Semantic Scholar*, 2011.
 - [111] S. Seibert *et al.*, “RAT-PAC analysis package,”
 - [112] T. Bolton, “The Braidwood reactor antineutrino experiment,” *Nucl. Phys. B Proc. Suppl.*, vol. 149, pp. 166–169, 2005.
 - [113]
 - [114] *et al.* A.R. Back, “Accelerator Neutrino Neutron Interaction Experiment (ANNIE): Preliminary Results and Physics Phase Proposal,” *FNAL Report No. P-1063*, arXiv:1707.08222 [physics.ins-det].
 - [115] WATCHMAN Collaboration, M. Askins *et al.*, “The Physics and Nuclear Nonproliferation Goals of WATCHMAN: A WATER CHerenkov Monitor for ANTineutrinos,” 2 2015.
 - [116] J. Gruszko, B. Naranjo, B. Daniel, A. Elagin, D. Gooding, C. Grant, J. Ouellet, and L. Winslow, “Detecting Cherenkov light from 1–2 MeV electrons in linear alkylbenzene,” *JINST*, vol. 14, no. 02, p. P02005, arXiv:1811.11144 [physics.ins-det].

- [117] *et al.* I. Anghel, “LETTER OF INTENT: The Accelerator Neutrino Neutron Interaction Experiment (ANNIE),” *FNAL Report No. P-1063*, 2015.
- [118] T. J. Pershing, *The Accelerator Neutrino-Neutron Interaction Experiment*. PhD thesis, University of California, Davis, 2020.
- [119] E. Graham, D. Gooding, J. Gruszko, C. Grant, B. Naranjo, and L. Winslow, “Light Yield of Perovskite Nanocrystal-Doped Liquid Scintillator,” arXiv:1908.03564 [physics.ins-det].
- [120] DUNE Collaboration, J. Strait *et al.*, “Long-Baseline Neutrino Facility (LBNF) and Deep Underground Neutrino Experiment (DUNE): Conceptual Design Report, Volume 3: Long-Baseline Neutrino Facility for DUNE June 24, 2015,” arXiv:1601.05823 [physics.ins-det].
- [121] DUNE Collaboration, R. Acciarri *et al.*, “Long-Baseline Neutrino Facility (LBNF) and Deep Underground Neutrino Experiment (DUNE): Conceptual Design Report, Volume 1: The LBNF and DUNE Projects,” arXiv:1601.05471 [physics.ins-det].
- [122] BOREXINO Collaboration, M. Agostini *et al.*, “Experimental evidence of neutrinos produced in the CNO fusion cycle in the Sun,” *Nature*, vol. 587, pp. 577–582, arXiv:2006.15115 [hep-ex].
- [123] A. Friedland, C. Lunardini, and C. Pena-Garay, “Solar neutrinos as probes of neutrino matter interactions,” *Phys. Lett. B*, vol. 594, p. 347, 2004.
- [124] H. Minakata and C. Pena-Garay, “Solar Neutrino Observables Sensitive to Matter Effects,” *Adv. High Energy Phys.*, vol. 2012, p. 349686, arXiv:1009.4869 [hep-ph].
- [125] S. D. Biller, “Probing Majorana neutrinos in the regime of the normal mass hierarchy,” *Phys. Rev. D*, vol. 87, no. 7, p. 071301, arXiv:1306.5654 [physics.ins-det].
- [126] A. Cabrera *et al.*, “Neutrino Physics with an Opaque Detector,” *Commun. Phys.*, vol. 4, p. 273, 2021.
- [127] C. Buck, B. Gramlich, and S. Schoppmann, “Novel Opaque Scintillator for Neutrino Detection,” *JINST*, vol. 14, no. 11, p. P11007, 2019.
- [128] MINER Collaboration, G. Agnolet *et al.*, “Background Studies for the MINER Coherent Neutrino Scattering Reactor Experiment,” *Nucl. Instrum. Meth. A*, vol. 853, pp. 53–60, arXiv:1609.02066 [physics.ins-det].
- [129] R. Strauss *et al.*, “The ν -cleus experiment: A gram-scale fiducial-volume cryogenic detector for the first detection of coherent neutrino-nucleus scattering,” *Eur. Phys. J. C*, vol. 77, p. 506, arXiv:1704.04320 [physics.ins-det].
- [130] R. Strauss *et al.*, “Gram-scale cryogenic calorimeters for rare-event searches,” *Phys. Rev. D*, vol. 96, no. 2, p. 022009, arXiv:1704.04317 [physics.ins-det].
- [131] CRESST Collaboration, G. Angloher *et al.*, “Results on MeV-scale dark matter from a gram-scale cryogenic calorimeter operated above ground,” *Eur. Phys. J. C*, vol. 77, no. 9, p. 637, arXiv:1707.06749 [astro-ph.CO].
- [132] C. Augier *et al.*, “Ricochet Progress and Status,” in *19th International Workshop on Low Temperature Detectors*, 11 2021, 2111.06745.
- [133] I. Colantoni, C. Bellenghi, M. Calvo, R. Camattari, L. Cardani, N. Casali, A. Cruciani, S. Di Domizio, J. Goupy, V. Guidi, H. Le Sueur, M. Martinez, A. Mazzolari, A. Monfardini, V. Pettinacci, G. Pettinari, M. Romagnoni, and M. Vignati, “BULLKID: BULky and Low-Threshold Kinetic Inductance Detectors,” *Journal of Low Temperature Physics*, vol. 199, pp. 593–597, Feb. 2020.
- [134] CONNIE Collaboration, A. Aguilar-Arevalo *et al.*, “Exploring low-energy neutrino physics with the Coherent Neutrino Nucleus Interaction Experiment,” *Phys. Rev. D*, vol. 100, no. 9, p. 092005, arXiv:1906.02200 [physics.ins-det].
- [135] D. Akimov, S. Alawabdeh, P. An, A. Arteaga, C. Awe, P. S. Barbeau, C. Barry, B. Becker, V. Belov, I. Bernardi, M. A. Blackston, L. Blokland, C. Bock, B. Bodur, A. Bolozdynya,

- R. Bouabid, A. Bracho, J. Browning, B. Cabrera-Palmer, N. Chen, D. Chernyak, E. Conley, J. Daughhetee, J. Daughtry, E. Day, M. d. V. Coello, J. Detwiler, K. Ding, M. R. Durand, Y. Efremenko, S. R. Elliott, L. Fabris, M. Febbraro, W. Fox, J. Galambos, A. G. Rosso, A. Galindo-Uribarri, C. Gilbert, M. P. Green, K. R. Hansen, B. Harris, M. R. Heath, S. Hedges, R. Henderson, D. Hoang, C. Hughes, M. Hughes, E. Iverson, P. Jairam, B. A. Johnson, T. Johnson, L. Kaufman, A. Khromov, A. Konovalov, J. Koros, E. Kozlova, A. Kumpan, L. Li, J. T. Librande, J. M. Link, J. Liu, A. Major, K. Mann, D. M. Markoff, J. Mastroberti, J. Mattingly, O. McGoldrick, M. McIntyre, Y. A. Melikyan, M. Mishra, P. E. Mueller, J. Newby, D. S. Parno, A. Penne, S. I. Penttila, D. Pershey, C. Prior, D. Radford, F. Rahman, R. Rapp, H. Ray, J. Raybern, O. Razuvaeva, D. Reyna, G. C. Rich, D. Rimal, J. Ross, A. Rouzky, D. Rudik, J. Runge, D. J. Salvat, A. M. Salyapongse, J. Sander, K. Scholberg, P. Siehien, A. Shakirov, G. Simakov, G. Sinev, W. M. Snow, V. Sosnovstsev, J. Steele, A. S. Hjelmstad, T. Subedi, B. Suh, R. Tayloe, K. Tellez-Giron-Flores, R. T. Thornton, I. Tolstukhin, S. Trotter, F. Tsai, Y. T. Tsai, E. Ujah, J. Vanderwerp, E. van Nieuwenhuizen, R. L. Varner, S. Vasquez, C. J. Virtue, G. Visser, K. Walkup, J. Wang, E. M. Ward, C. Wiseman, T. Wongjirad, D. Wu, J. Yang, Y. Yang, Y. R. Yen, J. Yoo, C. H. Yu, J. Zettlemoyer, and S. Zhang, “The coherent experimental program,” 2022.
- [136] CONUS Collaboration, H. Bonet *et al.*, “Constraints on Elastic Neutrino Nucleus Scattering in the Fully Coherent Regime from the CONUS Experiment,” *Phys. Rev. Lett.*, vol. 126, no. 4, p. 041804, arXiv:2011.00210 [hep-ex].
- [137] J. Colaresi, J. I. Collar, T. W. Hossbach, A. R. L. Kavner, C. M. Lewis, A. E. Robinson, and K. M. Yocum, “First results from a search for coherent elastic neutrino-nucleus scattering at a reactor site,” *Phys. Rev. D*, vol. 104, no. 7, p. 072003, arXiv:2108.02880 [hep-ex].
- [138] Presentation at the Magnificent CEvNS workshop, Nov 2021, <https://indico.cern.ch/event/1075677/contributions/4556660/>.
- [139] H. T.-K. Wong, “Taiwan EXperiment On Neutrino — History and Prospects,” *The Universe*, vol. 3, no. 4, pp. 22–37, arXiv:1608.00306 [hep-ex].
- [140] J. J. Choi, E. J. Jeon, J. Y. Kim, K. W. Kim, S. H. Kim, S. K. Kim, Y. D. Kim, Y. J. Ko, B. C. Koh, C. Ha, B. J. Park, S. H. Lee, I. S. Lee, H. Lee, H. S. Lee, J. Lee, Y. M. Oh, and S. L. Olsen, “Exploring coherent elastic neutrino-nucleus scattering using reactor electron antineutrinos in the neon experiment,” 2022.
- [141] E. Alfonso-Pita *et al.*, “Snowmass 2021 Scintillating Bubble Chambers: Liquid-noble Bubble Chambers for Dark Matter and CE ν NS Detection,” in *2022 Snowmass Summer Study*, 7 2022, 2207.12400.
- [142] I. Giomataris *et al.*, “A Novel large-volume Spherical Detector with Proportional Amplification read-out,” *JINST*, vol. 3, p. P09007, arXiv:0807.2802 [physics.ins-det].
- [143] D. Akimov *et al.*, “First constraint on coherent elastic neutrino-nucleus scattering in argon,” *Phys. Rev. D*, vol. 100, p. 115020, Dec 2019.
- [144] D. Y. Akimov *et al.*, “Status of the RED-100 experiment,” *JINST*, vol. 12, no. 06, p. C06018, 2017.
- [145] J. Xu, “"status of the chillax detector development"." Magnificent CEvNS 2021, 2021.
- [146] K. Ni, J. Qi, E. Shockley, and Y. Wei, “Sensitivity of a Liquid Xenon Detector to Neutrino–Nucleus Coherent Scattering and Neutrino Magnetic Moment from Reactor Neutrinos,” *Universe*, vol. 7, no. 3, p. 54, 2021.
- [147] B. Monreal and J. A. Formaggio, “Relativistic cyclotron radiation detection of tritium decay electrons as a new technique for measuring the neutrino mass,” *Phys. Rev. D*, vol. 80, p. 051301, Sep 2009.

- [148] C. Velte, F. Ahrens, A. Barth, K. Blaum, M. Braß, M. Door, H. Dorrer, C. E. Düllmann, S. Eliseev, C. Enss, P. Filianin, A. Fleischmann, L. Gastaldo, A. Goeggelmann, T. D. Goodacre, M. W. Haverkort, D. Hengstler, J. Jochum, K. Johnston, M. Keller, S. Kempf, T. Kieck, C. M. König, U. Köster, K. Kromer, F. Mantegazzini, B. Marsh, Y. N. Novikov, F. Piquemal, C. Riccio, D. Richter, A. Rischka, S. Rothe, R. X. Schüssler, C. Schweiger, T. Stora, M. Wegner, K. Wendt, M. Zampaolo, and K. Zuber, “High-resolution and low-background ^{163}Ho spectrum: interpretation of the resonance tails,” *The European Physical Journal C*, vol. 79, no. 12, p. 1026, 2019.
- [149] Nucciotti, Angelo, “Statistical sensitivity of ^{163}Ho electron capture neutrino mass experiments,” *Eur. Phys. J. C*, vol. 74, no. 11, p. 3161, 2014.
- [150] J. A. B. Mates, D. T. Becker, D. A. Bennett, B. J. Dober, J. D. Gard, J. P. Hays-Wehle, J. W. Fowler, G. C. Hilton, C. D. Reintsema, D. R. Schmidt, D. S. Swetz, L. R. Vale, and J. N. Ullom, “Simultaneous readout of 128 x-ray and gamma-ray transition-edge microcalorimeters using microwave squid multiplexing,” *Applied Physics Letters*, vol. 111, no. 6, p. 062601, 2017.
- [151] S. Betts *et al.*, “Development of a relic neutrino detection experiment at ptolemy: Princeton tritium observatory for light, early-universe, massive-neutrino yield,” 2013.
- [152] L. Pattavina, N. Ferreiro Iachellini, and I. Tamborra, “Neutrino observatory based on archaeological lead,” *Phys. Rev. D*, vol. 102, no. 6, p. 063001, arXiv:2004.06936 [astro-ph.HE].
- [153] S. Baum, A. K. Drukier, K. Freese, M. Górski, and P. Stengel, “Searching for Dark Matter with Paleo-Detectors,” *Phys. Lett. B*, vol. 803, p. 135325, arXiv:1806.05991 [astro-ph.CO].
- [154] K. Alfonso *et al.*, “Passive low energy nuclear recoil detection with color centers – PALEOCENE,” in *2022 Snowmass Summer Study*, 3 2022, 2203.05525.
- [155] N. Solomey *et al.*, “Science mission of a neutrino space-craft.” <https://www.nasa.gov/directorates/spacetech/niac/>.
- [156] S. Vahsen *et al.*, “CYGNUS: Feasibility of a nuclear recoil observatory with directional sensitivity to dark matter and neutrinos,” arXiv:2008.12587 [physics.ins-det].
- [157] D. Aristizabal Sierra, B. Dutta, D. Kim, D. Snowden-Ifft, and L. E. Strigari, “Coherent elastic neutrino-nucleus scattering with the $\nu\text{BDX-DRIFT}$ directional detector at next generation neutrino facilities,” *Phys. Rev. D*, vol. 104, no. 3, p. 033004, arXiv:2103.10857 [hep-ph].
- [158] J. Billard, L. Strigari, and E. Figueroa-Feliciano, “Implication of neutrino backgrounds on the reach of next generation dark matter direct detection experiments,” *Phys. Rev. D*, vol. 89, no. 2, p. 023524, arXiv:1307.5458 [hep-ph].
- [159] P. Adari *et al.*, “Excess workshop: Descriptions of rising low-energy spectra,” 2022.
- [160] NUCLEUS Collaboration, J. Rothe *et al.*, “NUCLEUS: Exploring Coherent Neutrino-Nucleus Scattering with Cryogenic Detectors,” *J. Low Temp. Phys.*, vol. 199, no. 1-2, pp. 433–440, 2019.
- [161] NUCLEUS Collaboration, G. Angloher *et al.*, “Exploring $\text{CE}\nu\text{NS}$ with NUCLEUS at the Chooz nuclear power plant,” *Eur. Phys. J. C*, vol. 79, no. 12, p. 1018, arXiv:1905.10258 [physics.ins-det].
- [162] V. Wagner *et al.*, “Development of a compact muon veto for the NUCLEUS experiment,” arXiv:2202.03991 [physics.ins-det].
- [163] T. Salagnac *et al.*, “Optimization and performance of the CryoCube detector for the future RICOCHET low-energy neutrino experiment,” in *19th International Workshop on Low Temperature Detectors*, 11 2021, 2111.12438.
- [164] S. M. Griffin, Y. Hochberg, K. Inzani, N. Kurinsky, T. Lin, and T. C. Yu, “Silicon carbide detectors for sub-gev dark matter,” *Phys. Rev. D*, vol. 103, p. 075002, Apr 2021.
- [165] N. Kurinsky, T. C. Yu, Y. Hochberg, and B. Cabrera, “Diamond detectors for direct detection of sub-gev dark matter,” *Phys. Rev. D*, vol. 99, p. 123005, Jun 2019.

- [166] L. Canonica, A. H. Abdelhameed, P. Bauer, A. Bento, E. Bertoldo, N. Ferreiro Iachellini, D. Fuchs, D. Hauff, M. Mancuso, F. Petricca, F. Pröbst, and J. Rothe, “Operation of a diamond cryogenic detector for low-mass dark matter searches,” *Journal of Low Temperature Physics*, vol. 199, no. 3, pp. 606–613, 2020.
- [167] A. E. Chavarria *et al.*, “Measurement of the ionization produced by sub-keV silicon nuclear recoils in a CCD dark matter detector,” *Phys. Rev. D*, vol. 94, no. 8, p. 082007, arXiv:1608.00957 [astro-ph.IM].
- [168] Y. Sarkis, A. Aguilar-Arevalo, and J. C. D’Olivo, “Study of the ionization efficiency for nuclear recoils in pure crystals,” *Phys. Rev. D*, vol. 101, no. 10, p. 102001, arXiv:2001.06503 [hep-ph].
- [169] Y. Sarkis, A. Aguilar-Arevalo, and J. C. D’Olivo, “A Study of the Ionization Efficiency for Nuclear Recoils in Pure Crystals,” *Phys. At. Nucl.*, vol. 84, no. 4, pp. 590–594, 2021.
- [170] <https://www.violetaexperiment.com>.
- [171] S. Eliseev, K. Blaum, M. Block, S. Chenmarev, H. Dorrer, C. E. Düllmann, C. Enss, P. E. Filianin, L. Gastaldo, M. Goncharov, U. Köster, F. Lautenschläger, Y. N. Novikov, A. Rischka, R. X. Schüssler, L. Schweikhard, and A. Türlér, “Direct measurement of the mass difference of ^{163}Ho and ^{163}Dy solves the q -value puzzle for the neutrino mass determination,” *Phys. Rev. Lett.*, vol. 115, p. 062501, Aug 2015.
- [172] A. K. Drukier, S. Baum, K. Freese, M. Górski, and P. Stengel, “Paleo-detectors: Searching for Dark Matter with Ancient Minerals,” *Phys. Rev. D*, vol. 99, no. 4, p. 043014, arXiv:1811.06844 [astro-ph.CO].
- [173] J. R. Jordan, S. Baum, P. Stengel, A. Ferrari, M. C. Morone, P. Sala, and J. Spitz, “Measuring Changes in the Atmospheric Neutrino Rate Over Gigayear Timescales,” *Phys. Rev. Lett.*, vol. 125, no. 23, p. 231802, arXiv:2004.08394 [hep-ph].
- [174] N. Tapia-Arellano and S. Horiuchi, “Measuring solar neutrinos over gigayear timescales with paleo detectors,” *Phys. Rev. D*, vol. 103, no. 12, p. 123016, arXiv:2102.01755 [hep-ph].
- [175] S. Baum, T. D. P. Edwards, B. J. Kavanagh, P. Stengel, A. K. Drukier, K. Freese, M. Górski, and C. Weniger, “Paleodetectors for Galactic supernova neutrinos,” *Phys. Rev. D*, vol. 101, no. 10, p. 103017, arXiv:1906.05800 [astro-ph.GA].
- [176] S. Baum, T. D. P. Edwards, K. Freese, and P. Stengel, “New Projections for Dark Matter Searches with Paleo-Detectors,” *Instruments*, vol. 5, no. 2, p. 21, arXiv:2106.06559 [astro-ph.CO].
- [177] S. Baum, W. DeRocco, T. D. P. Edwards, and S. Kalia, “Galactic geology: Probing time-varying dark matter signals with paleodetectors,” *Phys. Rev. D*, vol. 104, no. 12, p. 123015, arXiv:2107.02812 [astro-ph.GA].
- [178] B. K. Cogswell, A. Goel, and P. Huber, “Passive Low-Energy Nuclear-Recoil Detection with Color Centers,” *Phys. Rev. Applied*, vol. 16, no. 6, p. 064060, arXiv:2104.13926 [physics.ins-det].
- [179] M. Szydagis, C. Levy, Y. Huang, A. C. Kamaha, C. C. Knight, G. R. C. Rischbieter, and P. W. Wilson, “Demonstration of neutron radiation-induced nucleation of supercooled water,” *Phys. Chem. Chem. Phys.*, vol. 23, pp. 13440–13446, 2021.
- [180] R. Cooper, D. Radford, P. Hausladen, and K. Lagergren, “A novel hpge detector for gamma-ray tracking and imaging,” *Nuclear Instruments and Methods in Physics Research Section A: Accelerators, Spectrometers, Detectors and Associated Equipment*, vol. 665, pp. 25–32, 2011.
- [181] H. Bonet *et al.*, “Large-size sub-keV sensitive germanium detectors for the CONUS experiment,” *Eur. Phys. J. C*, vol. 81, no. 3, p. 267, arXiv:2010.11241 [physics.ins-det].
- [182] H. Bonet *et al.*, “Full background decomposition of the conus experiment,” arXiv:2112.09585 [physics.ins-det].
- [183] A. Bonhomme *et al.*, “Direct measurement of the ionization quenching factor of nuclear recoils in germanium in the kev energy range,” arXiv:2202.03754 [physics.ins-det].

- [184] J. Colaresi, J. I. Collar, T. W. Hossbach, C. M. Lewis, and K. M. Yocum, “Suggestive evidence for Coherent Elastic Neutrino-Nucleus Scattering from reactor antineutrinos,” arXiv:2202.09672 [hep-ex].
- [185] TEXONO Collaboration, H. Wong *et al.*, “A Search of Neutrino Magnetic Moments with a High-Purity Germanium Detector at the Kuo-Sheng Nuclear Power Station,” *Phys. Rev. D*, vol. 75, p. 012001, 2007.
- [186] J.-W. Chen, H.-C. Chi, H.-B. Li, C. P. Liu, L. Singh, H. T. Wong, C.-L. Wu, and C.-P. Wu, “Constraints on millicharged neutrinos via analysis of data from atomic ionizations with germanium detectors at sub-keV sensitivities,” *Phys. Rev. D*, vol. 90, no. 1, p. 011301, arXiv:1405.7168 [hep-ph].
- [187] COSINE-100 Collaboration, G. Adhikari *et al.*, “An experiment to search for dark-matter interactions using sodium iodide detectors,” *Nature*, vol. 564, no. 7734, pp. 83–86, arXiv:1906.01791 [astro-ph.IM].
- [188] COSINE-100 Collaboration, G. Adhikari *et al.*, “Search for a Dark Matter-Induced Annual Modulation Signal in NaI(Tl) with the COSINE-100 Experiment,” *Phys. Rev. Lett.*, vol. 123, no. 3, p. 031302, arXiv:1903.10098 [astro-ph.IM].
- [189] COSINE-100 Collaboration, G. Adhikari *et al.*, “Initial Performance of the COSINE-100 Experiment,” *Eur. Phys. J. C*, vol. 78, no. 2, p. 107, arXiv:1710.05299 [physics.ins-det].
- [190] COSINE-100 Collaboration, G. Adhikari *et al.*, “Lowering the energy threshold in COSINE-100 dark matter searches,” *Astropart. Phys.*, vol. 130, p. 102581, arXiv:2005.13784 [physics.ins-det].
- [191] J. Choi, B. Park, C. Ha, K. Kim, S. Kim, Y. Kim, Y. Ko, H. Lee, S. Lee, and S. Olsen, “Improving the light collection using a new NaI(Tl) crystal encapsulation,” *Nucl. Instrum. Meth. A*, vol. 981, p. 164556, arXiv:2006.02573 [physics.ins-det].
- [192] COSINE Collaboration, B. Park *et al.*, “Development of ultra-pure NaI(Tl) detectors for the COSINE-200 experiment,” *Eur. Phys. J. C*, vol. 80, no. 9, p. 814, arXiv:2004.06287 [physics.ins-det].
- [193] COSINE-100 Collaboration, G. Adhikari *et al.*, “The COSINE-100 Data Acquisition System,” *JINST*, vol. 13, no. 09, p. P09006, arXiv:1806.09788 [physics.ins-det].
- [194] B. Mosconi, P. Ricci, E. Truhlik, and P. Vogel, “Model dependence of the neutrino-deuteron disintegration cross sections at low energies,” *Phys. Rev. C*, vol. 75, p. 044610, Apr 2007.
- [195] SBC Collaboration, P. Giampa, “The Scintillating Bubble Chamber (SBC) Experiment for Dark Matter and Reactor CEvNS,” *PoS*, vol. ICHEP2020, p. 632, 2021.
- [196] SBC, CEvNS Theory Group at IF-UNAM Collaboration, L. J. Flores *et al.*, “Physics reach of a low threshold scintillating argon bubble chamber in coherent elastic neutrino-nucleus scattering reactor experiments,” *Phys. Rev. D*, vol. 103, no. 9, p. L091301, arXiv:2101.08785 [hep-ex].
- [197] K. Scholberg, “Prospects for measuring coherent neutrino-nucleus elastic scattering at a stopped-pion neutrino source,” *Phys. Rev. D*, vol. 73, p. 033005, arXiv:hep-ex/0511042 [hep-ex].
- [198] I. Katsioulas *et al.*, “A sparkless resistive glass correction electrode for the spherical proportional counter,” *JINST*, vol. 13, no. 11, p. P11006, arXiv:1809.03270 [physics.ins-det].
- [199] I. Giomataris *et al.*, “A resistive ACHINOS multi-anode structure with DLC coating for spherical proportional counters,” *JINST*, vol. 15, no. 11, p. 11, arXiv:2003.01068 [physics.ins-det].
- [200] A. Giganon *et al.*, “A multiball read-out for the spherical proportional counter,” *JINST*, vol. 12, no. 12, p. P12031, arXiv:1707.09254 [physics.ins-det].
- [201] E. Bougamont *et al.*, “Ultra low energy results and their impact to dark matter and low energy neutrino physics,” arXiv:1010.4132 [physics.ins-det].
- [202] G. Heusser and other, “GIOVE - A new detector setup for high sensitivity germanium spectroscopy at shallow depth,” *Eur. Phys. J. C*, vol. 75, no. 11, p. 531, arXiv:1507.03319 [astro-ph.IM].

- [203] C. Buck *et al.*, “A novel experiment for coherent elastic neutrino nucleus scattering: CONUS,” *J. Phys. Conf. Ser.*, vol. 1342, no. 1, p. 012094, 2020.
- [204] D. Akimov *et al.*, “Coherent 2018 at the spallation neutron source,” 2018.
- [205] RED-100 Collaboration, D. Y. Akimov *et al.*, “First ground-level laboratory test of the two-phase xenon emission detector RED-100,” *JINST*, vol. 15, no. 02, p. P02020, arXiv:1910.06190 [physics.ins-det].
- [206] B. Lenardo *et al.*, “Measurement of the ionization yield from nuclear recoils in liquid xenon between 0.3 - 6 keV with single-ionization-electron sensitivity,” arXiv:1908.00518 [physics.ins-det].
- [207] M. Abdullah *et al.*, “Coherent elastic neutrino-nucleus scattering: Terrestrial and astrophysical applications,” 2022.
- [208] B. Cabrera, L. M. Krauss, and F. Wilczek, “Bolometric Detection of Neutrinos,” *Phys. Rev. Lett.*, vol. 55, p. 25, 1985.
- [209] A. K. Drukier, K. Freese, and D. N. Spergel, “Detecting Cold Dark Matter Candidates,” *Phys. Rev. D*, vol. 33, pp. 3495–3508, 1986.
- [210] J. Monroe and P. Fisher, “Neutrino Backgrounds to Dark Matter Searches,” *Phys. Rev. D*, vol. 76, p. 033007, arXiv:0706.3019 [astro-ph].
- [211] J. D. Vergados and H. Ejiri, “Can Solar Neutrinos be a Serious Background in Direct Dark Matter Searches?,” *Nucl. Phys. B*, vol. 804, pp. 144–159, arXiv:0805.2583 [hep-ph].
- [212] L. E. Strigari, “Neutrino Coherent Scattering Rates at Direct Dark Matter Detectors,” *New J. Phys.*, vol. 11, p. 105011, arXiv:0903.3630 [astro-ph.CO].
- [213] A. Gutlein *et al.*, “Solar and atmospheric neutrinos: Background sources for the direct dark matter search,” *Astropart. Phys.*, vol. 34, pp. 90–96, arXiv:1003.5530 [hep-ph].
- [214] G. B. Gelmini, V. Takhistov, and S. J. Witte, “Casting a Wide Signal Net with Future Direct Dark Matter Detection Experiments,” *JCAP*, vol. 1807, no. 07, p. 009, arXiv:1804.01638 [hep-ph].
- [215] C. A. J. O’Hare, “New Definition of the Neutrino Floor for Direct Dark Matter Searches,” *Phys. Rev. Lett.*, vol. 127, no. 25, p. 251802, arXiv:2109.03116 [hep-ph].
- [216] J. B. Dent, B. Dutta, J. L. Newstead, and L. E. Strigari, “Dark matter, light mediators, and the neutrino floor,” *Phys. Rev. D*, vol. 95, no. 5, p. 051701, arXiv:1607.01468 [hep-ph].
- [217] J. H. Davis, “Dark Matter vs. Neutrinos: The effect of astrophysical uncertainties and timing information on the neutrino floor,” *JCAP*, vol. 1503, p. 012, arXiv:1412.1475 [hep-ph].
- [218] F. Ruppin, J. Billard, E. Figueroa-Feliciano, and L. Strigari, “Complementarity of dark matter detectors in light of the neutrino background,” *Phys. Rev. D*, vol. 90, no. 8, p. 083510, arXiv:1408.3581 [hep-ph].
- [219] A. Gaspert, P. Giampa, and D. E. Morrissey, “Neutrino backgrounds in future liquid noble element dark matter direct detection experiments,” *Phys. Rev. D*, vol. 105, no. 3, p. 035020, arXiv:2108.03248 [hep-ph].
- [220] C. A. J. O’Hare, “Can we overcome the neutrino floor at high masses?,” *Phys. Rev. D*, vol. 102, no. 6, p. 063024, arXiv:2002.07499 [astro-ph.CO].
- [221] C. A. J. O’Hare, A. M. Green, J. Billard, E. Figueroa-Feliciano, and L. E. Strigari, “Readout strategies for directional dark matter detection beyond the neutrino background,” *Phys. Rev. D*, vol. 92, no. 6, p. 063518, arXiv:1505.08061 [astro-ph.CO].
- [222] P. Grothaus, M. Fairbairn, and J. Monroe, “Directional Dark Matter Detection Beyond the Neutrino Bound,” *Phys. Rev. D*, vol. 90, no. 5, p. 055018, arXiv:1406.5047 [hep-ph].
- [223] F. Mayet *et al.*, “A review of the discovery reach of directional Dark Matter detection,” *Phys. Rept.*, vol. 627, pp. 1–49, arXiv:1602.03781 [astro-ph.CO].

- [224] C. A. J. O’Hare, B. J. Kavanagh, and A. M. Green, “Time-integrated directional detection of dark matter,” *Phys. Rev. D*, vol. 96, no. 8, p. 083011, arXiv:1708.02959 [astro-ph.CO].
- [225] T. Franarin and M. Fairbairn, “Reducing the solar neutrino background in dark matter searches using polarized helium-3,” *Phys. Rev. D*, vol. 94, no. 5, p. 053004, arXiv:1605.08727 [hep-ph].
- [226] S. E. Vahsen, C. A. J. O’Hare, and D. Loomba, “Directional recoil detection,” *Ann. Rev. Nucl. Part. Sci.*, vol. 71, pp. 189–224, arXiv:2102.04596 [physics.ins-det].
- [227] S. Sassi, A. Dinmohammadi, M. Heikinheimo, N. Mirabolfathi, K. Nordlund, H. Safari, and K. Tuominen, “Solar neutrinos and dark matter detection with diurnal modulation,” arXiv:2103.08511 [hep-ph].
- [228] LUX-ZEPLIN Collaboration, D. S. Akerib *et al.*, “Projected WIMP sensitivity of the LUX-ZEPLIN dark matter experiment,” *Phys. Rev. D*, vol. 101, no. 5, p. 052002, arXiv:1802.06039 [astro-ph.IM].
- [229] L. Baudis, A. Ferella, A. Kish, A. Manalaysay, T. Marrodan Undagoitia, and M. Schumann, “Neutrino physics with multi-ton scale liquid xenon detectors,” *JCAP*, vol. 01, p. 044, arXiv:1309.7024 [physics.ins-det].
- [230] DARWIN Collaboration, J. Aalbers *et al.*, “DARWIN: towards the ultimate dark matter detector,” *JCAP*, vol. 1611, p. 017, arXiv:1606.07001 [astro-ph.IM].
- [231] J. L. Newstead, R. F. Lang, and L. E. Strigari, “Atmospheric neutrinos in next-generation xenon and argon dark matter experiments,” *Phys. Rev. D*, vol. 104, no. 11, p. 115022, arXiv:2002.08566 [astro-ph.CO].
- [232] R. F. Lang, C. McCabe, S. Reichard, M. Selvi, and I. Tamborra, “Supernova neutrino physics with xenon dark matter detectors: A timely perspective,” *Phys. Rev. D*, vol. 94, no. 10, p. 103009, arXiv:1606.09243 [astro-ph.HE].
- [233] N. Raj, “Neutrinos from Type Ia and failed core-collapse supernovae at dark matter detectors,” *Phys. Rev. Lett.*, vol. 124, no. 14, p. 141802, arXiv:1907.05533 [hep-ph].
- [234] A. M. Suliga, J. F. Beacom, and I. Tamborra, “Towards Probing the Diffuse Supernova Neutrino Background in All Flavors,” arXiv:2112.09168 [astro-ph.HE].
- [235] R. Agnese, A. J. Anderson, T. Aramaki, I. Arnquist, W. Baker, D. Barker, R. Basu Thakur, D. A. Bauer, A. Borgland, M. A. Bowles, P. L. Brink, R. Bunker, B. Cabrera, D. O. Caldwell, R. Calkins, C. Cartaro, D. G. Cerdeño, H. Chagani, Y. Chen, J. Cooley, B. Cornell, P. Cushman, M. Daal, P. C. F. Di Stefano, T. Doughty, L. Esteban, S. Fallows, E. Figueroa-Feliciano, M. Fritts, G. Gerbier, M. Ghaith, G. L. Godfrey, S. R. Golwala, J. Hall, H. R. Harris, T. Hofer, D. Holmgren, Z. Hong, E. Hoppe, L. Hsu, M. E. Huber, V. Iyer, D. Jardin, A. Jastram, M. H. Kelsey, A. Kennedy, A. Kubik, N. A. Kurinsky, A. Leder, B. Loer, E. Lopez Asamar, P. Lukens, R. Mahapatra, V. Mandic, N. Mast, N. Mirabolfathi, R. A. Moffatt, J. D. Morales Mendoza, J. L. Orrell, S. M. Oser, K. Page, W. A. Page, R. Partridge, M. Pepin, A. Phipps, S. Poudel, M. Pyle, H. Qiu, W. Rau, P. Redl, A. Risetter, A. Roberts, A. E. Robinson, H. E. Rogers, T. Saab, B. Sadoulet, J. Sander, K. Schneck, R. W. Schnee, B. Serfass, D. Speller, M. Stein, J. Street, H. A. Tanaka, D. Toback, R. Underwood, A. N. Villano, B. von Krosigk, B. Welliver, J. S. Wilson, D. H. Wright, S. Yellin, J. J. Yen, B. A. Young, X. Zhang, and X. Zhao, “Projected sensitivity of the SuperCDMS SNOLAB experiment,” *Phys. Rev. D*, vol. 95, no. 8, pp. 082002/1–17, 2017.
- [236] SuperCDMS Collaboration, M. Al-Bakry, I. Alkhatib, D. Praia do Amaral, T. Aralis, T. Aramaki, I. Arnquist, I. Ataee Langroudy, E. Azadbakht, S. Banik, C. Bathurst, D. Bauer, L. Bezerra, R. Bhattacharyya, P. Brink, R. Bunker, B. Cabrera, R. Calkins, R. Cameron, C. Cartaro, D. Cerdeno, Y.-Y. Chang, M. Chaudhuri, R. Chen, N. Chott, J. Cooley, H. Coombes, J. Corbett, P. Cushman, F. De Brienne, S. Dharani, M. L. di Vacri, M. Diamond, E. Fascione, E. Figueroa, C. Fink, K. Fouts, M. Fritts, G. Gerbier, R. Germond, M. Ghaith, S. Golwala, J. Hall, N. Has-

- san, B. Hines, M. Hollister, Z. Hong, E. Hoppe, L. Hsu, M. Huber, V. Iyer, D. Jardin, A. Jastram, V. Kashyap, M. Kelsey, A. Kubik, N. Kurinsky, R. Lawrence, M. Lee, A. Li, J. Liu, Y. Liu, B. Loer, P. Lukens, D. MacFarlane, R. Mahapatra, V. Mandic, N. Mast, A. Mayer, H. M. z. Theenhausen, É. Michaud, E. Michielin, N. Mirabolfathi, B. Mohanty, S. Nagorny, J. Nelson, H. Neog, V. Novati, J. Orrell, M. Osborne, S. Oser, W. Page, R. Partridge, D. S. Pedreros, R. Podvianiuk, F. Ponce, S. Poudel, A. Pradeep, M. Pyle, W. Rau, E. Reid, T. Ren, T. Reynolds, A. Roberts, A. Robinson, T. Saab, B. Sadoulet, I. Saikia, J. Sander, A. Sattari, B. Schmidt, R. Schnee, S. Scorza, B. Serfass, S. Sharma Poudel, D. Sincavage, C. Stanford, J. Street, H. Sun, F. Thasrawala, D. Toback, R. Underwood, S. Verma, A. Villano, B. von Krosigk, S. Watkins, O. Wen, Z. Williams, M. Wilson, J. Winchell, C.-p. Wu, K. Wykoff, S. Yellin, B. Young, T. C. Yu, B. Zatschler, S. Zatschler, A. Zaytsev, E. Zhang, L. Zheng, and S. Zuber, “A Strategy for Low-Mass Dark Matter Searches with Cryogenic Detectors in the SuperCDMS SNOLAB Facility.” to be submitted to arXiv, 2022. to be submitted to the Proceedings of the US Community Study on the Future of Particle Physics (Snowmass 2021).
- [237] RES-NOVA Collaboration, L. Pattavina *et al.*, “RES-NOVA sensitivity to core-collapse and failed core-collapse supernova neutrinos,” *JCAP*, vol. 10, p. 064, arXiv:2103.08672 [astro-ph.IM].
- [238] D. P. Snowden-Ifft, C. J. Martoff, and J. M. Burwell, “Low pressure negative ion drift chamber for dark matter search,” *Phys. Rev. D*, vol. 61, p. 101301, 2000.
- [239] M. Ackermann *et al.*, “High-Energy and Ultra-High-Energy Neutrinos,” arXiv:2203.08096 [hep-ph].
- [240] ANTARES, IceCube, Pierre Auger, LIGO Scientific, Virgo Collaboration, A. Albert *et al.*, “Search for High-energy Neutrinos from Binary Neutron Star Merger GW170817 with ANTARES, IceCube, and the Pierre Auger Observatory,” *Astrophys. J. Lett.*, vol. 850, no. 2, p. L35, arXiv:1710.05839 [astro-ph.HE].
- [241] IceCube-Gen2 Collaboration, M. G. Aartsen *et al.*, “IceCube-Gen2: the window to the extreme Universe,” *J. Phys. G*, vol. 48, no. 6, p. 060501, arXiv:2008.04323 [astro-ph.HE].
- [242] S. Hallmann, B. Clark, C. Glaser and D. Smith for the IceCube-Gen2 Collaboration, “Sensitivity studies for the IceCube-Gen2 radio array,” *PoS*, vol. ICRC2021, p. 1183, arXiv:2107.08910 [astro-ph.HE].
- [243] “All-sky point-source IceCube data: years 2010-2012.” <https://icecube.wisc.edu/data-releases/2018/10/all-sky-point-source-icecube-data-years-2010-2012/>. Accessed: 2021-02-16.
- [244] IceCube Collaboration, M. G. Aartsen *et al.*, “All-sky Search for Time-integrated Neutrino Emission from Astrophysical Sources with 7 yr of IceCube Data,” *Astrophys. J.*, vol. 835, no. 2, p. 151, arXiv:1609.04981 [astro-ph.HE].
- [245] PUEO Collaboration, Q. Abarr *et al.*, “The Payload for Ultrahigh Energy Observations (PUEO): a white paper,” *JINST*, vol. 16, no. 08, p. P08035, arXiv:2010.02892 [astro-ph.IM].
- [246] T. M. Venters, M. H. Reno, J. F. Krizmanic, L. A. Anchordoqui, C. Guépin, and A. V. Olinto, “POEMMA’s Target of Opportunity Sensitivity to Cosmic Neutrino Transient Sources,” *Phys. Rev. D*, vol. 102, p. 123013, arXiv:1906.07209 [astro-ph.HE].
- [247] GRAND Collaboration, J. Álvarez-Muñiz *et al.*, “The Giant Radio Array for Neutrino Detection (GRAND): Science and Design,” *Sci. China Phys. Mech. Astron.*, vol. 63, no. 1, p. 219501, arXiv:1810.09994 [astro-ph.HE].
- [248] S. S. Kimura, K. Murase, P. Mészáros, and K. Kiuchi, “High-Energy Neutrino Emission from Short Gamma-Ray Bursts: Prospects for Coincident Detection with Gravitational Waves,” *Astrophys. J. Lett.*, vol. 848, no. 1, p. L4, arXiv:1708.07075 [astro-ph.HE].

- [249] A. van Vliet, R. Alves Batista, and J. R. Hörandel, “Determining the fraction of cosmic-ray protons at ultrahigh energies with cosmogenic neutrinos,” *Phys. Rev. D*, vol. 100, no. 2, p. 021302, arXiv:1901.01899 [astro-ph.HE].
- [250] M. S. Muzio, G. R. Farrar, and M. Unger, “Probing the environments surrounding ultrahigh energy cosmic ray accelerators and their implications for astrophysical neutrinos,” *Phys. Rev. D*, vol. 105, no. 2, p. 023022, arXiv:2108.05512 [astro-ph.HE].
- [251] K. Fang and K. Murase, “Linking High-Energy Cosmic Particles by Black Hole Jets Embedded in Large-Scale Structures,” *Nature Phys.*, vol. 14, no. 4, p. 396, arXiv:1704.00015 [astro-ph.HE].
- [252] D. Biehl, D. Boncioli, C. Lunardini, and W. Winter, “Tidally disrupted stars as a possible origin of both cosmic rays and neutrinos at the highest energies,” *Sci. Rep.*, vol. 8, no. 1, p. 10828, arXiv:1711.03555 [astro-ph.HE].
- [253] IceCube Collaboration, R. Abbasi *et al.*, “Improved Characterization of the Astrophysical Muon-Neutrino Flux with 9.5 Years of IceCube Data,” arXiv:2111.10299 [astro-ph.HE].
- [254] IceCube Collaboration, M. G. Aartsen *et al.*, “Characteristics of the diffuse astrophysical electron and tau neutrino flux with six years of IceCube high energy cascade data,” *Phys. Rev. Lett.*, vol. 125, no. 12, p. 121104, arXiv:2001.09520 [astro-ph.HE].
- [255] Pierre Auger Collaboration, A. Aab *et al.*, “Probing the origin of ultra-high-energy cosmic rays with neutrinos in the EeV energy range using the Pierre Auger Observatory,” *JCAP*, vol. 10, p. 022, arXiv:1906.07422 [astro-ph.HE].
- [256] ARA Collaboration, P. Allison *et al.*, “Constraints on the diffuse flux of ultrahigh energy neutrinos from four years of Askaryan Radio Array data in two stations,” *Phys. Rev. D*, vol. 102, no. 4, p. 043021, arXiv:1912.00987 [astro-ph.HE].
- [257] A. Anker *et al.*, “A search for cosmogenic neutrinos with the ARIANNA test bed using 4.5 years of data,” *JCAP*, vol. 03, p. 053, arXiv:1909.00840 [astro-ph.IM].
- [258] ANITA Collaboration, P. Gorham *et al.*, “Constraints on the ultrahigh-energy cosmic neutrino flux from the fourth flight of ANITA,” *Phys. Rev. D*, vol. 99, no. 12, p. 122001, arXiv:1902.04005 [astro-ph.HE].
- [259] IceCube Collaboration, M. G. Aartsen *et al.*, “The IceCube Neutrino Observatory: Instrumentation and Online Systems,” *JINST*, vol. 12, no. 03, p. P03012, arXiv:1612.05093 [astro-ph.IM].
- [260] S. Wissel *et al.*, “Prospects for high-elevation radio detection of >100 PeV tau neutrinos,” *JCAP*, vol. 11, p. 065, arXiv:2004.12718 [astro-ph.IM].
- [261] A. Romero-Wolf *et al.*, “An Andean Deep-Valley Detector for High-Energy Tau Neutrinos,” in *Latin American Strategy Forum for Research Infrastructure*, 2 2020, 2002.06475.
- [262] A. N. Otte, A. M. Brown, M. Doro, A. Falcone, J. Holder, E. Judd, P. Kaaret, M. Mariotti, K. Murase, and I. Taboada, “Trinity: An Air-Shower Imaging Instrument to detect Ultrahigh Energy Neutrinos,” arXiv:1907.08727 [astro-ph.IM].
- [263] S. Prohira *et al.*, “Observation of Radar Echoes From High-Energy Particle Cascades,” *Phys. Rev. Lett.*, vol. 124, no. 9, p. 091101, arXiv:1910.12830 [astro-ph.HE].
- [264] POEMMA Collaboration, A. V. Olinto *et al.*, “The POEMMA (Probe of Extreme Multi-Messenger Astrophysics) observatory,” *JCAP*, vol. 06, p. 007, arXiv:2012.07945 [astro-ph.IM].
- [265] RNO-G Collaboration, J. A. Aguilar *et al.*, “The Radio Neutrino Observatory Greenland (RNO-G),” *PoS*, vol. ICRC2021, p. 001, 2021.
- [266] D. Hooper, “Detecting MeV Gauge Bosons with High-Energy Neutrino Telescopes,” *Phys. Rev. D*, vol. 75, p. 123001, 2007.
- [267] K. Ioka and K. Murase, “IceCube PeV–EeV neutrinos and secret interactions of neutrinos,” *PTEP*, vol. 2014, no. 6, p. 061E01, arXiv:1404.2279 [astro-ph.HE].

- [268] K. C. Y. Ng and J. F. Beacom, “Cosmic neutrino cascades from secret neutrino interactions,” *Phys. Rev. D*, vol. 90, no. 6, p. 065035, arXiv:1404.2288 [astro-ph.HE]. [Erratum: *Phys. Rev. D* 90, 089904 (2014)].
- [269] M. Dhuria and V. Rentala, “PeV scale Supersymmetry breaking and the IceCube neutrino flux,” *JHEP*, vol. 09, p. 004, arXiv:1712.07138 [hep-ph].
- [270] M. Bustamante, C. Rosenstrøm, S. Shalgar, and I. Tamborra, “Bounds on secret neutrino interactions from high-energy astrophysical neutrinos,” *Phys. Rev. D*, vol. 101, no. 12, p. 123024, arXiv:2001.04994 [astro-ph.HE].
- [271] C. Creque-Sarbinowski, J. Hyde, and M. Kamionkowski, “Resonant neutrino self-interactions,” *Phys. Rev. D*, vol. 103, no. 2, p. 023527, arXiv:2005.05332 [hep-ph].
- [272] I. Esteban, S. Pandey, V. Brdar, and J. F. Beacom, “Probing secret interactions of astrophysical neutrinos in the high-statistics era,” *Phys. Rev. D*, vol. 104, no. 12, p. 123014, arXiv:2107.13568 [hep-ph].
- [273] IceCube Collaboration, M. G. Aartsen *et al.*, “A combined maximum-likelihood analysis of the high-energy astrophysical neutrino flux measured with IceCube,” *Astrophys. J.*, vol. 809, no. 1, p. 98, arXiv:1507.03991 [astro-ph.HE].
- [274] IceCube Collaboration, R. Abbasi *et al.*, “The IceCube high-energy starting event sample: Description and flux characterization with 7.5 years of data,” *Phys. Rev. D*, vol. 104, p. 022002, arXiv:2011.03545 [astro-ph.HE].
- [275] Y. Huang, H. Li, and B.-Q. Ma, “Consistent Lorentz violation features from near-TeV IceCube neutrinos,” *Phys. Rev. D*, vol. 99, no. 12, p. 123018, arXiv:1906.07329 [hep-ph].
- [276] U. Jacob and T. Piran, “Neutrinos from gamma-ray bursts as a tool to explore quantum-gravity-induced Lorentz violation,” *Nature Phys.*, vol. 3, pp. 87–90, 2007.
- [277] A. Addazi *et al.*, “Quantum gravity phenomenology at the dawn of the multi-messenger era – A review,” arXiv:2111.05659 [hep-ph].
- [278] S. W. Li, M. Bustamante, and J. F. Beacom, “Echo Technique to Distinguish Flavors of Astrophysical Neutrinos,” *Phys. Rev. Lett.*, vol. 122, no. 15, p. 151101, arXiv:1606.06290 [astro-ph.HE].
- [279] K. Murase and E. Waxman, “Constraining High-Energy Cosmic Neutrino Sources: Implications and Prospects,” *Phys. Rev. D*, vol. 94, no. 10, p. 103006, arXiv:1607.01601 [astro-ph.HE].
- [280] M. Ahlers and F. Halzen, “Pinpointing Extragalactic Neutrino Sources in Light of Recent IceCube Observations,” *Phys. Rev.*, vol. D90, p. 043005, arXiv:1406.2160 [astro-ph.HE].
- [281] K. Fang, K. Kotera, M. C. Miller, K. Murase, and F. Oikonomou, “Identifying Ultrahigh-Energy Cosmic-Ray Accelerators with Future Ultrahigh-Energy Neutrino Detectors,” *JCAP*, vol. 12, p. 017, arXiv:1609.08027 [astro-ph.HE].
- [282] I. Bartos, M. Ahrens, C. Finley, and S. Marka, “Prospects of Establishing the Origin of Cosmic Neutrinos using Source Catalogs,” *Phys. Rev. D*, vol. 96, no. 2, p. 023003, arXiv:1611.03861 [astro-ph.HE].
- [283] I. Bartos, D. Veske, M. Kowalski, Z. Marka, and S. Marka, “The IceCube Pie Chart: Relative Source Contributions to the Cosmic Neutrino Flux,” *Astrophys. J.*, vol. 921, no. 1, p. 45, arXiv:2105.03792 [astro-ph.HE].
- [284] IceCube Collaboration, R. Abbasi *et al.*, “Measuring total neutrino cross section with IceCube at intermediate energies (~ 100 GeV to a few TeV),” *PoS*, vol. ICRC2021, p. 1132, arXiv:2107.09764 [astro-ph.HE].
- [285] M. Bustamante and A. Connolly, “Extracting the Energy-Dependent Neutrino-Nucleon Cross Section above 10 TeV Using IceCube Showers,” *Phys. Rev. Lett.*, vol. 122, no. 4, p. 041101, arXiv:1711.11043 [astro-ph.HE].

- [286] IceCube Collaboration, M. G. Aartsen *et al.*, “Measurement of the multi-TeV neutrino cross section with IceCube using Earth absorption,” *Nature*, vol. 551, pp. 596–600, arXiv:1711.08119 [hep-ex].
- [287] P. B. Denton and Y. Kini, “Ultra-High-Energy Tau Neutrino Cross Sections with GRAND and POEMMA,” *Phys. Rev. D*, vol. 102, p. 123019, arXiv:2007.10334 [astro-ph.HE].
- [288] A. Connolly, R. S. Thorne, and D. Waters, “Calculation of High Energy Neutrino-Nucleon Cross Sections and Uncertainties Using the MSTW Parton Distribution Functions and Implications for Future Experiments,” *Phys. Rev. D*, vol. 83, p. 113009, arXiv:1102.0691 [hep-ph].
- [289] IceCube Collaboration, M. G. Aartsen *et al.*, “Measurements using the inelasticity distribution of multi-TeV neutrino interactions in IceCube,” *Phys. Rev. D*, vol. 99, no. 3, p. 032004, arXiv:1808.07629 [hep-ex].
- [290] I. Safa, A. Pizzuto, C. A. Argüelles, F. Halzen, R. Hussain, A. Kheirandish, and J. Vandenbroucke, “Observing EeV neutrinos through Earth: GZK and the anomalous ANITA events,” *JCAP*, vol. 01, p. 012, arXiv:1909.10487 [hep-ph].
- [291] KM3Net Collaboration, S. Adrian-Martinez *et al.*, “Letter of intent for KM3NeT 2.0,” *J. Phys. G*, vol. 43, no. 8, p. 084001, arXiv:1601.07459 [astro-ph.IM].
- [292] Baikal-GVD Collaboration, A. Avrorin *et al.*, “Neutrino Telescope in Lake Baikal: Present and Future,” *PoS*, vol. ICRC2019, p. 1011, arXiv:1908.05427 [astro-ph.HE].
- [293] P-ONE Collaboration, M. Agostini *et al.*, “The Pacific Ocean Neutrino Experiment,” *Nature Astron.*, vol. 4, no. 10, pp. 913–915, arXiv:2005.09493 [astro-ph.HE].
- [294] G. A. Askar’yan, “Excess negative charge of an electron-photon shower and its coherent radio emission,” *Zh. Eksp. Teor. Fiz.*, vol. 41, pp. 616–618, 1961.
- [295] L. A. Anchordoqui *et al.*, “Performance and science reach of the Probe of Extreme Multimessenger Astrophysics for ultrahigh-energy particles,” *Phys. Rev. D*, vol. 101, no. 2, p. 023012, arXiv:1907.03694 [astro-ph.HE].
- [296] D. García-Fernández, A. Nelles, and C. Glaser, “Signatures of secondary leptons in radio-neutrino detectors in ice,” *Phys. Rev. D*, vol. 102, no. 8, p. 083011, arXiv:2003.13442 [astro-ph.HE].
- [297] K.-C. Lai, C.-C. Chen, and P. Chen, “The Strategy of Discrimination between Flavors for Detection of Cosmogenic Neutrinos,” *Nucl. Phys. B Proc. Suppl.*, vol. 246-247, p. 95, arXiv:1303.1949 [hep-ph].
- [298] L. Gerhardt and S. R. Klein, “Electron and Photon Interactions in the Regime of Strong LPM Suppression,” *Phys. Rev. D*, vol. 82, p. 074017, arXiv:1007.0039 [hep-ph].
- [299] ARA Collaboration, P. Allison *et al.*, “First Constraints on the Ultra-High Energy Neutrino Flux from a Prototype Station of the Askaryan Radio Array,” *Astropart. Phys.*, vol. 70, p. 62, arXiv:1404.5285 [astro-ph.HE].
- [300] ARIANNA Collaboration, A. Anker *et al.*, “Targeting ultra-high energy neutrinos with the ARIANNA experiment,” *Adv. Space Res.*, vol. 64, pp. 2595–2609, arXiv:1903.01609 [astro-ph.IM].
- [301] A. Anker *et al.*, “White Paper: ARIANNA-200 high energy neutrino telescope,” arXiv:2004.09841 [astro-ph.IM].
- [302] J. Aguilar *et al.*, “The Next-Generation Radio Neutrino Observatory – Multi-Messenger Neutrino Astrophysics at Extreme Energies,” arXiv:1907.12526 [astro-ph.HE].
- [303] K. D. de Vries, K. Hanson, and T. Meures, “On the feasibility of RADAR detection of high-energy neutrino-induced showers in ice,” *Astropart. Phys.*, vol. 60, p. 25, arXiv:1312.4331 [astro-ph.HE].
- [304] S. Prohira and D. Besson, “Particle-level model for radar based detection of high-energy neutrino cascades,” *Nucl. Instrum. Meth. A*, vol. 922, p. 161, arXiv:1710.02883 [physics.ins-det].

- [305] D. Fargion, “Discovering Ultra High Energy Neutrinos by Horizontal and Upward τ Air-Showers: Evidences in Terrestrial Gamma Flashes?,” *Astrophys. J.*, vol. 570, p. 909, 2002.
- [306] Telescope Array Collaboration, R. U. Abbasi *et al.*, “Search for Ultra-High-Energy Neutrinos with the Telescope Array Surface Detector,” *J. Exp. Theor. Phys.*, vol. 131, no. 2, pp. 255–264, arXiv:1905.03738 [astro-ph.HE].
- [307] H. León Vargas, A. Sandoval, E. Belmont, and R. Alfaro, “Capability of the HAWC Gamma-Ray Observatory for the Indirect Detection of Ultrahigh-Energy Neutrinos,” *Adv. Astron.*, vol. 2017, p. 1932413, arXiv:1610.04820 [astro-ph.IM].
- [308] J. Nam *et al.*, “Design and implementation of the TAROGÉ experiment,” *Int. J. Mod. Phys. D*, vol. 25, no. 13, p. 1645013, 2016.
- [309] J. Nam *et al.*, “High-elevation synoptic radio array for detection of upward moving air-showers, deployed in the Antarctic mountains,” *PoS*, vol. ICRC2019, p. 967, 2020.
- [310] C. Deaconu *et al.*, “Searches for Ultra-High Energy Neutrinos with ANITA,” *PoS*, vol. ICRC2019, p. 867, arXiv:1908.00923 [astro-ph.HE].
- [311] C. Aramo, A. Insolia, A. Leonardi, G. Miele, L. Perrone, O. Pisanti, and D. Semikoz, “Earth-skimming UHE Tau neutrinos at the fluorescence detector of Pierre Auger observatory,” *Astropart. Phys.*, vol. 23, p. 65, 2005.
- [312] D. Góra, E. Bernardini, and A. Kappes, “Searching for tau neutrinos with Cherenkov telescopes,” *Astropart. Phys.*, vol. 61, p. 12, arXiv:1402.4243 [astro-ph.IM].
- [313] D. Góra and E. Bernardini, “Detection of tau neutrinos by Imaging Air Cherenkov Telescopes,” *Astropart. Phys.*, vol. 82, p. 77, arXiv:1606.01676 [astro-ph.IM].
- [314] MAGIC Collaboration, M. L. Ahnen *et al.*, “Limits on the flux of tau neutrinos from 1 PeV to 3 EeV with the MAGIC telescopes,” *Astropart. Phys.*, vol. 102, pp. 77–88, arXiv:1805.02750 [astro-ph.IM].
- [315] D. F. Fiorillo, G. Miele, and O. Pisanti, “Tau Neutrinos with Cherenkov Telescope Array,” arXiv:2007.13423 [hep-ph].
- [316] T. C. Weekes *et al.*, “Observation of TeV gamma rays from the Crab nebula using the atmospheric Cerenkov imaging technique,” *Astrophys. J.*, vol. 342, pp. 379–395, 1989.
- [317] A. N. Otte, “Studies of an air-shower imaging system for the detection of ultrahigh-energy neutrinos,” *Phys. Rev. D*, vol. 99, no. 8, p. 083012, arXiv:1811.09287 [astro-ph.IM].
- [318] M. Sasaki and G. W.-S. Hou, “Neutrino Telescope Array Letter of Intent: A Large Array of High Resolution Imaging Atmospheric Cherenkov and Fluorescence Detectors for Survey of Air-showers from Cosmic Tau Neutrinos in the PeV-EeV Energy Range,” arXiv:1408.6244 [astro-ph.IM].
- [319] J. H. Adams *et al.*, “White paper on EUSO-SPB2,” arXiv:1703.04513 [astro-ph.HE].
- [320] ATLAS Collaboration, G. Aad *et al.*, “The ATLAS Experiment at the CERN Large Hadron Collider,” *JINST*, vol. 3, p. S08003, 2008.
- [321] L. A. Anchordoqui *et al.*, “The Forward Physics Facility: Sites, Experiments, and Physics Potential,” arXiv:2109.10905 [hep-ph].
- [322] J. L. Feng *et al.*, “The Forward Physics Facility at the High-Luminosity LHC,” arXiv:2203.05090 [hep-ex].
- [323] FASER Collaboration, A. Ariga *et al.*, “Technical Proposal for FASER: ForwArd Search Experiment at the LHC,” arXiv:1812.09139 [physics.ins-det].
- [324] H. Abreu *et al.*, “Neutrino/dark particle detectors for the hl-lhc forward beam; snowmass 2021 loi,” 2021.
- [325] “Forward physics facility workshops.” <https://indico.cern.ch/category/13966/>.
- [326] FASER Collaboration, H. Abreu *et al.*, “First neutrino interaction candidates at the LHC,” *Phys. Rev. D*, vol. 104, no. 9, p. L091101, arXiv:2105.06197 [hep-ex].

- [327] DUNE Collaboration, B. Abi *et al.*, “The DUNE Far Detector Interim Design Report Volume 1: Physics, Technology and Strategies,” arXiv:1807.10334 [physics.ins-det].
- [328] W. A. Mann *et al.*, “Study of the reaction $\nu n \rightarrow \mu^- p$,” *Phys. Rev. Lett.*, vol. 31, pp. 844–847, 1973.
- [329] S. J. Barish *et al.*, “Study of Neutrino Interactions in Hydrogen and Deuterium. 1. Description of the Experiment and Study of the Reaction $\nu d \rightarrow \mu^- pp_s$,” *Phys. Rev.*, vol. D16, p. 3103, 1977.
- [330] K. L. Miller *et al.*, “Study of the reaction $\nu_\mu d \rightarrow \mu^- pp_s$,” *Phys. Rev.*, vol. D26, pp. 537–542, 1982.
- [331] N. J. Baker, A. M. Cnops, P. L. Connolly, S. A. Kahn, H. G. Kirk, M. J. Murtagh, R. B. Palmer, N. P. Samios, and M. Tanaka, “Quasielastic Neutrino Scattering: A Measurement of the Weak Nucleon Axial Vector Form-Factor,” *Phys. Rev.*, vol. D23, pp. 2499–2505, 1981.
- [332] T. Kitagaki *et al.*, “High-Energy Quasielastic $\nu_\mu n \rightarrow \mu^- p$ Scattering in Deuterium,” *Phys. Rev.*, vol. D28, pp. 436–442, 1983.
- [333] C. Wilkinson, P. Rodrigues, S. Cartwright, L. Thompson, and K. McFarland, “Reanalysis of bubble chamber measurements of muon-neutrino induced single pion production,” *Phys. Rev. D*, vol. 90, no. 11, p. 112017, arXiv:1411.4482 [hep-ex].
- [334] X. G. Lu, D. Coplowe, R. Shah, G. Barr, D. Wark, and A. Weber, “Reconstruction of Energy Spectra of Neutrino Beams Independent of Nuclear Effects,” *Phys. Rev. D*, vol. 92, no. 5, p. 051302, arXiv:1507.00967 [hep-ex].
- [335] P. Hamacher-Baumann, X. Lu, and J. Martín-Albo, “Neutrino-hydrogen interactions with a high-pressure time projection chamber,” *Phys. Rev. D*, vol. 102, no. 3, p. 033005, arXiv:2005.05252 [physics.ins-det].
- [336] Y. Sakai, H. Böttcher, and W. Schmidt, “Excess electrons in liquid hydrogen, liquid neon, and liquid helium,” *Journal of Electrostatics*, vol. 12, pp. 89 – 96, 1982.
- [337] H. Harrison and B. Springett, “Electron mobility variation in dense hydrogen gas,” *Chemical Physics Letters*, vol. 10, no. 4, pp. 418 – 421, 1971.
- [338] DUNE Collaboration, A. Abed Abud *et al.*, “Deep Underground Neutrino Experiment (DUNE) Near Detector Conceptual Design Report,” *Instruments*, vol. 5, no. 4, p. 31, arXiv:2103.13910 [physics.ins-det].
- [339] H. Bradner, “Bubble chambers,” *Annual Reviews of Nuclear Science*, vol. 10, pp. 109–160, [hep-ex/nuc-ex].
- [340] M. D. *et al.*, “Holographic photography of bubble chamber tracks: A feasibility test,” *Nuclear Instruments and Methods*, vol. 179, pp. 487–493, 1981.
- [341] D. G. Crabb and W. Meyer, “Solid polarized targets for nuclear and particle physics experiments,” *Ann. Rev. Nucl. Part. Sci.*, vol. 47, pp. 67–109, 1997.
- [342] A. Dael, D. Cacaute, H. Desportes, R. Duthil, B. Gallet, F. Kircher, C. Lesmond, Y. Pabot, and J. Thinel, “A Superconducting 2.5-T high accuracy solenoid and a large 0.5-T dipole magnet for the SMC target,” *IEEE Trans. Magnetics*, vol. 28, no. 1, pp. 560–563, 1992.
- [343] A. Berryhill and J. Ritter, “A Dual 5T Superconducting Magnet System for the Brookhaven National Lab Electron Beam Ion Source,” *IEEE Trans. Appl. Supercond.*, vol. 29, no. 5, p. 4100104, 2019.
- [344] E. Bunyatova, “Free radicals and polarized targets,” *Nuclear Instruments and Methods in Physics Research Section A: Accelerators, Spectrometers, Detectors and Associated Equipment*, vol. 526, no. 1, pp. 22–27, 2004. Proceedings of the ninth International Workshop on Polarized Solid Targets and Techniques.
- [345] B. van den Brandt, P. Hautle, J. A. Konter, and E. I. Bunyatova, “Progress in scintillating polarized targets for spin physics,” in *2nd International Symposium on the Gerasimov-Drell-Hearn Sum Rule and the Spin Structure of the Nucleon (GDH 2002)*, pp. 183–187, 7 2002.

- [346] B. van den Brandt, E. I. Bunyatova, P. Hautle, J. A. Konter, S. Mango, and I. B. Nemchonok, “An ‘active’ target for spin physics: Polarizing nuclei in plastic scintillators,” *Czech. J. Phys.*, vol. 52, pp. C689–C694, 2002.